SYNTHESIS AND CHARACTERIZATION OF COPPER PHTHALOCYANINE DEPOSITED MICA TITANIA PIGMENT

A THESIS SUBMITTED TO
THE GRADUATE SCHOOL OF NATURAL AND APPLIED SCIENCES OF
MIDDLE EAST TECHNICAL UNIVERSITY

BY

BERNA BURCU TOPUZ

IN PARTIAL FULFILLMENT OF THE REQUIREMENTS
FOR
THE DEGREE OF MASTER OF SCIENCE
IN
POLYMER SCIENCE AND TECHNOLOGY

JANUARY 2010

Approval of the thesis:

SYNTHESIS AND CHARACTERIZATION OF COPPER PHTHALOCYANINE DEPOSITED MICA TITANIA PIGMENT

submitted by **BERNA BURCU TOPUZ** in partial fulfillment of the requirements for the degree of **Master of Science in Polymer Science and Technology Departmant, Middle East Technical University** by,

Prof. Dr. Canan Özgen _____
Dean, Graduate School of **Natural and Applied Sciences**

Prof. Dr. Cevdet Kaynak _____
Head of Department, **Polymer Science and Technology**

Prof. Dr. Güngör Gündüz _____
Supervisor, **Chemical Engineering Dept., METU**

Asst. Prof. Dr. Bora Maviş _____
Co-Supervisor, **Mechanical Engineering Dept., HU**

Examining Committee Members:

Prof. Dr. Ülkü Yılmazer _____
Chemical Engineering Dept., METU

Prof. Dr. Güngör Gündüz _____
Chemical Engineering Dept., METU

Prof. Dr. Jale Hacaloğlu _____
Chemistry Dept., METU

Prof. Dr. Tülay Özbelge _____
Chemical Engineering Dept., METU

Prof. Dr. Leyla Aras _____
Chemistry Dept., METU

Date: 15/01/2010

I hereby declare that all information in this document has been obtained and presented in accordance with academic rules and ethical conduct. I also declare that, as required by these rules and conduct, I have fully cited and referenced all material and results that are not original to this work.

Name, Last name: Berna Burcu Topuz

Signature :

ABSTRACT

SYNTHESIS AND CHARACTERIZATION OF COPPER PHTHALOCYANINE DEPOSITED MICA TITANIA PIGMENT

Topuz, Berna Burcu

M.Sc., Department of Polymer Science and Technology

Supervisor: Prof. Dr. Güngör Gündüz

Co-Supervisor: Asst. Prof. Dr. Bora Maviş

January 2010, 104 pages

In the present work, anatase and rutile titanium dioxide (TiO_2) coated lustrous mica pigments were prepared by heterogeneous nucleation method. Anatase-rutile phase transformation of the TiO_2 on mica substrate was achieved by coating very thin layers of tin (IV) oxide on mica surfaces prior to TiO_2 deposition. Muscovite mica, which was used in the experiments was sieved, pre-treated with sodium bicarbonate and decantated before coating process. The surface morphology of mica titania pigments and anatase-rutile phase transformation were investigated by SEM and XRD analyse, respectively. Also, microwave-assisted synthesis of copper phthalocyanine and tetracarboxamide copper phthalocyanine pigments were carried out with phthalic anhydride and trimellitic anhydride precursors, respectively. Molecular structures of these pigments were confirmed by FT-IR and UV-visible spectroscopy analyse. Furthermore, combination pigments were obtained by the process of deposition of copper phthalocyanine pigments on

mica-titania pigment substrate in dimethyl formamide solvent. FT-IR analysis and XRD analyse were performed to observe the transformations in the crystal forms of copper phthalocyanines on the substrate. The surface morphologies of copper phthalocyanines on the mica titania pigments were investigated by SEM analysis. Varying amounts of copper phthalocyanines were deposited on the mica surfaces, and nitrogen elemental analysis was performed to determine the amount of copper phthalocyanines. The resulting pigments were incorporated into alkyd based resin to prepare paint samples. L*a*b* values, gloss property, and hardness of the paint samples were determined by color measuring device, gloss meter and hardness measuring device, respectively.

The resulting combination pigments obtained in this study showed improved luster, hue, and color intensity. Furthermore, in literature it was reported that these pigments have very high bleed resistance. This can be attributed to large macromolecular structure of copper phthalocyanine on the surface of mica titania pigment that prevents bleeding of the pigment from the paint. Moreover, the paint samples obtained from combination pigments showed higher hardness with respect to the paint sample of the mica titania pigment.

Key words: mica, titanium dioxide, tin oxide, copper phthalocyanine, combination pigment.

ÖZ

BAKIR FTALOSİYANİN ÇÖKTÜRÜLMÜŞ MİKA TİTAN PİGMENT SENTEZİ VE ÖZELLİKLERİNİN BELİRLENMESİ

Topuz, Berna Burcu

Yüksek Lisans, Polimer Bilim ve Teknolojisi Bölümü

Tez Yöneticisi: Prof. Dr. Güngör Gündüz

Ortak Tez Yöneticisi: Yard. Doç. Dr. Bora Maviş

Ocak 2010, 104 sayfa

Bu çalışmada rutil ve anataz fazda titanyum dioksit kaplı parlak mika pigmenti heterojen çekirdeklenme yöntemi ile hazırlanmıştır. Mika altlıkları üzerindeki titanyum dioksitin anataz-rutil faz dönüşümü, titanyum dioksit çökelmesinden önce mika yüzeylerine çok ince bir kalay oksit tabakası kaplanması ile gerçekleştirilmiştir. Deneylerde kullanılan muskovit mika kaplama işleminden önce elenip, sodyum bikarbonat önişlemine tabi tutulmuş ve dekantasyon ile arıtılmıştır. Mika titan pigmentlerinin yüzey morfolojileri ve anataz rutil faz dönüşümleri sırasıyla SEM ve XRD analizleri ile incelenmiştir. Bunun yanında, mikrodalga fırın kullanılarak bakır ftalosiyanin ve tetrakarboksamid bakır ftalosiyanin sentezi ftalik anhidrit ve trimellitik anhidrit maddeleri kullanılarak gerçekleştirilmiştir. Bu pigmentlerin molekül yapıları, FT-IR ve UV-Vis spektroskopi analizleri ile incelenmiştir. Ayrıca, bakır ftalosiyaninlerin rutil fazda mika titan pigmentinin üzerine çökelmesi işlemi ile dimetilformamit çözücüsü içerisinde çift bileşenli yeni pigmentler elde

edilmiştir. Bakır ftalosiyanin pigmentlerinin mika titan pigmenti üzerindeki kristal formlarındaki dönüşümleri incelemek için FT-IR ve XRD analizlerinden yararlanılmıştır. Bakır ftalosiyaninlerin mika titan pigment üzerindeki yüzey morfolojileri SEM analizi ile incelenmiştir. Değişik miktarlarda bakır ftalosiyaninler mika titan pigment yüzeylerine çöktürülmüş ve mika titan pigment yüzeylerindeki bakır ftalosiyaninlerin miktarları azot elementel analizi ile elde edilmiştir. Elde edilen pigmentler boya örnekleri hazırlanması amacıyla alkid esaslı reçinelere katılmışlardır. Boya örneklerinin L*a*b* değerleri, parlaklık özellikleri ve sertlikleri, renk ölçüm cihazı, parlaklık ölçüm cihazı ve sertlik ölçüm cihazı ile belirlenmiştir.

Bu çalışmada elde edilen çift bileşenli pigmentler iyileşmiş parlaklık, renk tonu ve renk gücü göstermiştir. Bunun dışında, mika titan pigment yüzeylerindeki bakır ftalosyaninlerin büyük makromolekül yapıları sayesinde pigmentin boya dışına çıkmasını önleyebilmesi ile pigmentlerin boya kusmasına karşı dirençlerinin yüksek olması gerektiği belirtilmiştir. Ayrıca, çift bileşenli pigmentler ile elde edilen boya örnekleri yalnızca mika titan pigmenti ile elde edilen boya örneklerine göre daha yüksek sertlik değerleri göstermiştir.

Anahtar Sözcükler: mika, titanyum dioksit, kalay oksit, bakır ftalosiyanin, çift bileşenli pigment.

To Nerzan and Hüsnü Topuz

ACKNOWLEDGEMENTS

I would like to express my sincere appreciation to Prof. Dr. Güngör Gündüz for his supervision and valued guidance. As my supervisor; he guided me on my thesis and my life, especially in personal matters.

I am very thankful to my co-supervisor Asst. Prof. Dr. Bora Maviş for his understanding, support, and his motivating speeches during my thesis period.

I would like to thank Prof. Dr. Üner Çolak for his invaluable suggestions, support and encouragement throughout this study.

My special thanks go to Gülden Eroğlu and Simge Çınar for being my family in Ankara. The friendship of Anisa Coniku, Sevinç Kahya, Korhan Sezgiker, İrem Vural, Nagihan Keskin, and Nasser Khazeni, Elif Karatay, Berker Fıçıcılar is much appreciated.

I wish to express my sincere thanks to Demet İzol Mekereci, Ceren Büyükyıldız and Can Olgaç Şengül for their friendship, help and patience in whole period of my thesis.

I am also very thankful to Ümit Sayıner and Selin Çiftçi for their encouragement and motivation throughout this study.

I would like to thank to Tuğçe Şentürk and Lütfi Oduncuoğlu for their endless support during writing my thesis.

I would like to thank to Kaltun Mining Co, for supplying me basic materials necessary in my thesis.

I would also thank to Mihrican Açıkgöz and Kerime Güney from Chemical Engineering Department at METU for helping me in analysis.

I am very thankful to Rüyam Kısakürek for doing color measurements of my samples which are important in my thesis.

I want to thank to Dr. Cemil Alkan, for his technical support in the beginning of this study.

I would like to thank my family for every beautiful thing in my life. Among them, special thanks to my nephew, Bartu Darendeli. His existence is enough to make me feel better and motivated.

TABLE OF CONTENTS

LIST OF TABLES

TABLES

LIST OF FIGURES

FIGURES

LIST OF SYMBOLS AND ABBREVIATIONS

°C	Celcius Degree
nm	Nanometer
n	Refractive index
W	Watt
ml	Mililiter
g	Gram
h	Hour
min	Minute
°	Degree
μm	Micrometer
cm^{-1}	Wavenumber
DMF	Dimethyl formamide
2θ	Two theta
SEM	Scanning Electron Spectroscopy
UV-vis	Ultraviolet - Visible Spectroscopy
XRD	X-Ray Diffractometer
BET	Brunauer ,Emmett, Teller
CP	Copper Phthalocyanine
TCP	Tetracarboxamide Copper Phthalocyanine
CPM	Copper Phthalocyanine Deposited Mica Titania Pigment
TCPM	Tetracarboxamide Copper Phthalocyanine Deposited Mica Titania Pigment

CHAPTER 1

INTRODUCTION

Recently, the angle-dependent optical effects depicted by pigments, have received significant attention because of their broad applications. Intense research is under way for different types of pigments and their processing methods. There are prominent requirements of the angle-dependent pigments. Generally, these optical effects can be achieved by using thin films and coatings that contain special effect pigments. Among them, pearlescent pigments are the most used in practice due to their easier synthesis methods [1]. Besides, they serve a growing economic significance due to its utility in various industrial products and end-user applications [2].

A pearlescent pigment is a kind of luster pigment which shows a pearl-shine due to angle-dependent optical effects deriving from transparent layers of particle with different refractive indices [3]. Today, they have found very broad application for decorative and functional purposes in systems like automotive top coatings, plastics, printing inks, and cosmetics because of their unique possibilities for the achievement of optical impressions such as eye-catching effects, angle-dependent interference colors, pearl luster, or multiple reflection [2]. The most widely used effect pigments consist of mica flakes coated with TiO_2 (Figure 1.1).

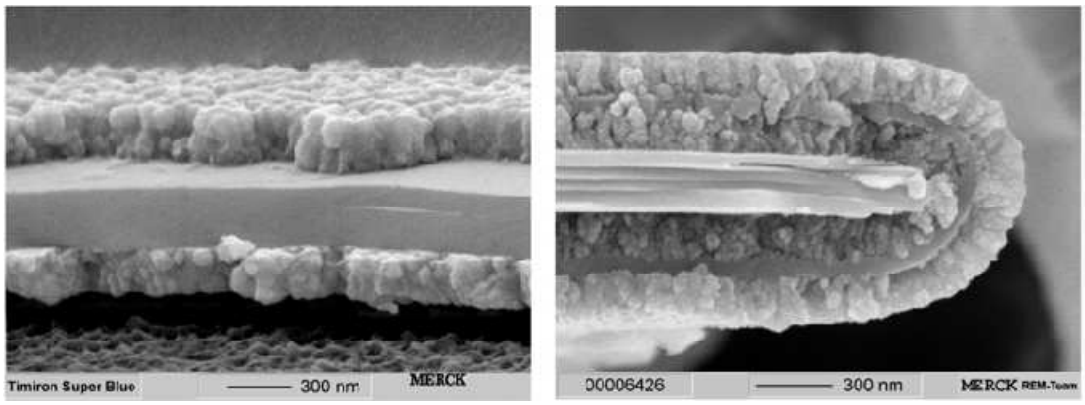

Figure 1.1 SEM micrographs of mica titania pigment.

Unique pearlescent effect occurs because the layers of the transparent mica particles allow a portion of the incident light to be transmitted. When this transmitted light meets further boundary surfaces, with different refractive indices, a portion of the light is reflected. The total reflected light is made up of portions that have travelled on different paths producing optical interference. Mica particle size also affects this luster appearance. The coarser platelets shine stronger while the small ones cause a satin appearance [3]. Among effect pigments, the choice of mica titania pigment depends on not only its aesthetic features but also excellent thermal stability up to 800 ^{O}C and chemical stability that copes with acid or alkali media [3] [4]. Furthermore, these pigments are non-combustible, not self-igniting, do not conduct electricity and are harmless to human health [3].

Mica titania pigments can be synthesized by several techniques. The most common technique is the heterogeneous nucleation in solution reactions. It is the most widely used and best controlled process [5]. This technique consists of two alternatives, homogeneous hydrolysis and titration method [6]. In homogeneous hydrolysis method, addition of titanyl sulfate solution to

the mica suspension is accompanied by hydrolysis with urea and the thickness of the layer and the associated interference color is predetermined by the amount of titanyl sulfate solution [5,7]. By creating a basic environment, the rate of hydrolysis can be controlled and urea gradually decomposes during heating. After drying and filtering, calcination process is applied to obtain crystalline form of TiO_2 on mica [8]. However the control of the rate of hydrolysis is very difficult in this method and titanyl sulfate produced titania coated mica is subject to considerable stripping [8-9]. This method is preferred by some researchers because of ease of operation and simplicity [9]. In titration method, pigment is prepared by precipitation of titanium hydroxide on the surface of mica via hydrolysis of $TiCl_4$ by the addition of a suitable base. This process is followed by drying, filtering, and calcination respectively. During coating, the pH should be adjusted and kept constant by simultaneous addition of a base [10]. This method is widely used in most studies because of the better quality of the final product. For example, the adhesion of the TiO_2 is good when this method is employed, and no stripping is observed [9]. It also avoids excess use of titanium salt by supplying to the hydrolysis only that quantity which is necessary for uniform coating per unit time. There is therefore no production of hydrated TiO_2 particles freely present in the pigment [10]. In both methods TiO_2 that coats mica in anatase crystalline form. However, thermodynamically stable phase of TiO_2 which is rutile is preferred in coatings due to many reasons. The refractive index of rutile (2.903) is higher than that of anatase (2.488) [11]. Thus, rutile form of TiO_2 coated mica results in a product with better luster and reflectivity, better color and color homogeneity, and also contains fewer small particles [12]. In other words, phase transformation between rutile and anatase and their proportion of TiO_2 layers has a significant influence on the pearlescent appearance of TiO_2 mica pigments [11]. In addition, rutile is known to have a lower photocatalytic activity than anatase, showing that

rutile transformation is more desirable to prevent the oxidation of binder in outdoor weathering. However, muscovite mica, which is used as a substrate of mica titania pearlescent pigment, is known to have template effect, namely, muscovite mica is anatase directing [13]. If a rutile crystalline form is desired, generally a layer of hydrous tin oxide is first precipitated on the surface of mica followed by a layer of hydrous TiO_2 by titration method. Tin (IV) oxide can influence TiO_2 to form rutile crystallinity on mica substrate after calcination [12]. The use of tin oxide is the method of choice and is used universally in all commercial rutile TiO_2 coated mica pigments [14].

Although anatase-rutile phase transformation has been studied extensively using pure or doped TiO_2, the effect of surface morphology to the quality and property of pigment and the anatase-rutile transformation of TiO_2 thin layers coated on the substrate of pearlescent pigments is not much studied. In this study, synthesis of mica titania pigment was performed and the effect of a rutile promoting additive on the phase transformation of TiO_2 thin layers during preparation of pearlescent pigments was investigated. Pre-treatment of the mica substrate was carried out to improve its surface properties and to cleave its layers.

Phthalocyanine is a symmetrical 18 π-electron aromatic macrocycle, closely related to the naturally occuring porphyrins [15-19] (Figure 1.2). Since its discovery over seventy years ago, phthalocyanines and its derivatives have been extensively used as colorants [16-17,20]. The peripheral and non-peripheral positions on the benzenoid ring of phthalocyanines can be substituted with many molecules and over seventy different metal ions can be introduced into the cental cavity to improve physical properties to suit a desired technological application [17,21].

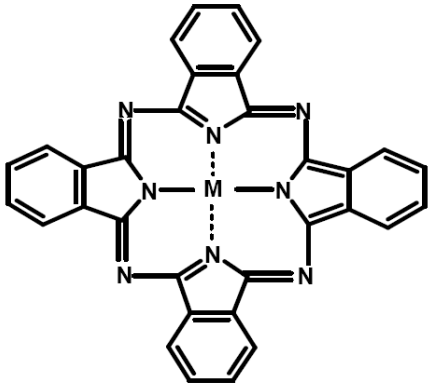

Figure 1.2 Molecular structure of a phthalocyanine; M represents H and a metal for metal free phthalocyanines and metallated phthalocyanines, respectively.

Metal free, unsubstituted and substituted metallophthalocyanines can be obtained by different methods of preparation. Among them, unsubstituted or substituted metallophthalocyanines have drawn increasing interest due to considerably extended applications including commercial dyes, photosensitizers for photodynamic terapy, optical and electrical materials, catalysts, chemicals sensors, liquid crystals, and photoconductive agents [17, 20-22].

Especially, copper phthalocyanine is one of the most important class of colorants and has found extensive use in many modern high technologies. Copper phthalocyanine is greenish-blue crystalline pigment with a high chemical and thermal stabilities. Due to its stability, it is used in inks, coatings, and many plastics.

The synthesis of metallophthalocyanines is usually achieved in high yields by cyclotetramerization of phthalonitrile, diiminoisoindoline, phthalic anhydride or phthalimide in the presence of a metal salt at high temperatures. When

phthalic anhydride or phthalimide is used, a nitrogen donor, like urea should be used in order to conduct the reaction. This method is favored in industry due to the cheaper precursor while other methods are generally cleaner reactions [23-24]. In order to synthesize peripherally or nonperipherally functionalized phthalocyanine, precursors which have desired substituents have been used. In some cases, the substituent can be converted to other molecule with the reaction conditions during phthalocyanine synthesis.

Phthalocyanines can be produced in the medium of solvents or under microwave irradiation. In the last decade, increased interest has been focused on the application of microwave irradiation in organic synthesis. Numerous reactions can be performed under microwave assisted conditions in which significant rate enhancements, improved yield and selectivity, and a reduction in thermal by-products have been achieved [25-26]. In particular, the reaction time and energy input are supposed to be mostly reduced in the reactions that last for a long time at high temperatures under conventional conditions [25,27]. One of the goals of this study comprises preparation of copper phthalocyanine and tetracarboxamide copper phthalocyanine without solvent under microwave irradiation.

Absorption pigments like phthalocyanines have several disadvantages in some applications because of their dispersion problem associated with their small particle size and high surface area [28-29]. By combining these absorption pigments with pearlescent pigments it is possible to produce pearlescent pigments coated with a layer of absorption colorant to realize more significant brilliant colors, and the problems mentioned above can be eliminated [29]. One possibility to obtain attractive combination pigments is the coating of mica titania pigments with an additional layer of an organic colorant. Examples of organic pigments are phthalocyanines, quinacridones,

perylenes, dioxazines and carbon black .They have high color intensity, light fastness and bleed resistance. Such properties make the resulting combination pigments suitable for automotive finishes as well as for general use in paints, cosmetics and in plastics [29-30]. There are very few studies related with the synthesis of combination pigments. These studies are quite complex because their method involves several steps and components to synthesize the desired combination pigment. For example milling was done in order to disperse pigment in water solution and/or some compounds were utilized to prevent the coagulation of the pigment and improve compatibility. All these additional steps are not economically acceptable and also time consuming.

The main objective of this work is to make combination pigment which includes mica titania as a pearlescent pigment and copper phthalocyanine and tetracarboxamide copper phthalocyanine as absorption pigments. Phthalocyanines were dissolved in DMF and because of their solubility in DMF, the dispersion was successfully achieved. Hence, no additional dispersing agents or processing steps were required in our method. Moreover, we did not need to use any binders to adhere the phthalocyanines onto mica surfaces. Simple stirring of this dispersion with mica titania pigment gives the desired pigments with enhanced gloss, hue and color properties. Different amounts of phthalocyanine pigments were used to synthesize combination pigments. Color effects and paint properties were determined by using these pigments in an alkyd resin. Besides, crystalline form of phthalocyanines on mica titania surfaces were investigated.

CHAPTER 2

LITERATURE REVIEW

In this chapter, properties and synthesis methods of mica titania pigments and phthalocyanines were described and previous studies in the literature was surveyed. Also, the definition and the properties of the combination pigments were given and the advantages and the disadvantages in the methods of synthesis were further explained by utilizing literature studies.

2.1 Effect Pigments: Types and Properties

Effect pigments are important class of pigments that give angle-dependent optical properties such as pearl luster, multiple reflection or eye-catching effects when applied in an application medium. Due to their several advantages associated with the achievement of optical impressions such as eye-catching effects, angle-dependent interference colors, pearl luster, or multiple reflection, they are meanwhile irreplaceable in many application systems [2]. The term 'luster pigments' is often applied to effect pigments, because, almost all effect pigments provide lustrous effects in practical applications. Luster pigments tend to be composed of predominantly platelet like particles, that readily align with a parallel orientation to the surface to which they are applied. For example metal effect pigments consist of thin metal (mostly aluminum) platelets; they are not transparent and reflect all incident light in one direction. The pigment particles act like small mirrors leading to a reflecting metal luster when applied to give an aligned parallel

orientation. Pearl luster or pearlescent pigments on the other hand are luster pigments consisting of transparent or semitransparent platelets of metal oxides or other materials with high refractive index [6]. Therefore, a completely different optical behavior can be observed with the pearl luster and metal effect pigments.

The strong demand for pearl effects came from the growing coatings and plastics industries, which wanted to improve the acceptance and popularity of their products. Furthermore, pearlescent pigments also allowed artists and designers to create new visual effects similar to those found in nature. The breakthrough for pearlescent pigments came with the invention of mica coated with metal oxides. Mica based pearlescent pigments now account for 90% of the world market [29]. The most important applications are thermoplastics, cosmetics, food packaging, children toys, paints, and automobile coatings. These pigments can also be utilized for security purposes, because their angle-dependent optical effects cannot be easily imitated with copier machines or photographic techniques, leading to be used on banknotes in many countries [3].

The effect pigments can be divided into two groups: substrate-free pigments which consist of basically one optically homogeneous material, and substrate-based pigments that can be formed by coating substrates with thin layers of metal oxides. The substrate-free pearlescent pigments show a low mechanical stability in some cases and are limited by their chemical composition. In recent years, the substrate-based effect pigments are gaining popularity in various end user applications. In substrate-based pearlescent pigments, the substrate can act as a mechanical support of thin optical layer and as a template for the synthesis. In the case of the substrate with narrow thickness distribution, the substrate can also act as an optical

layer. The substrate-based effect pigments are typically produced by the deposition of metal oxide layers on the substrate in aqueous suspension followed by a calcination process. The typical optical metal oxide layers consist of titanium oxide, iron oxide, mixed titanium-iron oxides and chromium oxide [13]. Among them, TiO_2 is the most widely used as optical metal oxide layer because its refractive index is the highest after diamond. (anatase n=2.488 and rutile n=2.903) [13,31].

Various flaky materials, including natural and synthetic mica platelets, alumina flake and silica flake, can be used as substrates for the pearlescent pigments [13]. Among them muscovite which is a potassium aluminum silicate hydroxide mineral of the mica group known by its layered platelet structure with a formula of $KAl_2(AlSi_3O_{10})(F,OH)$ found various applications in the synthesis of pearlescent (luster, nacreous) pigments (Figure 2.1).

(a) (b)

Figure 2.1. Pictures of muscovite mica (a) and crushed muscovite mica (b).

2.1.1 Pearl luster and interference effect

Natural pearls are made of recurrently alternating layers of transparent media with differing refractive index. They are layers of calcium carbonate (aragonite, n=1.7) and protein (n=1.4). [6,29]. Thus, a very narrow ray of light hitting the surface reflects in such a way that it obeys the laws of reflection, but at the same time it diffuses and gives the impression of gradually reducing intensity. To the eye, the luster takes on a three dimensional character, because at times it seems to come from inside the object. This effect is increased by the rounded shape of the pearl and is referred to as 'pearl luster' [6].

A phenomenon, which occurs with pearl luster pigments, is the interaction of light waves through the other phenomenon of interference. Figure 2.2 shows optical representation of mica pigment coated with a metal oxide. In summary, pearlescent pigments selectively reflect part of the light that is directly incident on the smooth platelet surface. The other part of light enters into the transparent particles and is partially reflected either at interfaces within the pigments or at the bottom of the platelets. The internally reflected light leaves the platelets leading to interactions with adjoining pigment particles to create further reflections (multiple reflection). The partial reflection of light and optical superimposition create interference phenomena, which together with multiple internal reflections lead to the characteristic appearance of pear luster pigments [6]. The thickness of the metal oxide layer determines the size of the phase shift, and so determines the color of iridescence. For coatings of titania, the lower section of the figure shows the thickness of the titania layers on mica. The increase in coating thickness changes the iridescence through yellow, red, blue and

green. The brilliance of iridescence declines if coating is much thicker than 150 nm.

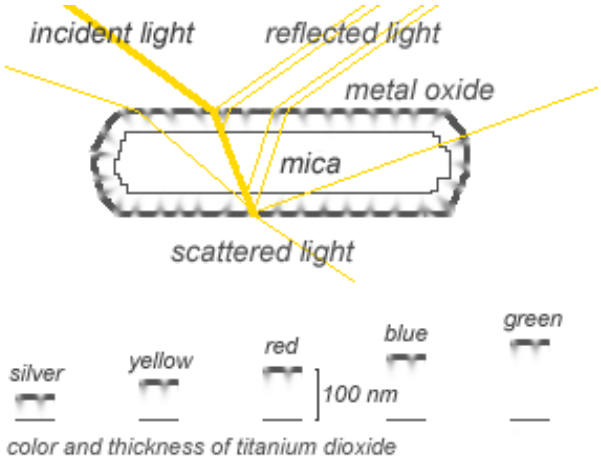

Figure 2.2. Optical representation of mica pigment coated with TiO_2.

2.1.2 Mica titania Pigments

2.1.2.1 Properties

The dominant class of pearlescent pigments is based on platelets of natural mica coated with thin films of transparent metal oxides. The mica substrate acts as a template for the synthesis and as a mechanical support for the deposited thin optical layers of the pearlescent pigments [29]. Possessing a very high refractive index and chemical stability and thermal stability, renders TiO_2 very attractive in mica coatings for the preparation of pearlescent pigments. The presence of a highly refractive and reflective surface layer, covering the less refractive support material results in a significant pearlescent effect and provides different colors resulting from light

interference [32]. Additional advantages can be found in its light stability, low price, and non-toxicity [6]. However, in order to obtain a smooth coating of the final pigment, the dimensions should be 10 to 20 times of the thickness of the flakes, the thickness of the particles should be less than 2 μm and the operation conditions should be carefully and precisely controlled during TiO_2 deposition [31,33].

2.1.2.2 Rutile Modification

Mica substrate stabilizes the anatase crystal form of TiO_2 and minimizes the formation of rutile during TiO_2 deposition. This behavior is due to the migration of Al^{+3} ions out of muscovite mica into the anatase layer leading to the inhibition of phase transformation [29]. Tin (IV) chloride is generally used to form nucleating surfaces to facilitate the deposition of TiO_2 in rutile crystalline form. Tin (IV) chloride is the preferred tin compound for use, as it is easily soluble in water and forms clear and stable solutions with the addition of small amounts of a mineral acid**.** Usually, mica flake particles are pre-treated with a tin compound solution and thereafter coated with TiO_2 particles to promote rutile form after calcinations. However, it is possible to coat mica particles with titanium hydroxide without use of tin and then treat the coated amorphous product with an aqueous solution of a tin compund and obtain rutile form. Although such after treatment is effective it is less convenient [34]. Furthermore, to obtain TiO_2 layer in the desired rutile structure, a tin salt can be used in mica suspension, and is hydrolyzed together with the titanyl sulfate by homogeneous hydrolysis method [7].

Additives other than tin for forming rutile modification of TiO_2 on mica while maintaining all other desirable characteristics are not known [14]. Tin oxide deposition onto mica substrate orient TiO_2 to form rutile crystalline phase

and this process is carried out by heterogeneous nucleation in solution technique [12,14,34].

The mechanism by which the tin compound treatment of mica substrate facilitates the formation of rutile coatings is not fully understood. One possibility is that the amorphous hydrated tin compound which deposits on mica changes into cassiterite, the only crystal form of SnO_2. Since cassiterite is isomorphous with rutile, it promotes the crystallization of the TiO_2 to rutile form upon calcinations [34].

2.1.2.3 Methods of Synthesis

The preparation methods can be classified into several general techniques. The most common technique is certainly the heterogeneous nucleation in solution reactions. Other processes done are gas or aerosol techniques, where a gaseous precursor is adsorbed and reacted onto an existing particle. Last but not least important is the hetero-coagulation process when particles of one material is covered on the surface with smaller particles of a different composition. In other cases, which will not be discussed in further detail here, a compositional gradient may occur within particles due to different reaction rates of the two precursor materials which may be used to precipitate a mixed powder particle [31].

2.1.2.3.1 Hetero-coagulation

The basic principle behind this technique is that particles having different surface charges will attract each other and coagulate. If one particle is much smaller in size compared to the second material, this coagulation will essentially form a coating layer. Figure 2.3 shows the schematic principle of

that process [5,31]. The larger particles have a positive surface charge in this case and the negatively charged particles in B will adhere to the surface when the two solutions are mixed.

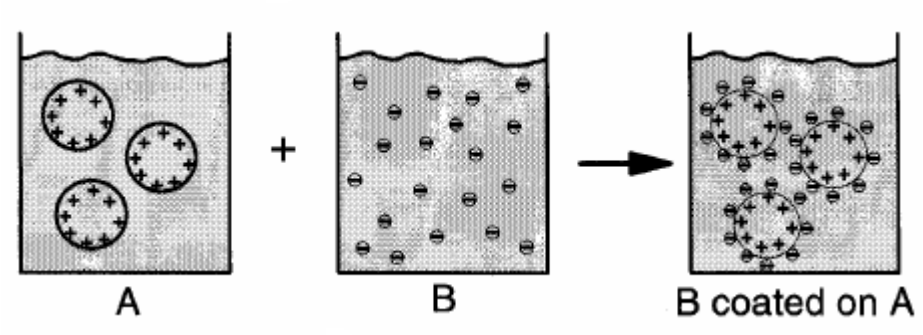

Figure 2.3. Schematic representation of coated powders by hetero-coagulation process.

The process is very simple and can be applied to a wide variety of materials without major problems. The disadvantage, however, is that the particle sizes have to be substantially different, it is not possible to form dense coatings by this process, the adhesion forces are usually weak and if no precautions are taken the coated particles can be washed off during processing steps. The essential part of this process is the adjustment of surface charges for A and B particles. This can be either done by properly adjusting the pH and using the natural surface charge of the two materials. The process can also be assisted by a prior surface modification process of one or both powders by a chemical reaction or by creating a temporary surface charge by adsorption of specific electrolytes [5]. Because of the aforementioned disadvantages associated with this method, very few studies have been done with this technique to obtain mica titania pigment.

Ren et. al synthesized rutile TiO_2 coated mica based on direct deposition of rutile TiO_2 nanoparticles on lamellar cericite by heterocoagulation method [33]. Firstly, by adding dropwise Na_2CO_3 aqueous solution into titanium tetrachloride solution which was diluted with 0.5 M HCl solution folllowed by nitric acid treatment were carried out for the preparation of rutile TiO_2 nanoparticles. Then, HCl treated lamellar cericite solution was added into the sonicated rutile TiO_2 aqueous suspension. The pH of the mixed suspension of cericite and rutile was adjusted to 2.2 and stirred in a water bath at 85°C for 3 h in order to deposit rutile TiO_2 nanoparticles on the surface of cericite. After rinsing with distilled water, dried and calcined at 400°C, rutile TiO_2 coated mica was obtained which was confirmed by XRD analysis. SEM images showed that TiO_2 particles anchored on the flat mica surfaces to form island-like structure which shows that TiO_2 particles were not well dispersed to coat mica particles homogeneously. Besides, brightness, whiteness and reflectance of the prepared TiO_2 coated mica were analyzed by using a spectrophotometer.

Çağlar et. al. prepared TiO_2 coated mica pigment by determining the optimum pH to coat mica surfaces by TiO_2 [31]. First, commercial TiO_2 was used to coat mica flakes at different pH values, namely, pH=0.8, 1.6, 2.4, 3.8 and 6.2. The best result was obtained at pH=2.4. At pH=0.8 and 6.2, it was observed that no coating of the titania was achieved on mica substrate because, the isoelectric point of mica and titania are close to each other at these pH values. In the case of pH values of 1.6 and 3.8, both uncoated mica flakes and agglomerated titania clusters onto the substrate were observed. In such a case, although both mica and TiO_2 were charged at these pH values, excess charges on one of them caused TiO_2 particles to form large cluster with the micas that met first. Therefore, they used a pH of 2.4. XRD results showed that TiO_2 particles formed were in rutile phase. SEM

analysis revealed that all TiO_2 particles were on mica particles and there were no free TiO_2 around. However, mica particles were not coated homogeneously, and there were some coagulates of TiO_2 particles or uncoated parts of the surfaces.

2.1.2.3.2 Heterogeneous nucleation in solution or in the gas phase

This coating technique is the most widely used and best controlled process. Each process has its unique synthesis condition, but it also allows for the best control of coating thickness and chemical composition within the coating layer. In principle it follows a LaMer type nucleation process.

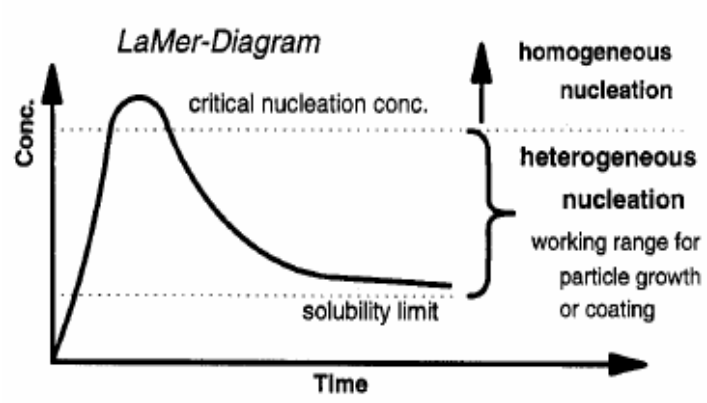

Figure 2.4. The LaMer-Diagram related to nucleation and growth mechanism and formation of coating layers.

However, it is important that the critical nucleation concentration is never exceeded. Thus, the system is forced to follow a heterogeneous nucleation and growth mechanism, schematically illustrated in Figure 2.4 [5,31].

The major disadvantage of this technique is the low particle concentration and long reaction times which are usually required. One can still achieve a sufficient coating at higher concentrations or at faster reaction rates, however, there are clearly compromises in the coating quality with respect to a uniform thickness and dense coating layers as well as the coating of individual particles instead of gluing together agglomerated structures [5,31].

In a very similar way the reaction can also be done in the gas phase ,similar to a chemical vapor deposition process. Instead of a solid substrate surface individual particles are suspended in a gas stream and the surface of those particles is coated. At low particle concentrations this can also lead to very uniform and controlled coating layers, whereas at higher particle concentrations, for example in a fluidized bed reactor, the particles come in contact with each other and agglomerated structures occur [5,31].

In heterogeneous nucleation technique two methods are used; homogeneous hydrolysis and titration method.

a) Homogeneous Hydrolysis

A measured amount of titanium sulfate is added to an aqueous mica suspension. By slowly heating the suspension the titanium salt is hydrolyzed to insoluble TiO_2 hydrate, which steadily deposits homogeneously on mica particles. After all titanium salt has been hydrolyzed, the coated particles are filtered off, dried, and finally calcined at 700 to 900°C in a kiln. At these high temperatures, water is eliminated and a thin compact coating of TiO_2 is formed on mica [6]. Equations 2.1 and 2.2 for the main reactions are as follows:

a) Coating

$TiOSO_4 + mica + nH_2O \longrightarrow TiO_2.(n-1)H_2O/mica + H_2SO_4$ (2.1)

b) Calcination

$TiO_2.(n-1)H_2O/mica \xrightarrow{-(n-1)H2O} TiO_2/mica$ (2.2)

Obtaining a homogeneous coating with this method is inconvenient because of the difficulty to control the rate of hydrolysis [6].

Deluca et. al. patented the synthesis of rutile coated mica by homogeneous hydrolysis method [34]. Firstly, mica flakes were treated with an acidic solution of a tin compound. The treatment was done both at room temperature and at 55°C by mixing mica with $SnCl_4.5H_2O$ solution. After filtering the solution, the wet cake was mixed with titanyl sulfate solution, containing 10% TiO_2 and 26% H_2SO_4 and refluxed until the suspension displayed the desired color. The same experiment was repeated without pretreatment of tin compound. XRD results indicated that tin chloride pretreated mica pigments showed rutile crystalline structure as expected while untreated pigments showed anatase form.

Bayat et. al. synthesized mica titania pigment by homogeneous hydrolysis method in which $TiCl_4$ was used as the precursor for TiO_2 [8]. Urea was used to conduct the reaction as it gradually decomposes upon heating and the difficulty in the control of the rate of hydrolysis was minimized by creating highly acidic environment (pH<2). XRD analysis showed an interesting result that grown phase on mica flakes was rutile. Besides, SEM analysis confirmed the uniformity of the coatings. The effect of solution concentration, temperature and time were studied.

Çağlar et. al. prepared TiO_2 coated mica by utilizing titanyl sulfate precursor [31]. During synthesis, 40% titanyl sulfate solution was added to mica suspension in water and stirred for 6 h at boiling temperature. After filtration, drying and calcination mica titania pigment was obtained. XRD analysis showed that there were both anatase and rutile peaks of titania. The coating of TiO_2 onto mica surface was seen by SEM analysis in the platelet form instead of coagulated particles with spherical morphology. Although perfect coatings with uniform thickness were seen on some mica substrates, some of the flakes were not properly coated.

b) Titration method

This method is easier to control than the hydrolysis method. An aqueous acidic $TiOCl_2$ solution is continuously added to a mica suspension at a pH of about 2 and temperatures in the range of 60 to 90°C. The precipitation of TiO_2 hydrate occurs at a fixed acidic pH level. The pH is held at a constant value by continuous addition of sodium hydroxide solution [6]. A highly simplified equation for this reaction is as follows:

$$TiOCl_2 + 2NaOH + \text{mica } nH_2O \longrightarrow TiO_2.(n+1)H_2O/\text{mica} + 2NaCl \qquad (2.3)$$

The further processing of pigment particles is identical to the homogeneous hydrolysis method [6].

Hildenbrand et al. investigated the crystallization of wet-chemically synthesized thin anatase coatings which was obtained by titration of $TiCl_4$ solution with a sodium hydroxide solution in an aqueous suspension of muscovite by X-ray line broadening (XRD) and transmission electron microscopy (TEM) [35]. They showed that TiO_2 films consisted of anatase

phase and the intrinsic macrostrains of unit cells of the anatase coatings. They proposed that crystallite size of thin anatase films is proportional to the height of coating layer and anisotropic crystallization growth starts at the interface between thin anatase films and muscovite substrate.

Song et. al. studied the deposition of TiO_2 on muscovite flakes and the effect of doping with different metal ions (Al^{3+}, Sn^{4+}, Fe^{3+}, Zn^{2+}, Mn^{2+}, Co^{2+} or Cu^{2+}) on anatase-rutile transformation [11]. XRD analysis revealed that Al^{3+}, Co^{2+}, or Cu^{2+} doped ions retarded the anatase-rutile transformation of TiO_2 while Sn^{4+}, Fe^{3+}, Zn^{2+}, Mn^{2+} doped ions promoted the anatase-rutile transformation. They claimed that the influence of doped metal ions on anatase-rutile transformation is influenced by the presence of the doped metal ions on top of titania layer. Thus, metal ions are exchanged with Ti^{4+} and promote either anatase or rutile crystalline formation depending on the type of the ion. Furthermore, SEM analysis showed that euhedral pillared rutile grains were found in the samples doped with Fe^{3+}, Zn^{2+}, Mn^{2+} ions and uniform circular grains were seen in the samples doped with Al^{3+}, Sn^{4+}, Co^{2+}, or Cu^{2+} ions.

Ryu et. al. prepared titania-substrate pearlescent pigments by the hydrolysis of $TiOCl_2$ on natural mica (muscovite), synthetic mica (fluorophlogopite) and α-alumina substrate followed by a calcination process [13]. They were selected as the substrates for pearlescent pigments. It was found that TiO_2 layer deposited on α-alumina has higher rutile fraction than those on the natural and synthetic mica. Also the XPS analysis showed that the cations originally present in the substrates diffused into TiO_2 layer and retarded the anatase rutile phase transformation of TiO_2. The TiO_2 layer deposited on α-alumina contains Al^{3+}, while those on the natural and synthetic mica substrates contain Si^{2+} and K^{+} in addition to Al^{3+} cations. The suppressing

effect on anatase rutile transformation by mixed cations seems to be much stronger than that of a single cation.

2.2 Phthalocyanines

2.2.1 Types and Properties

Phthalocyanine is a planar 18 π-electron heterocyclic aromatic system with alternating nitrogen-carbon atom ring structure derived from porphyrin [19]. Since their accidental discovery in 1907 and subsequent structure identification, phthalocyanines have been one of the most studied classes of organic materials [36]. They have attracted notable interest and have been found to be significant candidates for a variety of uses such as liquid crystals, photosensitizers, non-linear optics, solar cells, catalysis, and in various chemical sensing applications [22]. Besides, traditionally they have been used as dyes and pigments due to their characteristic blue-green color [25]. They are attractive dyes because of intense π–π* absorption in the visible region of the spectrum, which gives blue-green color. They are chemically strong and photochemically stable and show high resistance to chemical and photochemical degradation due to nitrogens located within the aromatic macrocycle and the peripherally fused benzene rings. Other properties that make phthalocyanines attractive include, absorption and emission in the deep red region of the electromagnetic spectrum and a wide range of accessible chemical structures allowing the design of compounds capable of meeting certain needs [22].

The difficulties in the preparation of these dyes consist of their limited solubility in aqueous media, formation of mixed isomers of some phthalocyanines during synthesis, and difficulties in purifications of some

kind of these dyes which cannot be purified even with standard chromatographic methods [22]. Moreover, owing to their extended planar hydrophobic aromatic surface, phthalocyanine molecules can interact with each other by attractive π-π stacking interactions leading aggregation both in solution and in the solid state [37]. One of the principal strategies to eliminating these disadvantages and to control their properties involves ring substitution on the peripheral and non-peripheral positions of the phthalocyanine ring [38]. The other way is to introduce a different kind of metal to the central cavity. Phthalocyanines can coordinate a variety of main group metals as well as numerous transition metals in their central core [19, 22]. Among them copper phthalociyanine is a blue semiconductor organic material due to its superior properties such as light fastness, tinting strength, covering power, and resistance to alkalies and acids [39]. This pigment is insoluble in water and in most solvents and has no tendency to migrate in the material. The outstanding chemical and physical stabilities of copper phthalocyanine blue permit their use in most applications for blue organic pigments as well as in some nonpigmentary areas. It is widely used as a color pigment in printing ink and packaging industry.

Peripheral or nonperipheral ring substitution also improves many properties of the molecule such as enhancing the solubility and changing the spectral properties of the macromolecule [15, 38]. Long alkyl, alkyloxy, alkylsulfanyl or bulky apolar groups lead to soluble products in common organic solvents while anionic or cationic substituents (e.g. sulfo groups, carboxylic acids, ammonium groups) result in products soluble in aqueous media [21].

2.2.2 Synthesis Methods

Synthesis of phthalocyanines can be achieved using different routes depending on the type of phthalocyanines to be synthesized, whether it is metal free, symmetrical, or asymmetrical. Among them, metallophthalocyanines can be synthesized by using various precursors such as phthalonitrile, phthalic acid, phthalic anhydride, and phthalimide. Also a metal free phthalocyanine can be metallated by heating in the presence of a metal or metal salt (Figure 2.5) [24].

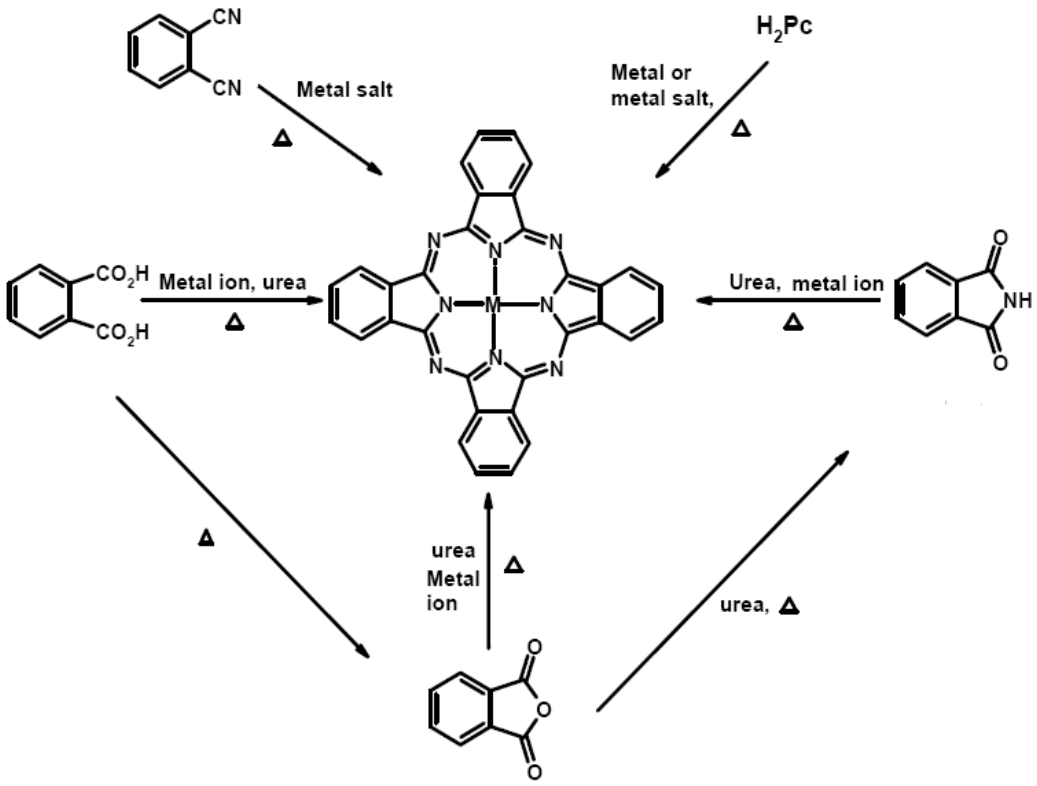

Figure 2.5. Synthesis of metallated phthalocyanine from some precursors [24].

In terms of choice of precursors for phthalocyanines synthesis, the use of phthalonitrile provides a mild and clean process with high yields of very pure metallophthalocyanines suitable for research purposes while the use of phthalic anhydride is relatively a cheap method but the metallophthalocyanines obtained are usually not as pure as the former. Synthesis by using phthalic anhydride also requires the presence of nitrogen source such as urea. Basically, the reactions involve cyclotetramerization of the precursor by heating it at high temperature with a suitable metal or metal salt in the presence of a catalyst and a solvent [23-24].

The most effective catalyst used in the preparation of the phthalocyanines is ammonium molybdate and the synthesis can be carried out in the presence of high boiling solvents like nitrobenzene, trichlorobenzene dimethyl formamide (DMF), dimethyl sulphoxide (DMSO) or quinoline [24]. Metal phthalocyanine syntheses have been mostly carried out in a solvent medium for years. However, in recent years researchers have a great attention for the synthesis of metal phthalocyanines quickly and very efficiently without solvent under microwave irradiation [40].

The traditional synthesis of phthalocyanine, no matter what starting material is used, required a quite long reaction time and a particularly high energy input. Because, it needs sufficient kinetic energy to overcome the reaction kinetic barrier and promote the collision probability and energy of molecules, which results in low efficiency. Microwave heating is different from conventional heating method mostly in its mode of energy delivery. Traditional heating method delivers heat energy by conducting through a container containing the solution, and homogeneously distributes the heat to the solution and hence raising the temperature. On the other hand, microwave heating delivers heat by radiation, and therefore, can heat

reactants directly and accordingly promoting its efficiency [41]. Also solvent is not used in microwave process which simplifies the purification steps. However it is not a dry reaction because water needs to be added at the beginning of the reaction to absorb microwave radiation. Water allows also the diffusion of metallic salt and plays a role in the redox process of formation of phthalocyanine. The melted phase allows also the diffusion of the necessary salt for the course of reaction, and thus, precursor can be used in excess [40]. One of the important reason to prefer microwave method is that microwave-promoted reactions are well known as environmentally benign methods that does not require high boiling solvents [26].

Villemin et. al. obtained metallophthalocyanine complexes very quickly and efficiently by the reaction of phthalodinitrile with hydrated metallic salts without solvent under microwave irradiation [40]. Metallophthalocyanines and metallododecachlorophthalocyanines of some divalent metals was also obtained in the presence of phthalic or tetrachlorophthalic anhydrides with hydrated metallic salt and urea under microwave irradiation and without solvent. When phthalodinitrile was used as precursor, it was finely ground with hydrated metallic salt and ammonium formate was added as catalyst. Water was added to the mixture and the mixture was irradiated for five minutes (at a power of 480 W). It was purified by water, acetone, and dichloromethane and extracted by soxhlet extraction with acetonitrile solvent. After drying at 110°C, the pure phthalocyanine was analyzed. By using phthalic or tetrachlorophthalic anhydride as a precursor, the method involves grounding urea with one of these precursors in a mortar in the presence of ammonium molybdate by subsequent addition of metallic salt . The mixture was irradiated under microwave radiation. The final product was washed with HCl, neutralized with soda and washed with water. The solid

dried at 110°C was purified by soxhlet extraction with acetonitrile as solvent for eight hours. The phthalocyanine obtained was identified with FT-IR and UV-Vis spectroscopic analysis.

Jung et. al. synthesized copper phthalocyanine by the reaction of phthalic anhydride, urea, and copper (I) chloride at various temperatures and times under conventional and microwave processes [42]. It was observed that microwave irradiation leads to acceleration of crystallization of copper phthalocyanine. Particle size analysis showed that the samples synthesized under the microwave process had small average size and narrow size distribution, which helped the pigments to be dispersed more stably in aqueous medium. SEM pictures indicated that all of the samples synthesized under both processes were well crystallized with acicular shape. The size of crystals was more uniform under the microwave process.

Exsted et. al. synthesized tetraamide nickel phthalocyanine to obtain tetracarboxy nickel phthalocyanine upon saponification for incorporation into melamine-based polyester resins [43]. Tetraamide nickel phthaloyanine was synthesized by mixing and heating trimellitic anhydride; nickel sulfate hexahydrate; urea; ammonium molybdate; ammonium chloride for 4 hours in nitrobenzene. Excess metal salts were removed after boiling the crude product for 12 h in hydrochloric acid, saturated with sodium chloride. Solvent removal brought in extra purification steps that the product was pulverized with a mortar and pestle into a fine powder and repeatedly Buchner-filtered with acetone.

Özil et. al. prepared the monomeric phthalocyanines with four naphthalene amide substituents by conventional and microwave methods [36]. In both methods cyclotetramerization of phthalonitrile derivatives containing

naphthalene-amide group was carried out by mixing and heating it with anhydrous CuCl and N,N-dimethylaminoethanol. However, in microwave method, little amounts of solvent was used to start the reaction while conventional method requires much more solvent to conduct the reaction. Besides, the yield in microwave method was found to be more than the conventional method and the reaction time was reduced from 24 hour to 8 minutes.

2.2.3 Polymorphic Forms of Phthalocyanines

Copper phthalocyanine (CuPc) has alternate single and double bond structure existing in alpha (α), beta (β), gamma (γ), and chi (χ) -polymorphic forms [44]. Polymorphism of phthalocyanine crystals has been the subject of a large number of studies and the most commonly studied forms are α and β polymorphs [45-46].

It is reported that the metastable α polymorph undergoes a polymorphic transition to the stable β polymorph when heated over 250°C or treated with some aromatic hydrocarbons, like xylene [44, 47-48]. It was found that the transformation was not a simple process, but the metastable powder grew to a considerable extent without changing its crystal structure before the actual transformation took place [49]. The resulting β polymorph is comparatively in a larger crystalline form. β polymorph is transformed to α phase when mechanically ground [45, 48].

The α form of copper phthalocyanine tends to grow large crystals and transform to β phase when incorporated into paints because many organic liquids which have a solvent action on the α form of copper phthalocyanine are commonly used as thinners or diluents in surface coating compositions

[50-51]. Large crystals change the shade and the tinctional strength of the paint in a storage period between the preparation of the composition and its final use [50-51]. For these reasons, β form is preffered in industrial use [51]. In this study unsubstituted and tetracarboxamide copper phthalocyanine were synthesized and phase transformation of the molecules on mica titania pigment at different temperatures were investigated.

2.3 Mica Based Combination Pigments

Absorption pigments, such as phthalocyanines, quinacridones, perylenes, dioxazines and carbon black organic colorants possess very high surface area energy and therefore are present in an unstable state and tend to cohere to coarser pigment particles in paint formulations or in some other applications [28]. To prevent this, the cohering coarse pigment particles are generally mechanically crushed into smaller particles or high shear mixing or ultrasonic dispersion is done [28,30]. The surface of crushed pigment particles can also be chemically treated to enable the individual particles to stay in a stably dispersed state. However, when it is stored for a long time the pigment particles can agglomerate again adversely effecting its color [28].

Combination pigments can be produced by the deposition of absorption pigments on the surface of a flaky substrate coated with a metal oxide whereby pigment particles adhere quickly in a state free from cohesion producing combination pigments which exhibit satisfactory spreading properties, high color effect and good color saturation [28]. So the tendency of absorption pigment particles to flocculate is eliminated or greatly reduced when the particles are bound to the mica surfaces. Also absorption pigments have high color intensity, light fastness and bleed resistance properties which

make the resulting combination pigments suitable for automobile finishes and other paint applications [30].

Pearlescent pigments of titania coated on mica are of particular interest because the color is derived entirely from the interference effect. They make possible combination pigments with the widest range of colors. Hence, any desired reflection color is obtainable by controlling the thickness of the oxide coating and absorption pigments of any desired color available for overcoating. In the case of colored oxides coated mica, the final color of combination pigments will be determined by both colored oxides and absorption colorants [30].

Noguchi patented the synthesis of colored flaky pigments by adhering a finely divided color pigment (Ultramarine blue, iron blue, phthalocyanine blue, etc.) onto a flaky substrate (mica, talk, mica titania) [28]. To adhere the color pigment to the flaky substrate high molecular organic compounds (polyvinyl alcohol, polyvinyl pyrrolidone) was used because of their sufficient binding properties to adhere the color pigment onto the flaky substrate without effecting its color properties. One of the method involves mixing the ultramarine blue with polyethylene glycol in water and alcohol solution and dispersing with the aid of sand mill. The mica titania pigment was also suspended in water and polyethylene glycol mixture and dispersed pigment solution is added dropwise to obtain the desired combination pigment with new color effects

Armanini et. al. patented the coating dispersed insoluable colored pigments (phthalocyanine blue, carbon black, quinacridone red) on the surface of mica and oxide coated mica pigments by deposition in a precipitate of a polyvalent cation (Al, Cr) and anionic polymeric substance (albumin, xanthan gum) [30].

Anionic polymeric substance is used to prevent the agglomeration of absorption pigment. Also polyvalent cations were used to help the precipitation of the dye on substrate surface. One of the methods comprises dispersing the colorant and xanthan gum in water by ultrasonic homogenizer. Mica pigment was also suspended in water and mixed with this dispersion. Then the solution pH was adjusted in a range suitable for the precipitation of the polyvalent cation which was aluminum hydroxide. Aluminum chloride was added drop wise while the pH was held constant with the addition of sodium hydroxide. The desired combination pigments were obtained with brilliant color properties.

2.4 Deposition of Copper Phthalocyanine on Different Substrates

The substrates such as glass, quartz, or silica were generally used for deposition of copper phthalocyanine. For a thin coating, copper phthalocyanines were vacuum deposited on substrates and the effects of substrate materials and annealing temperature on film morphology and crystalline structure were investigated [47].

Lee et. al. deposited unsubstituted and tetra-tert-butyl copper phthalocyanine onto glass and gold substrate by vacuum deposition technique [52]. The effect of annealing and different substrates to the phase transformations of copper phthalocyanines was investigated by XRD analysis. Also the effect of substrate on the morphology of copper phthalocyanine films was observed by SEM analysis. It was found that varying substrates leads to different morphologies depending on the interaction between substrate and copper phthalocyanines. Besides, crystalline phases of phthalocyanines change with differing annealing temperature and substrates. Unsubstituted copper phthalocyanine displays β form crystalline structure on

glass substrate, but an amorphous structure formed on gold due to higher nucleation rate of CuPc molecules on gold surface. Heat treatment gives no change in crystalline form on glass substrate while on gold substrate a diffraction peak at $2\theta=7.03$ was observed. Tetra-tert-butyl copper phthalocyanine shows amorphous structure on both glass and gold. After heat treatment, a diffraction peak at $2\theta=5.51$ appears both on glass and gold. This increase in the interplanar spacing in the substituted one should be due to distortion of the orientation of molecules by side groups.

CHAPTER 3

EXPERIMENTAL

In this chapter, the preparation methods of rutile titania deposited mica pigments and copper phthalocyanine pigments are described in detail. The procedure for the combination of these pigments is also explained. The characterization of all pigments, (i) titania deposited pigments, (ii) copper phthalocyanine pigments, and (iii) combination pigments are described. In addition, the properties of paints made by using combination pigments are presented.

3.1 Materials

3.1.1 Muscovite Mica

Muscovite mica is a phyllosilicate mineral of aluminium and potassium with a structural formula of $KAl_2(AlSi_3O_{10})(F,OH)_2$. The mineral ground by a jetmill was supplied by Sabuncular Mining Co. The particle size distribution analysis tests were performed, and the d_{50} of the mica was found to be 53 μm. It was used as a flaky substrate to synthesize mica titania pigment.

3.1.2 Titanium Tetrachloride

$TiCl_4$ is a colorless fuming inorganic compound. It was purchased from Merck, KgaA, Germany and used as a precursor for TiO_2.

3.1.3 Stanic Chloride Pentahydrate

$SnCl_4.5H_2O$ is a white colored solid soluble in water. It was purchased from Sigma-Aldrich, Germany and used as a rutile promoting agent in mica titania pigments.

3.1.4 Phthalic Anhydride

Phthalic anhydride is a white or pale yellow organic compound. It was purchased from Sigma-Aldrich, Germany and utilized as a precursor to synthesize copper phthalocyanine pigment. Its structural formula is given in Figure 3.1.

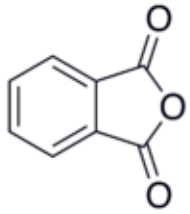

Figure 3.1 Structural formula of phthalic anhydride.

3.1.5 Trimellitic Anhydride

Trimellitic anhydride is a white organic compound. It was purchased from Sigma-Aldrich, Germany, and used as a precursor for the preparation of the tetracarboxamide substituted copper phthalocyanine pigment. Its structural formula is given in Figure 3.2.

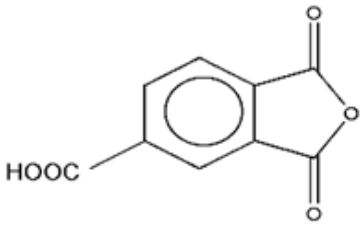

Figure 3.2 Structural formula of trimellitic anhydride.

3.1.6 Ammonium Heptamolybdate

Ammonium heptamolybdate is an odorless crystalline compound with a formula of $(NH_4)_6Mo_7O_{24}{\cdot}4H_2O$. It was purchased from Merck, KgaA, Germany, and used to catalyze the phthalocyanine synthesis reaction.

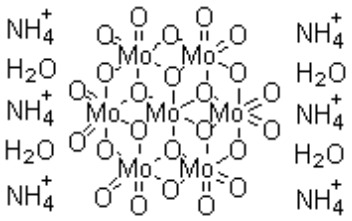

Figure 3.3 Structural formula of ammonium heptamolybdate.

3.1.7 Urea

Urea ($(NH_2)_2CO$) is a white crystalline organic compound. It was purchased from Merck, KgaA, Germany, and used as a nitrogen donor in the preparation of copper phthalocyanines. Its structural formula is given in Figure 3.4.

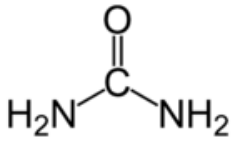

Figure 3.4 Structural formula of urea.

3.1.8 Copper (II) Chloride

Copper (II) chloride ($CuCl_2$) is yellow-brown solid. It was purchased from Merck, KgaA, Germany, and used as a copper source for the synthesis of copper phthalocyanines.

3.1.9 Dimethyl formamide (DMF)

Dimethyl formamide is a polar organic solvent with a chemical formula of $(CH_3)_2NC(O)H$. It was purchased from Merck, KgaA, Germany. It was used as a solvent in the production of combination pigments. Its structural formula is given in Figure 3.5.

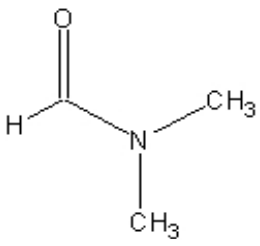

Figure 3.5 Structural formula of dimethyl formamide.

3.1.10 Other chemicals

Long oil alkyd resin was used for paint preparation. White spirit was used as a solvent; cobalt and lead naphthenates were used as drying agents.

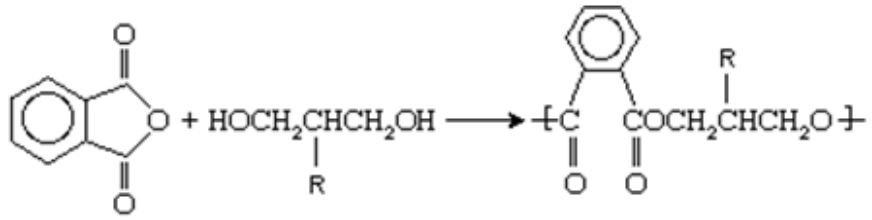

Phthalic anhydride Monoglyceride Alkyd resin

Figure 3.6 The molecular structure of an alkyd resin.

3.2 Synthesis of materials

3.2.1 Mica Pre-treatment

Mica was sieved through 270 mesh sieve to obtain particles with a size less than 53 μm. The thickness of mica platelets was reduced by sodium bicarbonate treatment and the surface characteristics of the mineral were improved by decantation procedure.

In sodium bicarbonate procedure, mica is heated to 800 ^{o}C and damped into saturated sodium bicarbonate solution as quickly as possible. After quenching, the solution was stirred with a mechanical stirrer, and 5% HCl solution was added to provide carbon dioxide evolution. The mixture was

stirred for an hour with a mechanical stirrer. Then it was washed and filtered to remove the excess salts [53].

The particles smaller than 10 μm were removed by decantation process. Decantation was carried out by calculating the time required to move a particle down through a quiescent viscous liquid at a specific distance according to the Stoke's law. First, settling velocity was calculated with the equation 3.1 given below and by specifying the distance, time was found.

$$V_s = (2/9).(\rho_p - \rho_f).g.R^2/\mu \quad (3.1)$$

V_s, ρ_p, ρ_f, R, μ, and g represent settling velocity, density of the particle, density of the fluid, radius of the particle, viscosity of the medium, and gravitational acceleration, respectively.

In the decantation procedure, first, mica particles were suspended in distilled water in a beaker. The settling distance was chosen as 3 cm and the time required to fall through this distance was found to be 5 minutes. The required distance was measured from the top of the liquid. The suspension was stirred with a glass stick and waited for 5 minutes to travel of particles larger than 10 μm with a distance of 3 cm. After 5 minutes, the supernatant liquid above 3 cm distance was removed by using a hose. The process was repeated until the supernatant liquid above 3 cm distance was clear. After decantation was finished, the mica particles were dried in an oven.

3.2.2 Preparation of Mica-titania Pigment

3.2.2.1 Sol Preparation

Dilution of $TiCl_4$ is very difficult, because concentrated $TiCl_4$ gives a sudden reaction with water at room temperature and undesired $Ti(OH)_4$ phase forms. In order to prevent this, the necessary amount of $TiCl_4$ was added dropwise into the HCl solution at 5°C to obtain 0.1 M solution of $TiOCl_2$.

3.2.2.2 Synthesis of Mica-titania Pigment

First of all, preliminary experiments were conducted with raw mica and the procedure described below was followed to synthesize mica titania pigment. Then pre-treated mica was used for the preparation of the pigment.

The synthesis of TiO_2 coated mica was carried out in the following way: 3 g pre-treated mica was suspended in distilled water and was heated to 75°C . The pH value of solution was adjusted to 2.0 with 5% (by weight) hydrochloric acid. Next, 50 ml 0.1 M of $TiOCl_2$ solution was introduced to the agitated slurry at a rate of 0.8 ml min^{-1}. The pH value of the slurry was kept constant by simultaneous addition of 1 M sodium hydroxide solution. After the addition was completed, the slurry was aged for 10 minutes. The slurry was then allowed to settle and cool to room temperature. The particles were separated, washed with distilled water, and dried for 24 h at 60°C. The final product was calcined at 800°C for 2 hours [54].

In order to obtain rutile phase of TiO_2 on mica substrate, SnO_2 was coated before TiO_2 coating. First, 0.05 M $SnCl_4$ solution was prepared by dissolving necessary amount of $SnCl_4.5H_2O$ in HCl solution. Then 3 g mica was

suspended in distilled water and heated to 75°C. The pH of the solution was adjusted to a value of 1.8, and 1 ml 0.05 M of $SnCl_4$ solution was added dropwise while pH was held constant with simultaneous additon of NaOH. After aging the slurry for 10 minutes, the TiO_2 synthesis procedure was applied as described above. The same procedure was applied by using 2ml, 3ml, and 4ml 0.05 M of $SnCl_4$ solution.

Figure 3.6 shows the experimental steps carried out for the preparation of mica titania pigments.

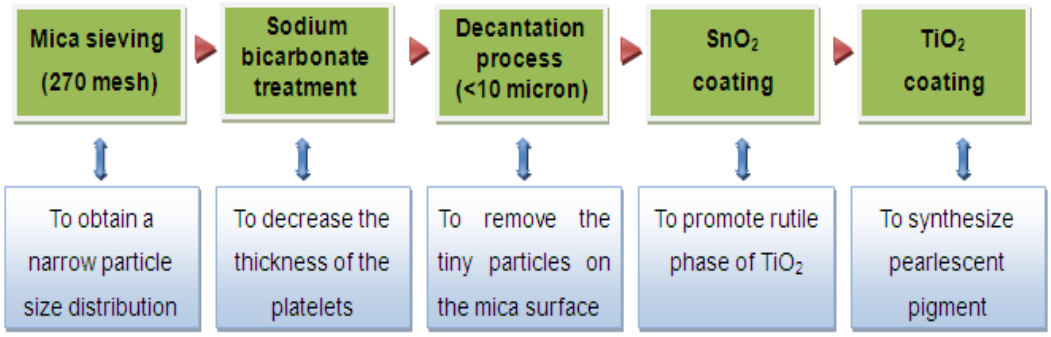

Figure 3.7 The synthesis route of mica titania pigment.

3.2.3 Synthesis of Copper Phthalocyanine Pigments

3.2.3.1 Synthesis of Unsubstituted Copper Phthalocyanine (CP)

Urea (92 mmol), phthalic anhydride (18 mmol), Copper (II) chloride (5mmol), and ammonium molybdate (59.6 mmol) were ground for 30 minutes by an agate mortar. The mixture was put into a flask and wetted

with 5 ml distilled water, and then heated in a microwave oven (600 W). The crude product was purified by washing in sequence with hot water (70°C), 6 M HCl, 1 M NaOH and with hot water again followed by filtration. After these steps, the pigment was washed with ethanol and filtered until the filtrate was colorless. The resulting pigment was dried in an oven at 100°C. Figure 3.7 shows the synthesis route of unsubstituted copper phthalocyanine.

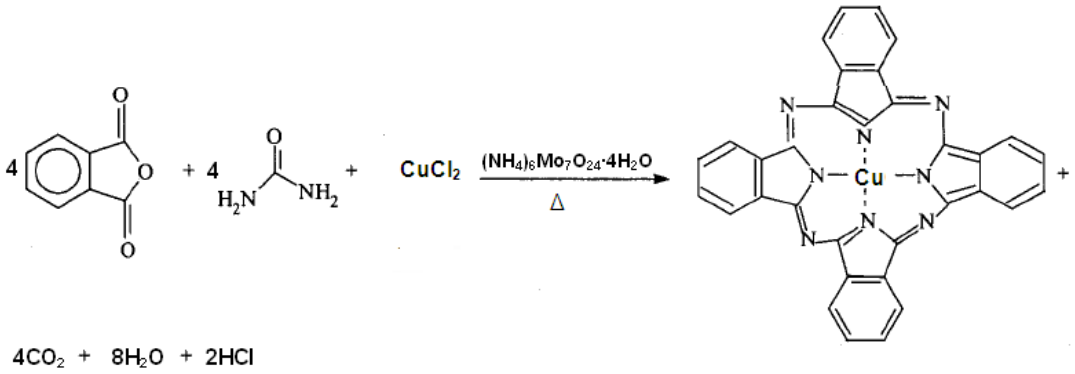

Figure 3.8 Synthesis of unsubstituted copper phthalocyanine.

3.2.3.2 Synthesis of Tetracarboxamide Copper Phthalocyanine (TCP)

Urea (92 mmol), trimellitic anhydride (18 mmol), Copper (II) chloride (5 mmol), and ammonium molybdate (59.6 mmol) were powdered for 30 minutes by an agate mortar. The mixture was put into a flask and wetted with 5 ml distilled water; then it was heated in a microwave oven (600 W). The crude product was purified by hot water (70°C), and then by 6 M HCl. It was washed with hot water again and filtered. Afterwards, it was washed with ethanol and filtered until the filtrate was colorless. The resulting

pigment was dried in an oven at 100°C. Figure 3.8 shows the synthesis route of tetracarboxamide copper phthalocyanine.

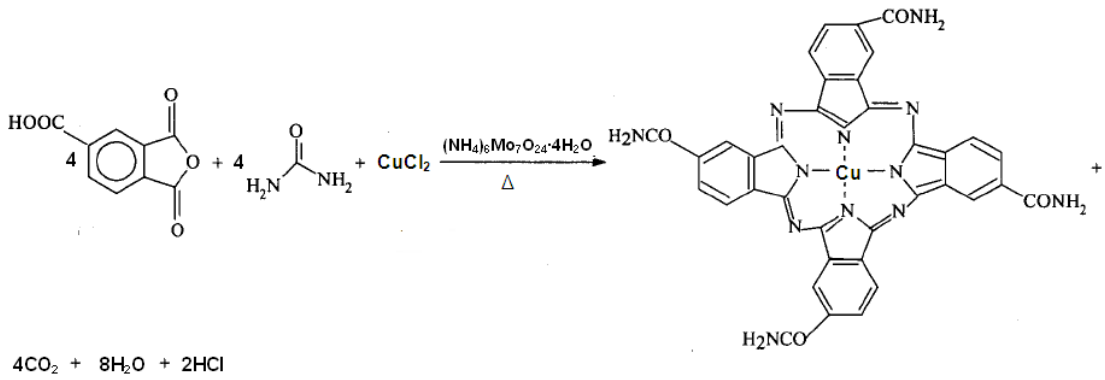

Figure 3.9 Synthesis of tetracarboxamide copper phthalocyanine.

3.2.4 Synthesis of Combination Pigments

3.2.4.1 Synthesis of Copper Phthalocyanine Deposited Mica Titania Pigment (CPM)

The preparation of combination pigment was carried out by mixing copper phthalocyanine with mica-titania pigment in DMF solvent. For this purpose, titania coated mica particles with the highest rutile content were selected. First, unsubstituted copper phthalocyanine was dissolved in 10 ml DMF. While mixing the solution, 0.3 g mica-titania pigment was added and stirred for an hour. The suspension was then filtered and washed with DMF. In order to get rid of free phthalocyanine particles, wet cake was suspended in DMF and kept for a while to settle down CPM particles while the supernatant liquid containing free phthalocyanine particles was removed from the solution. This process was repeated until the supernatant liquid was colorless. The wet cake was filtered and dried at 90°C in an oven. Different

amounts of phthalocyanine were deposited on the mica pigment surfaces synthesized at different temperatures which were given in Table 3.1.

Table 3.1 Description of CPM pigments prepared at different temperature.

Sample	Description
CPM005	CPM pigment with 0.005g CP used (25°C, 60°C, 90°C)
CPM010	CPM pigment with 0.01g CP used (25°C, 60°C, 90°C)
CPM020	CPM pigment with 0.02g CP used (25°C, 60°C, 90°C)
CPM040	CPM pigment with 0.04g CP used (25°C, 60°C, 90°C, 120°C)

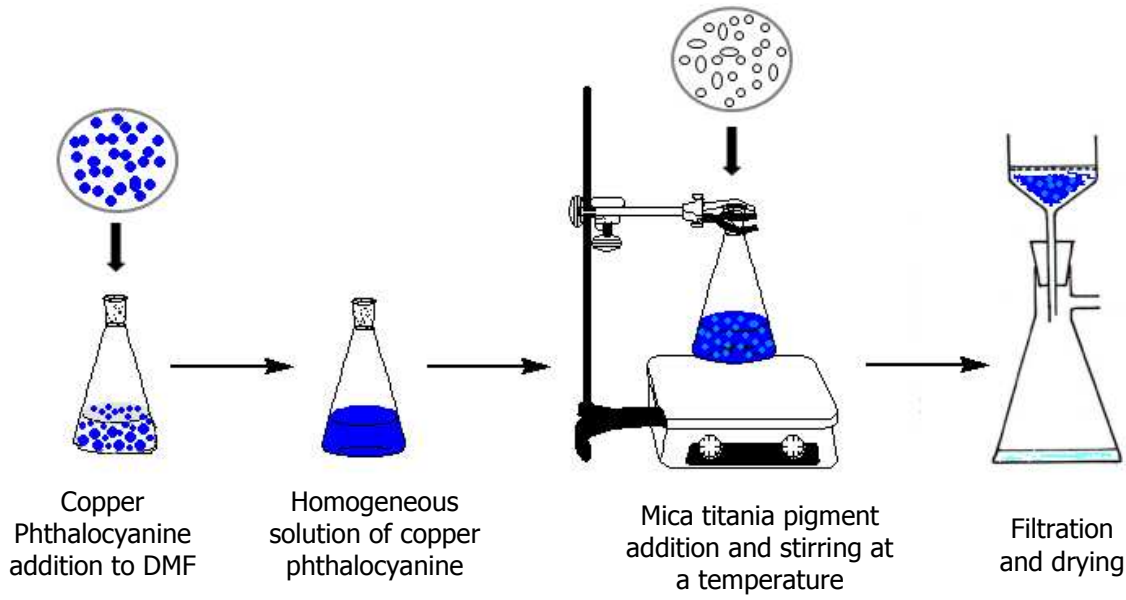

Figure 3.10 The method of synthesis of combination pigment.

3.2.4.2 Synthesis of Tetracarboxamide Copper Phthalocyanine Deposited Mica Titania Pigment (TCPM)

A similar procedure to the one explained above was applied except TCP was used instead of CP for the deposition. The amount of TCP used and the reaction temperatures were given in Table 3.2. Also, sample pictures of synthesized combination pigments are shown in Figure 3.10.

Table 3.2 Description of TCPM pigments that prepared at different temperatures.

Sample	Description
TCPM0065	TCPM pigment with 0.0065g TCP used (25°C, 60°C, 90°C)
TCPM013	TCPM pigment with 0.013g TCP used (25°C, 60°C, 90°C)
TCPM026	TCPM pigment with 0.026g TCP used (25°C, 60°C, 90°C)
TCPM052	TCPM pigment with 0.052g TCP used (25°C, 60°C, 90°C, 120°C)

Figure 3.11 Pictures of combination pigments; left one is CPM pigment and right one is TCPM pigment.

3.2.5 Preparation of a Alkyd Based Paint Formulations

Mica phthalocyanine pigments which were obtained at 90°C were used to prepare alkyd paint. The recipe used for the synthesis of the paints is given in Table 3.3. White spirit was used as solvent while cobalt and lead naphthenate were used as surface and inner drying agent, respectively.

The principle materials involved in the preparation of alkyd resins are polyhydric alcohols (polyols) and dibasic acid (or corresponding anhydrides) together with the modifying oils (or corresponding acids).

Table 3.3 Alkyd paint formulation.

Formulation	% (w/w)
Long oil alkyd resin (60%)	89.52
White spirit	7.96
Cobalt naphtanate	0.31
Lead naphthenate	0.24
Mica phthalocyanine pigment	2.00

Long oil alkyd resin (18 ml), white spirit (1.6 ml), cobalt naphthenate (0.06 ml), lead naphthenate (0.05 ml), and mica phthalocyanine pigment (0.4 g) were mixed by a magnetic stirrer for 15 minutes. When homogeneous distribution was achieved it was poured onto glass plates spread on by paint applicator at a film thickness of 50 µm, and left to dry at room temperature.

Generally, the paint synthesis was carried out in a paint production unit and mixing was carried out by a mechanical stirrer in the presence of zirconia beads. However, copper phthalocyanine and TiO_2 particles can leave out mica surfaces in this harsh grinding process. So, in order to avoid pigment damage, simple agitation was performed by a magnetic stirrer, and homogeneous distribution of the particles was successfully obtained. The pigments used in paint are copper phthalocyanine deposited mica-titania pigments that were synthesized at 90°C by using 0.005 g, 0.01 g, 0.02 g or 0.04 g copper phthalocyanine, and tetracarboxamide copper phthalocyanine deposited mica-titania pigments that were synthesized at 90°C by using 0.0065 g, 0.013 g, 0.026 g, or 0.052 g tetracarboxamide copper phthalocyanine.

3.3 Characterization

Crude mica, pre-treated mica, TiO_2 coated mica, copper phthalocyanine deposited mica-titania pigments were characterized by SEM (Model no: Quanta 400F Field Emission) in Central Laboratory, METU, to observe their morphology. BET analysis was performed for the raw and pre-treated micas to see the change in the specific surface area of the samples after cleaving. Particle size analysis (PSA) was carried out for crude mica and decantated mica to determine the effect of decantation on the particle size distribution (Sympatec PM-Tour 2000). Copper phthalocyanine pigments were analyzed by FT-IR spectroscopy (IR Prestige-21 SHIMADZU). Also mica-titania pigment and combination pigments were characterized by this analysis. UV-visible spectroscopy analysis was done for copper phthalocyanine and tetracarboxamide copper phthalocyanine to determine their characteristic absorbance values (Perkin Elmer Lambda 35). The crystal structure of TiO_2 on mica surfaces was determined by XRD analysis (Model no: RIGAKU-

D/Max-2200/PC) in Metallurgical and Materials Engineering, METU. Also the crystal form of copper phthalocyanines and combination pigments were found by XRD, and their phase were investigated. The nitrogen analysis was performed for the combination pigments by elemental analysis device (LECO, CHNS-932) in Central Laboratory, METU to determine the amount of copper phthalocyanine deposited on mica surfaces.

Apart from these characterizations, in order to determine the paint properties, gloss of the paint samples were measured by glossmeter at different angles 25°, 60°, and 85° (Rhopoint, Novo-Gloss). Hardness of samples were determined by Persoz Pendulum Hardness Tester (Braive Instruments Hardness Tester, Model 3034). This method evaluates hardness by measuring the damping time of an oscillating pendulum. The colors of the paints were determined by a color measuring device (Datacolor 400^{TM}).

CHAPTER 4

RESULTS AND DISCUSSION

4.1 Preliminary studies

In the first set of experiments, raw mica which was not sieved, decantated, or cleaved was used to synthesize mica titania pigment. Mica which has a 53 μm d_{50} value and 100 μm d_{98} value was coated with TiO_2 according to the procedure described in the experimental section except 2 M NaOH was used for the hydrolysis.

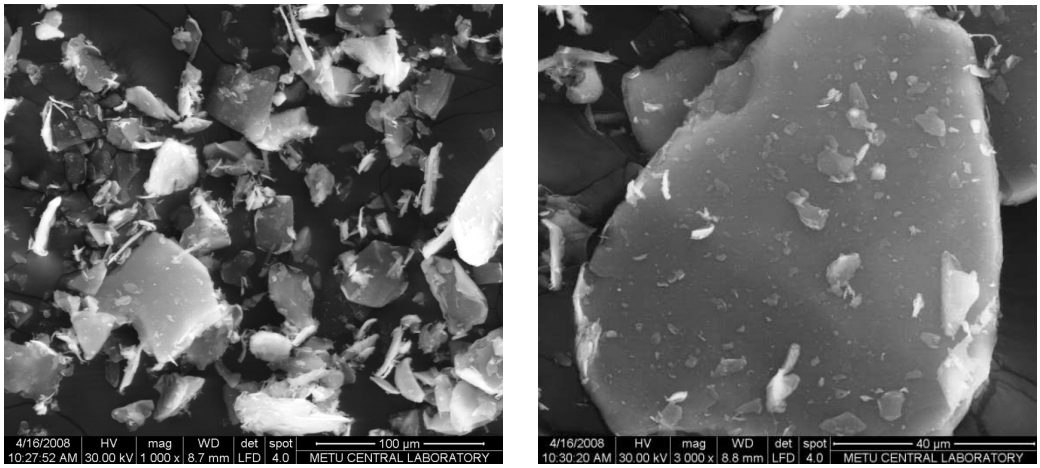

(a)

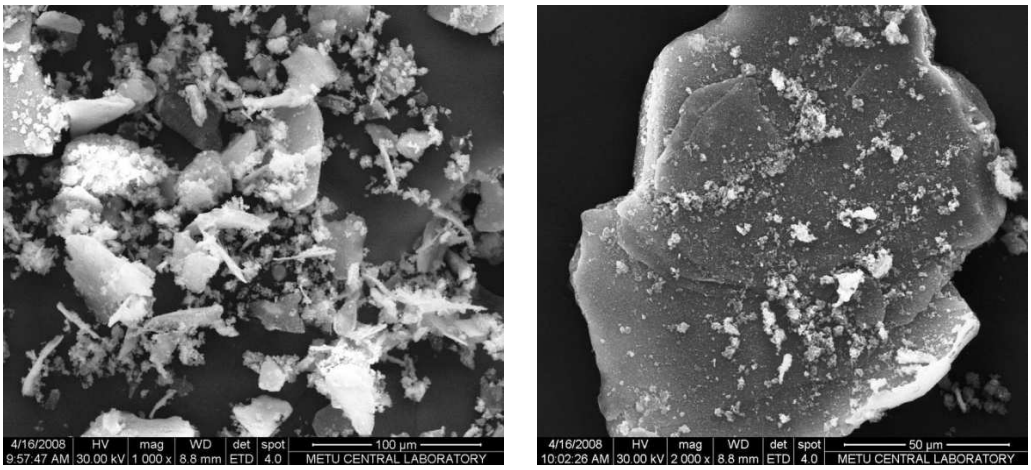

(b)

Figure 4.1 SEM micrographs of (a) untreated mica, (b) TiO_2 coated mica.

Figure 4.1 shows the SEM micrographs of crude mica and TiO_2 coated micas. In Figure 4.1 (a), the tiny particles were seen on mica surfaces which can scatter light and decrease the gloss and the pearlescent effect of the resulting pigment. Also the thickness of the mica particles was high and this should also decrease the interference effect of the resulting pigment. In Figure 4.1 (b), TiO_2 is seen to precipitate not only on the mica substrate but also freely existed in the medium. This is because $TiOCl_2$ was introduced through a burette to the solution and pH could not be carefully controlled due to unsteady rate of addition, and NaOH (2 M) addition caused significant changes in pH of the solution during the experiment. It can be interpreted that critical nucleation concentration was exceeded which causing homogeneous nucleation formation of TiO_2 in the solution. Consequently, the resulting pigment was seen to have no pearlescent effect.

The preliminary results showed that crude mica was not suitable to obtain the mica-titania pigment with the desired properties and it required some pre-treatments before coating. Also, it was thought that the experimental

conditions should be carefully controlled by changing the experimental set up in a way to provide the constant rate of addition of $TiOCl_2$. Besides, it was obvious that NaOH concentration should be reduced to avoid homogeneous precipitation of TiO_2.

4.2 Mica Pre-treatment

Mica pretreatment comprised sieving mica through 270 mesh (53 μm), sodium bicarbonate treatment and decantation process. In sodium bicarbonate treatment, it was aimed to decrease the thickness of the mica platelets through cleaving.

Table 4.1 BET analysis results of mica samples.

Sample	Specific Surface Area (m^2/g)
Mica (sieved+decantated)	4.54
Mica (sieved+decantated+$NaHCO_3$)	6.69

Table 4.1 shows the results of the BET analysis of the (i) sieved, decantated mica and (ii) sieved, sodium bicarbonate treated and decantated mica. Approximately 1.5 fold of increase in specific surface area was achieved after the treatment with sodium bicarbonate.

A considerable decrease in the number of particles below 10 μm size can be seen from the particle size distribution graph (Figure 4.2).

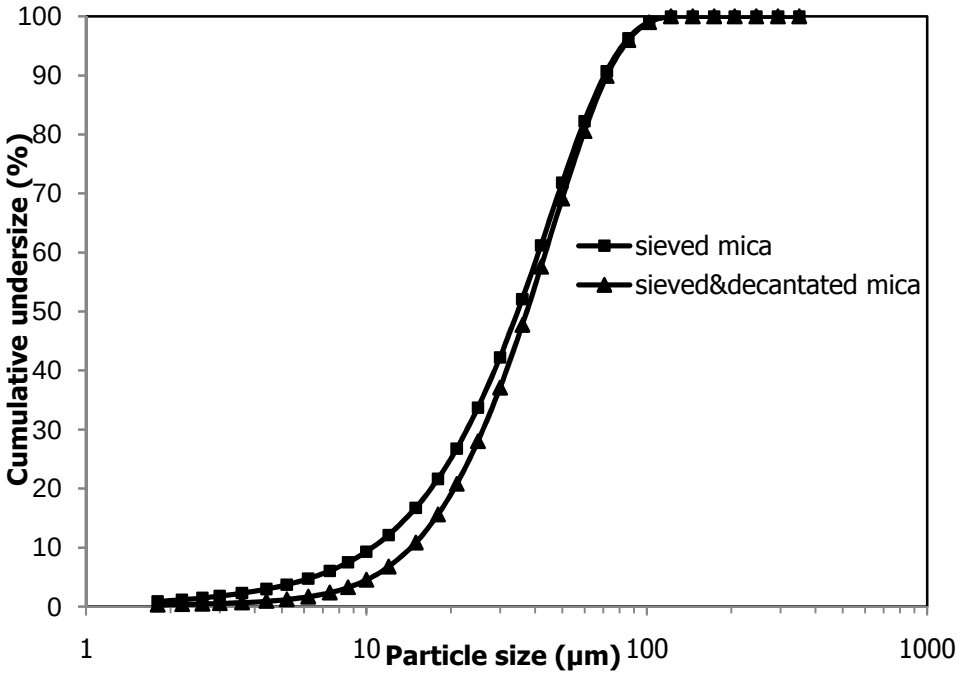

Figure 4.2 The particle size distribution of sieved mica (270 mesh) and sieved and decantated mica

The SEM results also showed that particles on mica surfaces was successfully removed and smooth mica surfaces were obtained (Figure 4.3). By removing tiny particles which scatter light and prevent pearlescence, mica-titania pigment with improved gloss property could be obtained.

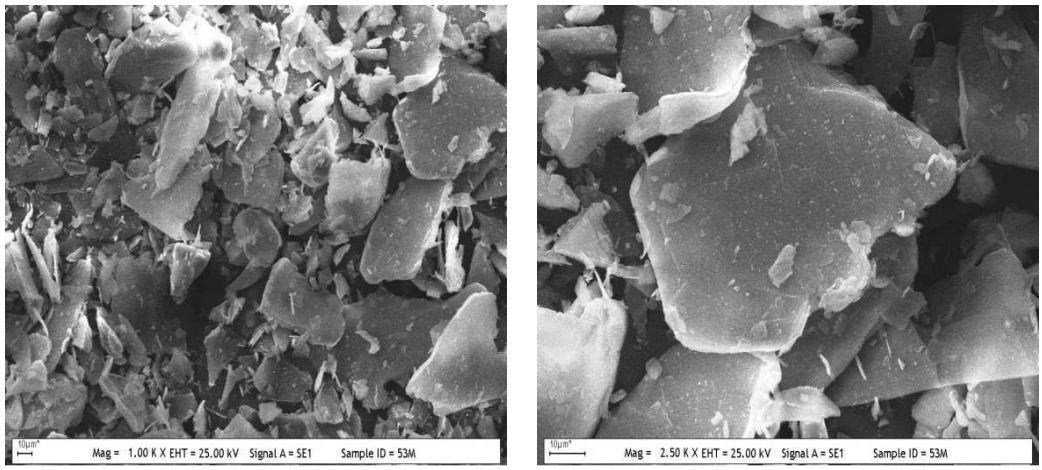

(a)

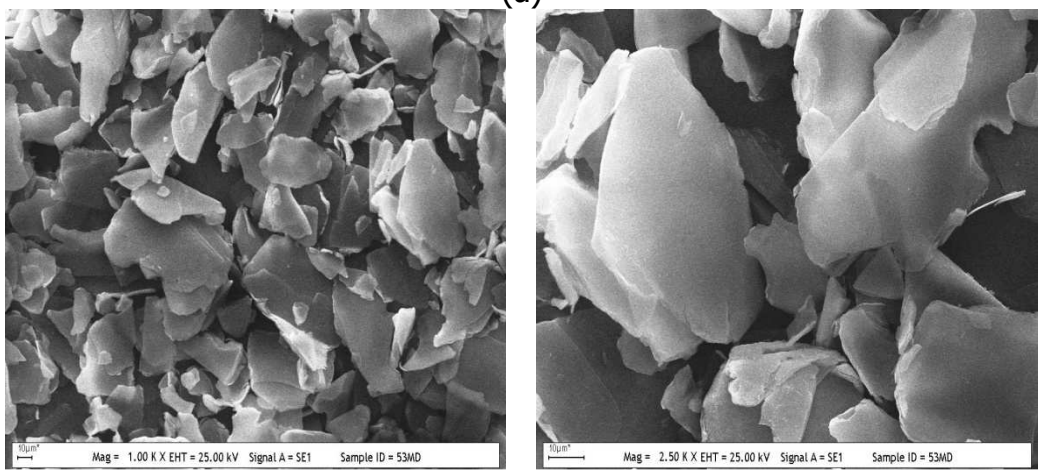

(b)

Figure 4.3 SEM micrographs of (a) sieved (270 mesh), (b) sieved and decantated mica

4.3 Mica Titania Pigment

In order to eliminate the disadvantages in the preliminary studies, firstly 1 M NaOH was used instead of 2 M for hydrolysis to control the pH of the solution more precisely. Furthermore, $TiOCl_2$ addition was decided to be carried out by a peristaltic pump to provide a constant rate of addition, and the pre-treated mica was used for the synthesis of mica titania pigment.

Figure 4.4 shows the SEM micrographs of TiO_2 coated mica pigment. It could be clearly seen that TiO_2 was smoothly deposited onto mica surfaces with no agglomerations by controlling the rate of hydrolysis. In order to obtain rutile phase of TiO_2 on mica platelets, 1 ml, 2 ml, 3 ml, and 4 ml of $SnCl_4$ (0.05 M) were used to precoat tin oxide on mica prior to titania deposition.

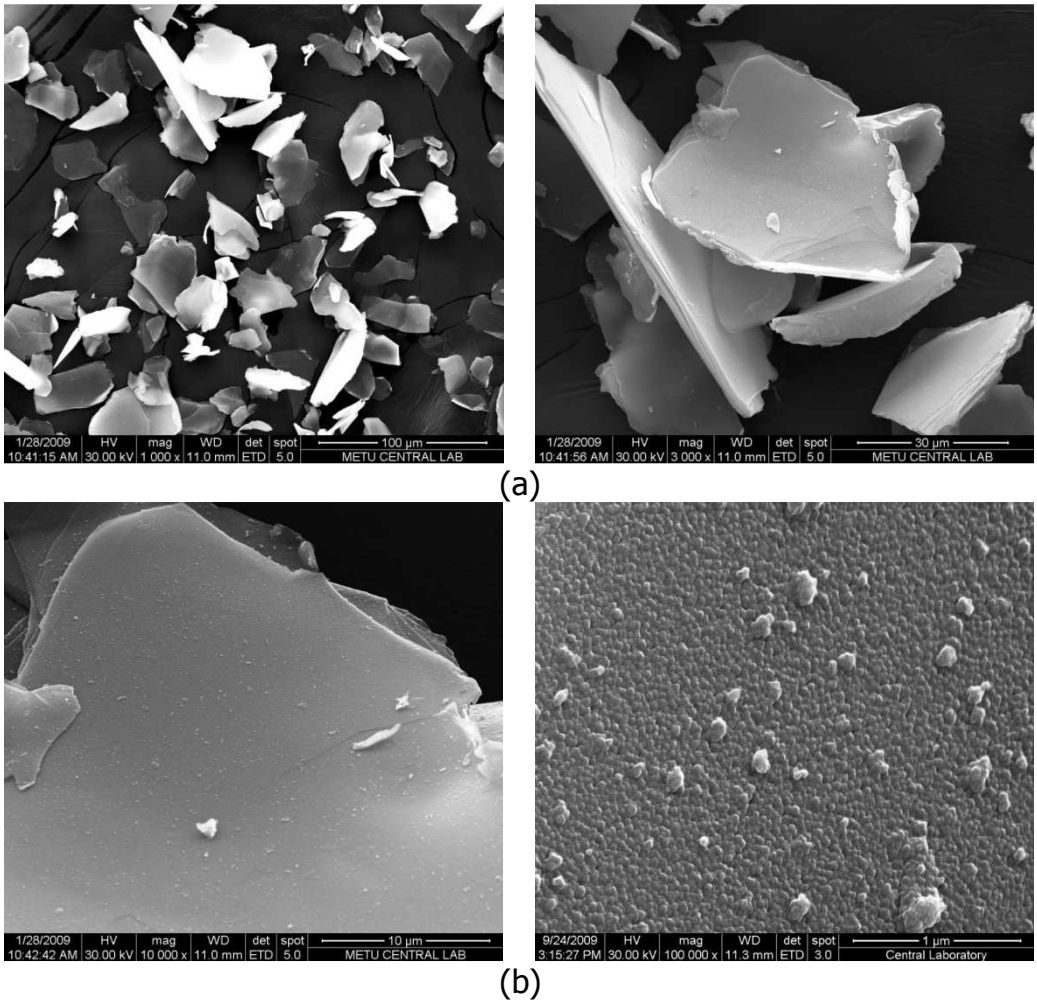

Figure 4.4 SEM micrographs of mica-titania pigment; (a) low magnifications, (b) high magnifications.

Figure 4.5 shows the SEM photographs of SnO_2 and TiO_2 coated mica samples at varying SnO_2 amounts. It can be easily seen that TiO_2 homogeneously covered mica surfaces, but the increase of SnO_2 caused inhomogeneous growth of TiO_2, and the surface roughness increased.

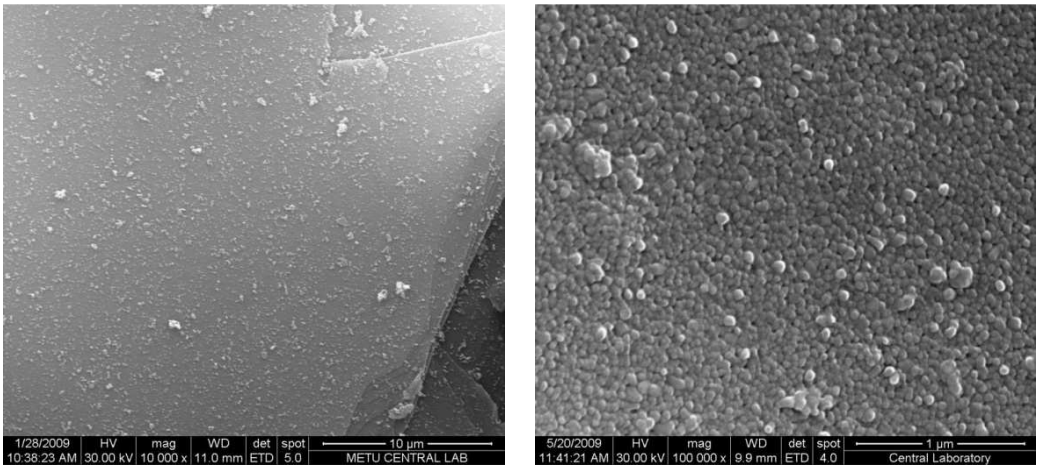

(a)

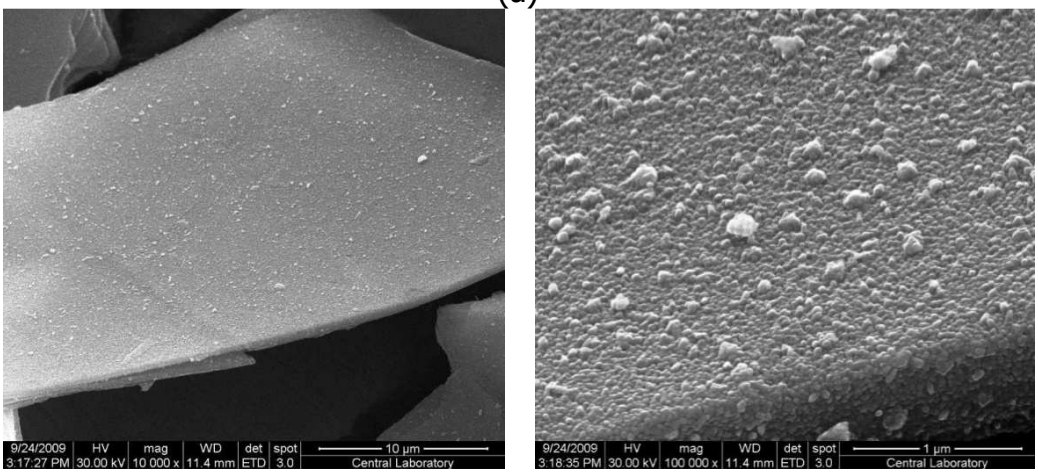

(b)

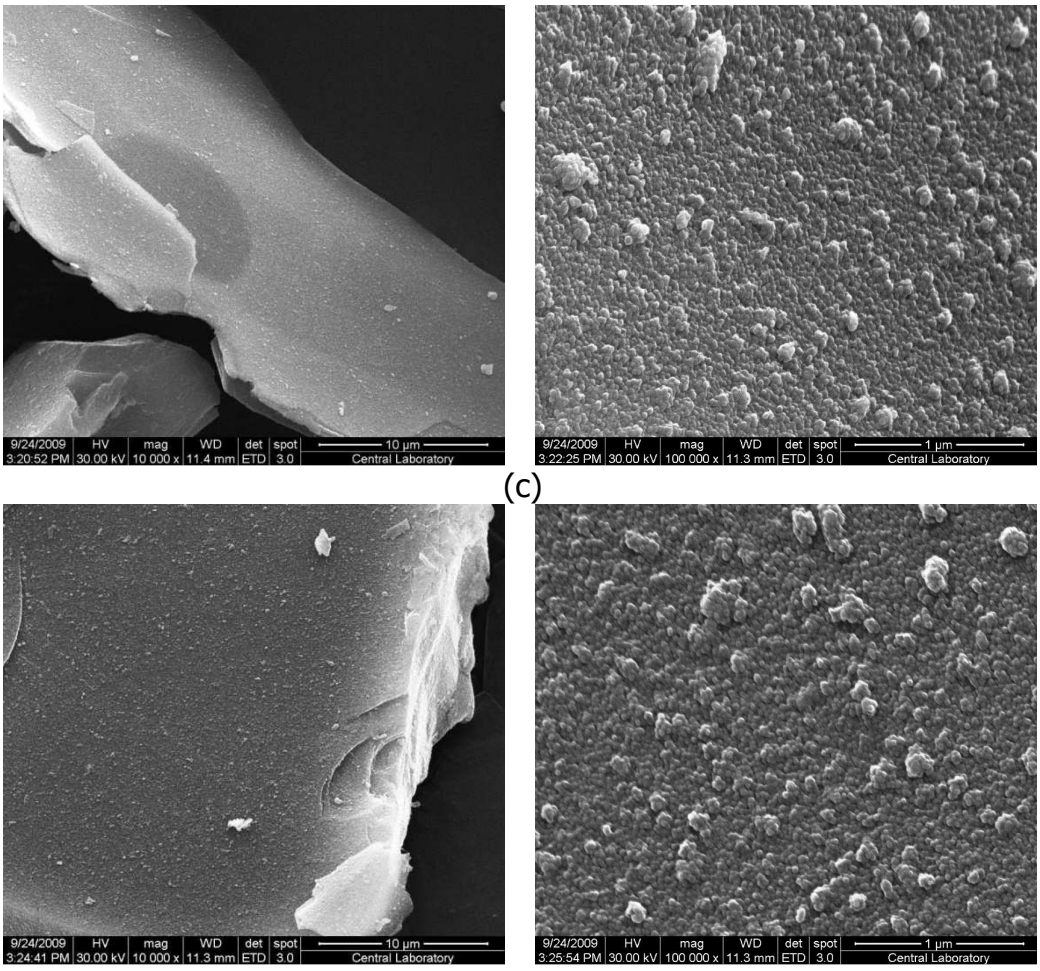

Figure 4.5 SnO_2 and TiO_2 coated mica samples; (a) 0.22 % SnO_2, (b) 0.44 % SnO_2, (c) 0.66 % SnO_2, (d) 0.88 % SnO_2.

In order to see the effect of SnO_2 from SEM analysis clearly, TiO_2 amount that was coated the mica surfaces was doubled with prior coating of 0.88 % SnO_2. In Figure 4.6 (a) smoothly grown TiO_2 is seen on mica surfaces while in Figure 4.6 (b) some discrete nucleation points of TiO_2 are seen. This pigment with yellow reflecting appearance was not used in the proceeding experiments.

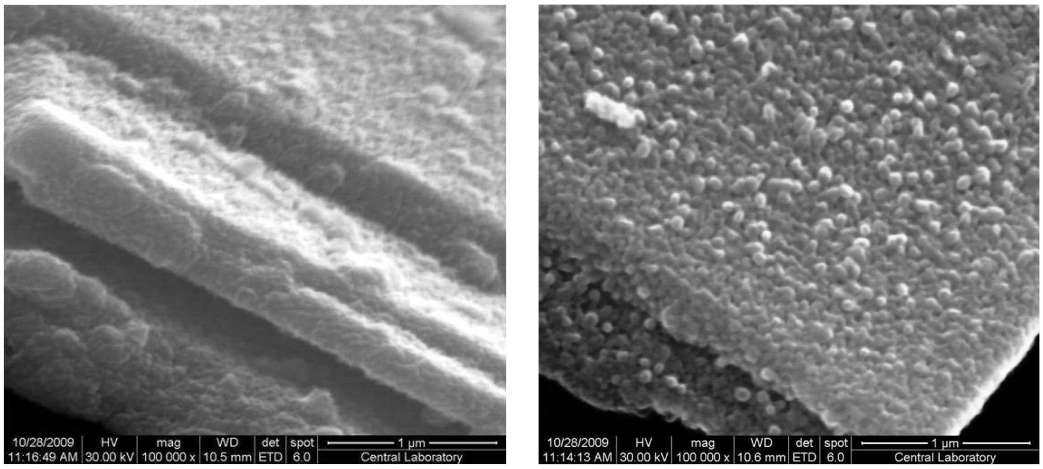

(a) (b)

Figure 4.6 (a) TiO_2 coated mica, (b) SnO_2 and TiO_2 coated mica.

XRD analysis was performed to observe the phase transformation of TiO_2 on mica surfaces at different amounts of SnO_2 deposition. In Figure 4.7, it was observed that the most intense peaks of rutile at 2θ=27.49° was intensified with increasing amount of SnO_2 while the most intense peak of anatase at 2θ=25.36° was seem to decrease. This can be interpreted as the transformation of anatase to rutile phase was promoted. Also the disappearance of the second most intense peak of anatase (2θ=48.14°) and the appearance of second most intense peak of rutile (2θ=36.15°) with increasing amount of SnO_2 confirmed this phase transformation.

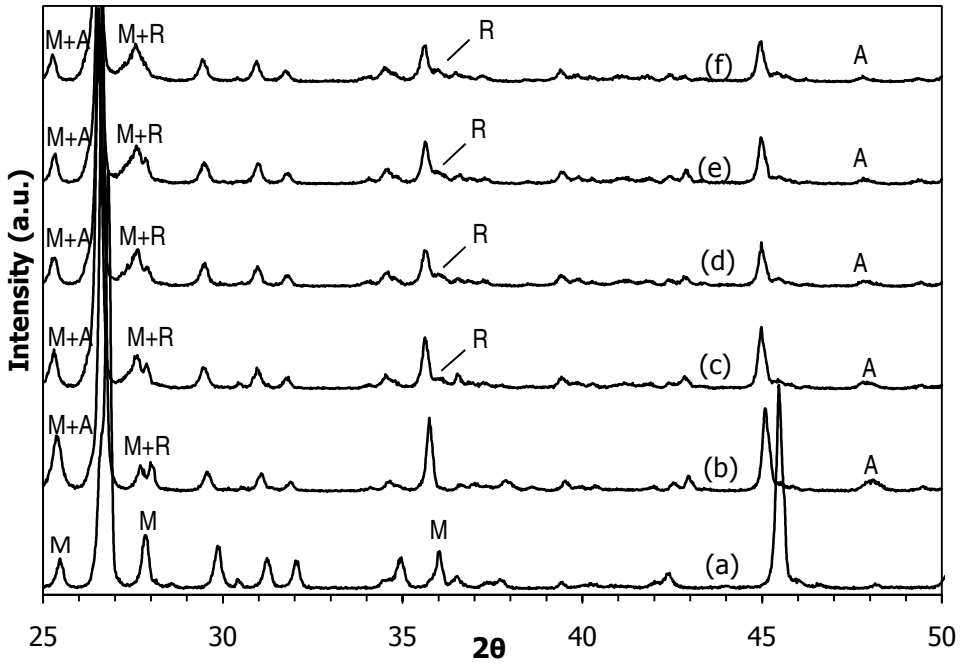

Figure 4.7 XRD analysis results of mica titania pigments with varying SnO_2 amounts. (a) muscovite mica, (b) only TiO_2, (c) 0.22 % SnO_2 and TiO_2 (d) 0.44 % SnO_2 and TiO_2, (e) 0.66 % SnO_2 and TiO_2, (f) 0.88 % SnO_2 and TiO_2.

However, the most intense peaks of rutile and anatase at 2θ=25.36° and 27.49° were seen to interfere with mica peaks, respectively. So in order to deconvole these combined peaks and calculate the mole percents of anatase and rutile phases, the areas of these corresponding peaks were calculated by using Peak Fit software (Peakfit, v. 4.11).

The results which consist of the mol percentages of rutile and anatase crystalline form of TiO_2 on mica substrate are given in Table 4.2. The calculations of mole percentages of TiO_2 phases are given in Appendix B in detail.

Table 4.2 Rutile and anatase mole percent in mica titania pigments.

Sample	Rutile (Mole %)	Anatase (Mole %)
Mica Titania	2.55	97.45
Mica titania (0.22 % SnO_2)	24.55	75.45
Mica titania (0.44 % SnO_2)	71.28	28.72
Mica titania (0.66 % SnO_2)	95.64	4.36
Mica titania (0.88 % SnO_2)	91.64	8.36

Figure 4.8 shows the change in the crystalline form of TiO_2 on mica with varying SnO_2. It was clearly seen that with increasing amount of SnO_2, except 0.88 % SnO_2, mole percent of anatase phase decreased while mole percent of rutile phase increased significantly. Mica titania pigment with 0.88 % SnO_2 displayed very little decrease with respect to the pigment with 0.66 % SnO_2. That is, further increase of SnO_2 had an adverse effect on anatase-rutile transformation.

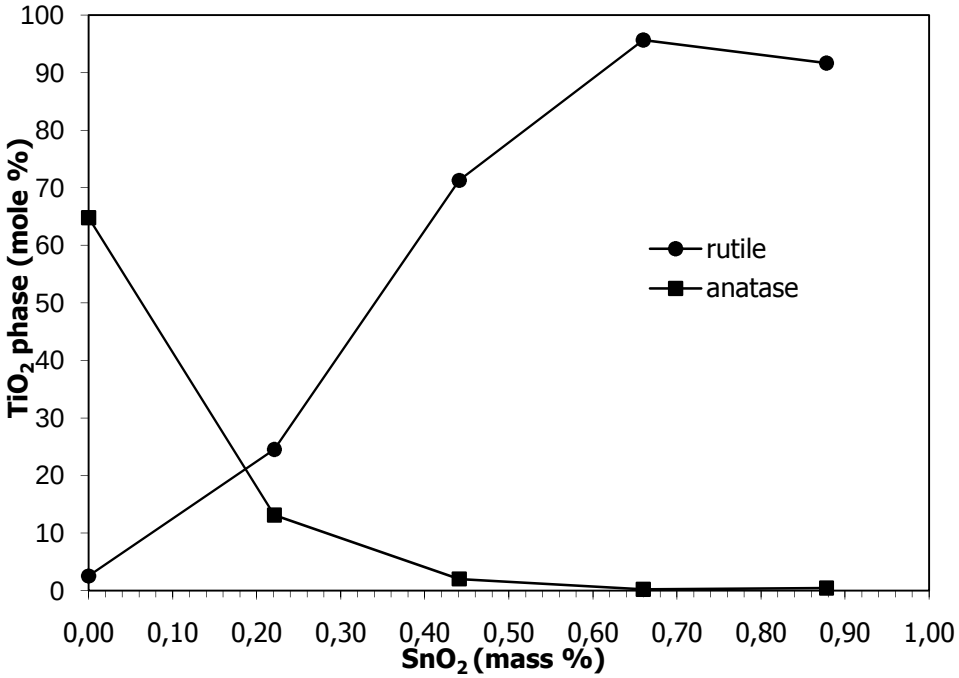

Figure 4.8 The mole percents of anatase and rutile crystalline phases of the mica titania pigments with varying SnO_2 amount.

4.4 Copper Phthalocyanines

The FT-IR spectrum of unsubstituted copper phthalocyanine(CP) is given in Figure 4.9. It has characteristic peaks at 3041 and 2910 cm^{-1} for aromatic C-H stretching, at 1610 cm^{-1} for C=C macrocycle ring deformation, at 1506 cm^{-1} for C=N stretching, at 1333 cm^{-1} for C-C stretching in isoindole, at 1091 cm^{-1} for C-H in plane deformation and at 723 cm^{-1} for C-H out of plane deformation of phenyl. The other peaks at 1286 cm^{-1}, 1165 cm^{-1} and 1119 cm^{-1} correspond to C-N stretching in isoindole, C-N in plane bending, C-H in plane bending, respectively.

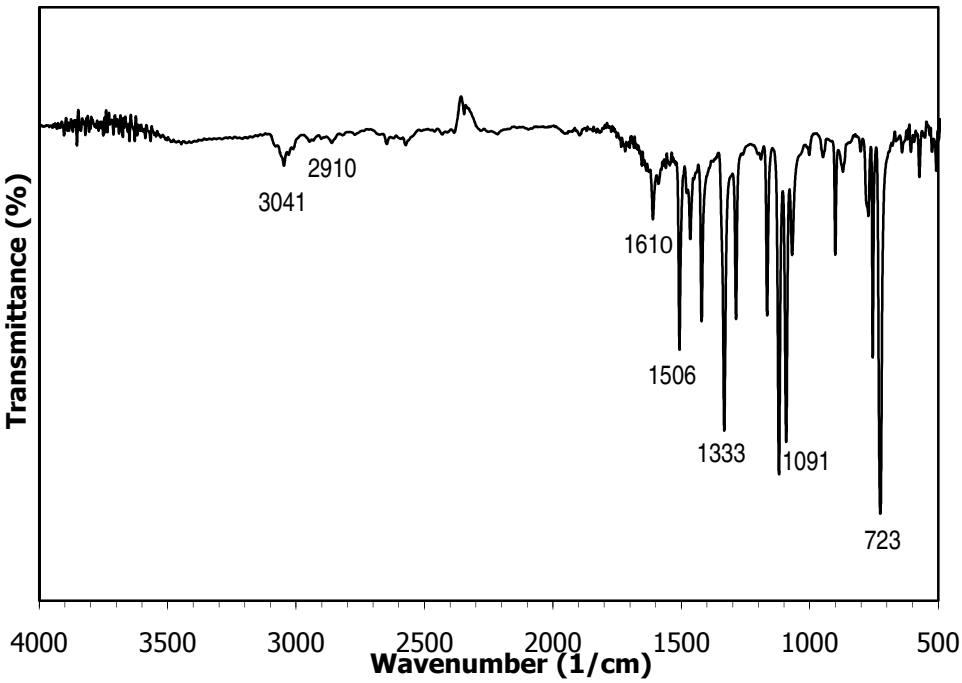

Figure 4.9 FT-IR spectra of unsubstituted copper phthalocyanine.

The FT-IR spectrum of tetracarboxamide copper phthalocyanine (TCP) is given in Figure 4.10. It has characteristic peaks at 3037 and 2912 cm^{-1} for aromatic C-H stretching, at 1614 cm^{-1} for C=C macrocycle ring deformation, at 1504 cm^{-1} for C=N stretching, at 1328 cm^{-1} for C-C stretching in isoindole, at 1093 cm^{-1} for C-H in plane deformation and at 738 cm^{-1} for C-H out of plane deformation of phenyl which differed from CP in some extent due to substitution.

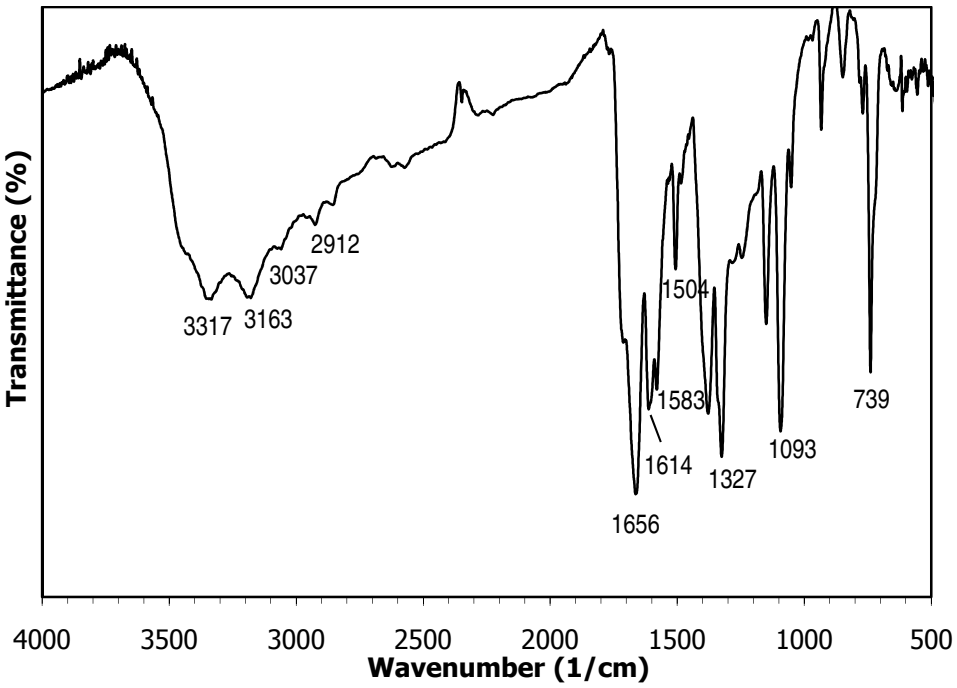

Figure 4.10 FT-IR spectra of tetracarboxamide copper phthalocyanine.

In Figure 4.11, the comparison of the FT-IR spectrum of TCP with that of CP is given. The FT-IR spectrum of TCP shows additional bands that is not existing in CP spectrum due to its four amide groups bonded to peripheral benzenoid rings of the macrocycle. These peaks include N-H stretching bands at 3317 cm^{-1} and 3167 cm^{-1}, C=O stretching of the amide at 1656 cm^{-1}, and N-H bending combined with C-N stretching at 1583 cm^{-1}.

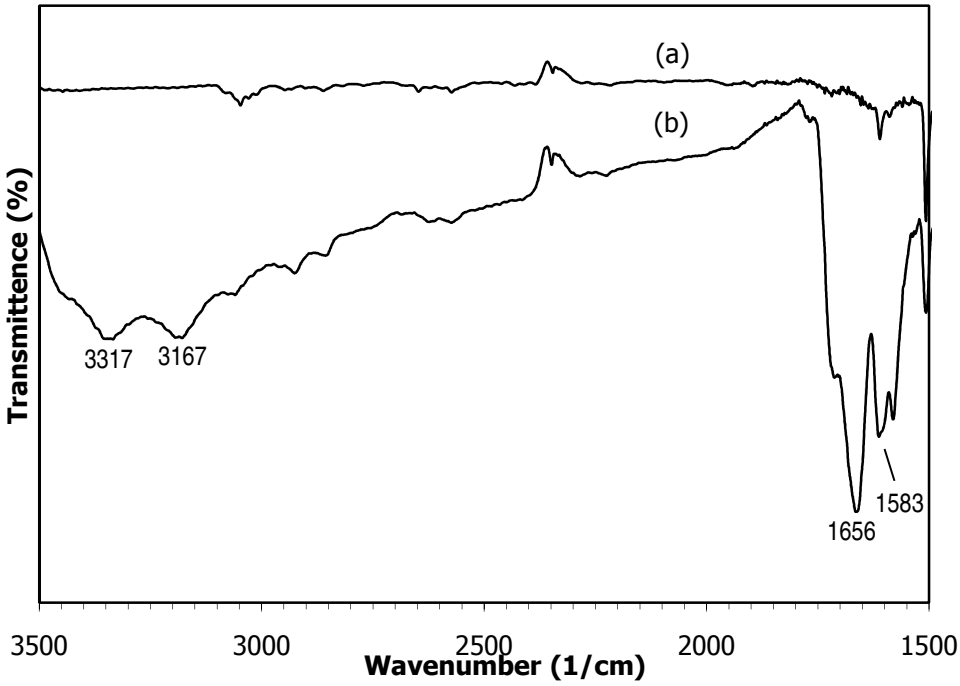

Figure 4.11 Comparison of FT-IR spectra of (a) CP with (b) TCP.

The UV-visible absorption spectra of CP and TCP pigments are shown in Figure 4.12. UV-visible spectra of phthalocyanine complexes exhibit characteristic absorptions in the Q band region at 650-700 nm and in the B band region (UV region) at around 300-400 nm. CP and TCP complexes are deep in blue color due to absorption in the B band region at 345 nm and at 348 nm, respectively. Furthermore, CP shows absorption in Q band region at 671 nm, and TCP shows absorption at 674 nm.

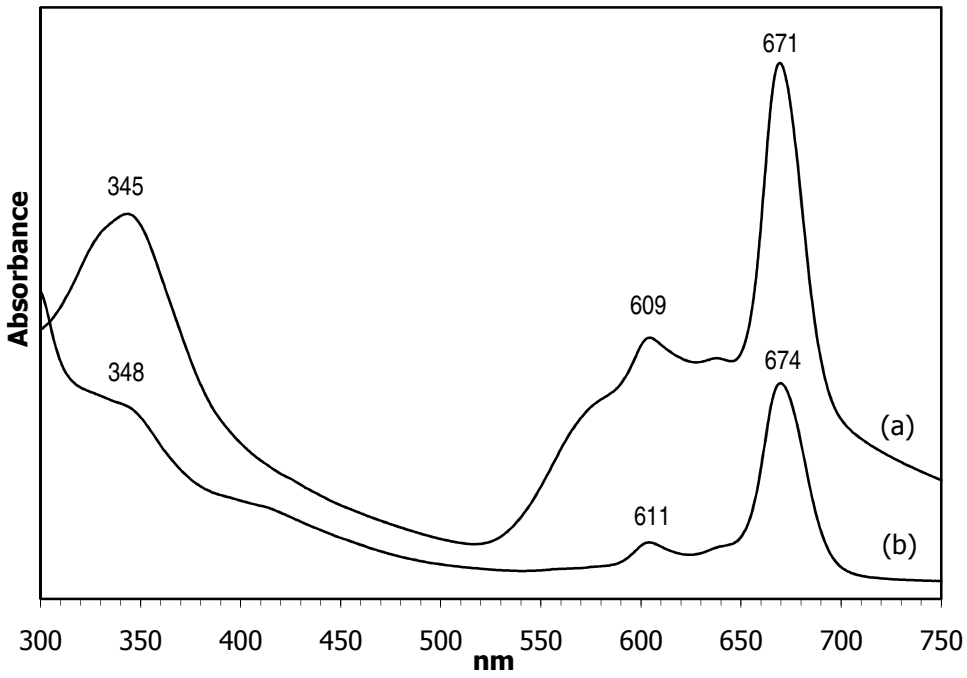

Figure 4.12 UV-visible absorption spectra of (a) CP and (b) TCP pigment.

The appearance of the band in the higher energy part of Q band region is due to aggregation species formed in DMF solution. This small band formed at 609 nm for CP and at 611 nm for TCP. Aggregation occurs when the dye-dye interaction is strong enough to overcome any other forces which favor the solvation of monomer. The broadened or split Q band is the evidence of the aggregation with the high energy band being due to the aggregate and the low energy band due to the monomer. So, the broadening of Q band of CP at 609 nm was due to enhanced aggregation with respect to TCP which can be because of π-π interactions of the peripheral benzenoid rings of the molecule. On the other hand, amide groups in the peripheral sides of TCP could interact with DMF in the form of hydrogen bonding which minimizes the self association of the molecules.

4.5 Combination Pigments

4.5.1 FT-IR and XRD Analysis Results of CPMO40 Pigment

Figure 4.13 shows the FT-IR spectra of CPM040 pigment at different temperatures, mica titania pigment and CP pigment.

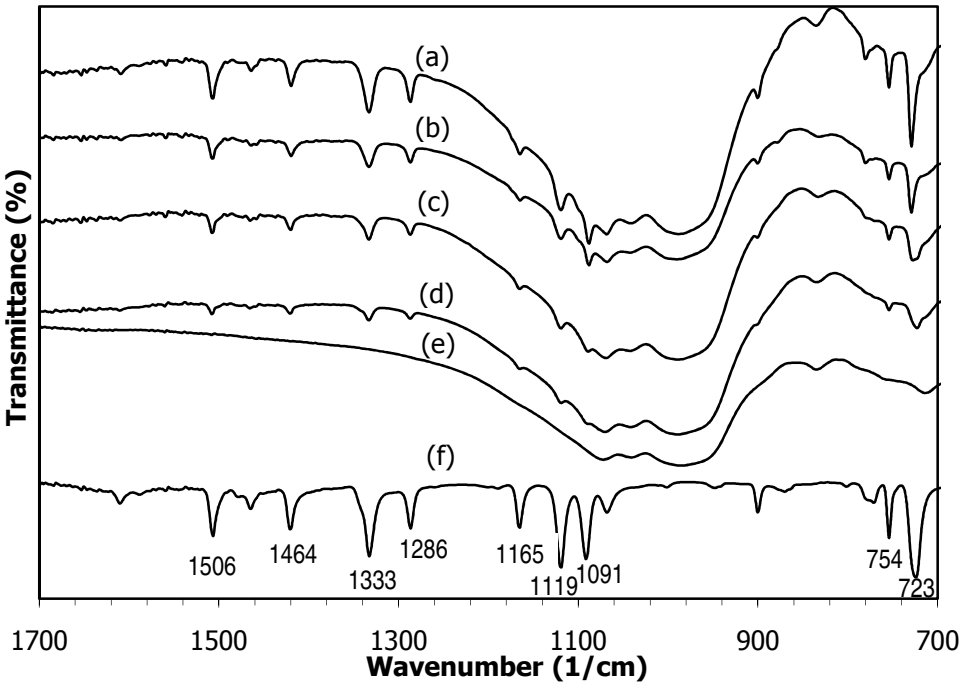

Figure 4.13 FT-IR spectra of CPM040 pigment at (a) 120°C, (b) 90°C, (c) 60°C (d) 25°C, (e) mica titania, (f) CP.

The characteristic peaks of CP can be seen in Figure 4.13 at all temperatures studied, and these peaks became quite intensified with increasing temperature. Also peak shifts were observed with the increase in temperature. It should be due to crystal phase transformation of CP on mica substrate. The synthesized CP powder is in alpha phase which was confirmed

by FT-IR spectra at peaks of 1190 cm^{-1}, 941 cm^{-1}, 871 cm^{-1}, 864 cm^{-1}, 771 cm^{-1} and 723 cm^{-1}. However, some peaks corresponding to beta phase can also be seen with very small intensity which were at 779 cm^{-1} and 984 cm^{-1}. In order to see these peaks clearly, FT-IR in the range between 700 cm^{-1} and 900 cm^{-1} is given in Figure 4.14.

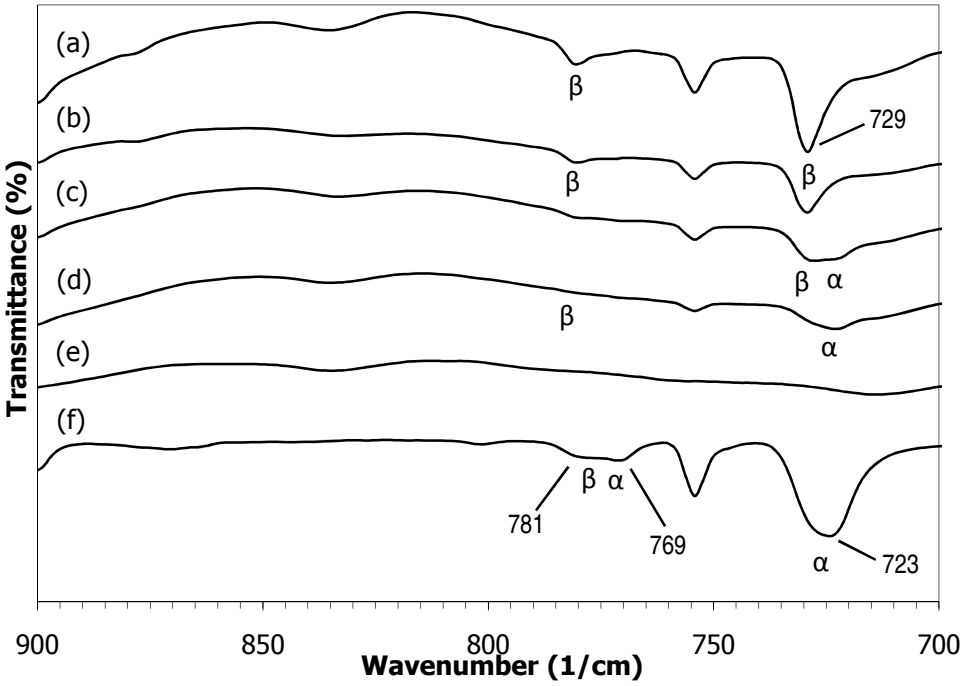

Figure 4.14 FT-IR spectra of CPM040 pigment between 700- 900 cm^{-1} at (a) 120°C, (b) 90°C, (c) 60°C (d) 25°C, (e) mica titania, (f) CP.

The most intense peaks of CP correspond to alpha polymorphic form which could be distinguishable in the figure at 723 and 769 cm^{-1}. The CP was found to be in alpha phase on mica titania pigment at 25°C which was confirmed by the peak of 723 cm^{-1} that corresponded to alpha form. As the temperature increased to 60°C, the peak at 723 cm^{-1} broadened and created

a peak at 729 cm^{-1} which corresponded to beta phase. At 60°C alpha peak at 769 cm^{-1} shifted to 777 cm^{-1} which could be interpreted as the presence of both alpha and beta phases. Also, at 90°C and 120°C only beta phase peaks could be observed which are at 729 cm^{-1} and 780 cm^{-1}. The same trends were observed when the quantity of copper phthalocyanine was altered. However, the peaks were less significant as the amount of copper phthalocyanine decreased (Appendix A).

The alpha-beta phase transformation detected from FT-IR results was also confirmed by XRD analysis given in Figure 4.15.

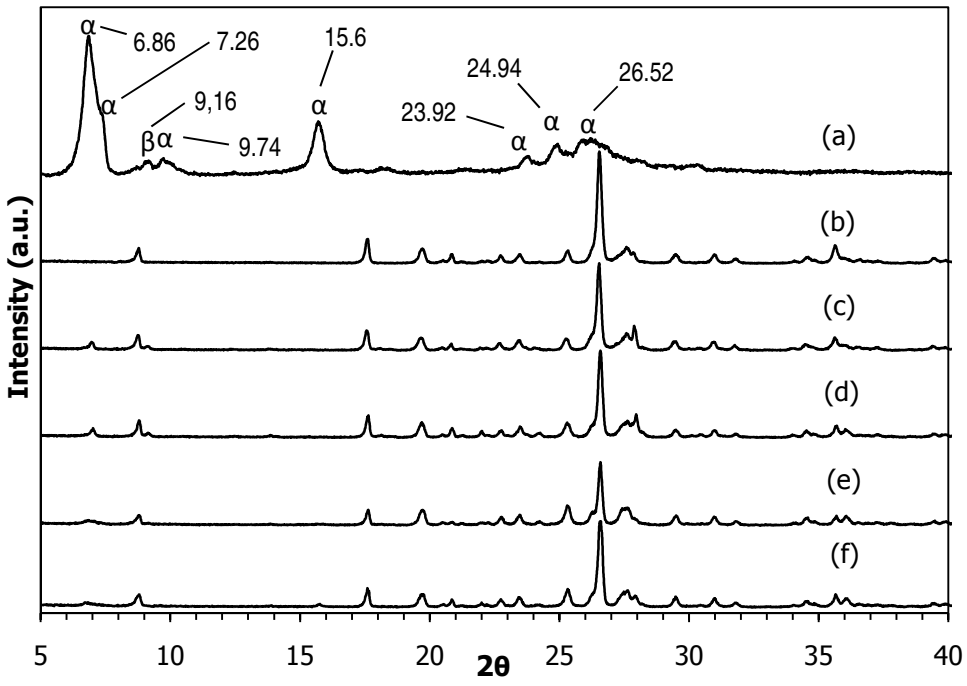

Figure 4.15 XRD patterns of (a) CP, (b) mica titania, CPM040 pigment at (c) 120°C, (d) 90°C, (e) 60°C, (f) 25°C.

XRD peaks of copper phthalocyanine that are located at 2θ=6.86° and 7.26° belong to the alpha form of copper phthalocyanine and they have 100% and 34% theoretical intensities, respectively. The other distinctive peaks at 2θ= 9.74°, 15.6°, 23.92°, 24.94° and 26.52° also confirmed the alpha phase.

XRD pattern of CPM pigment obtained at different deposition temperatures, showed peaks of CP between 2θ values of 6° and 18°, because the most intense peaks of phthalocyanine appeared in this region. In other regions, peaks of mica-titania pigment crowds the patterns, and it is difficult to isolate and distinguish less intense peaks of CP.

When the same XRD patterns are plotted in Figure 4.16 that are expanded in the 2θ range between 6° to 18°, peaks of phthalocyanine could be seen with more ease. At 25°C the copper phthalocyanine pigment showed alpha polymorphic phase with peaks at 2θ=6.82° and 15.68°. When the reaction temperature was increased to 60°C, beta and alpha peaks were observed to coexist in the pattern. This means that some of CP on the mica-titania substrate have an alpha crystalline form while the rest transforms to the beta form.

When the temperature was further increased above 90°C, the peaks that are ascribed to alpha crystalline form disappeared, and the most intense beta peaks showed themselves distinctly at 2θ=7.02° and 9.16°. Also at 120°C beta crystalline form is identifiable from the peaks situated at 2θ=6.98° and 9.14°.

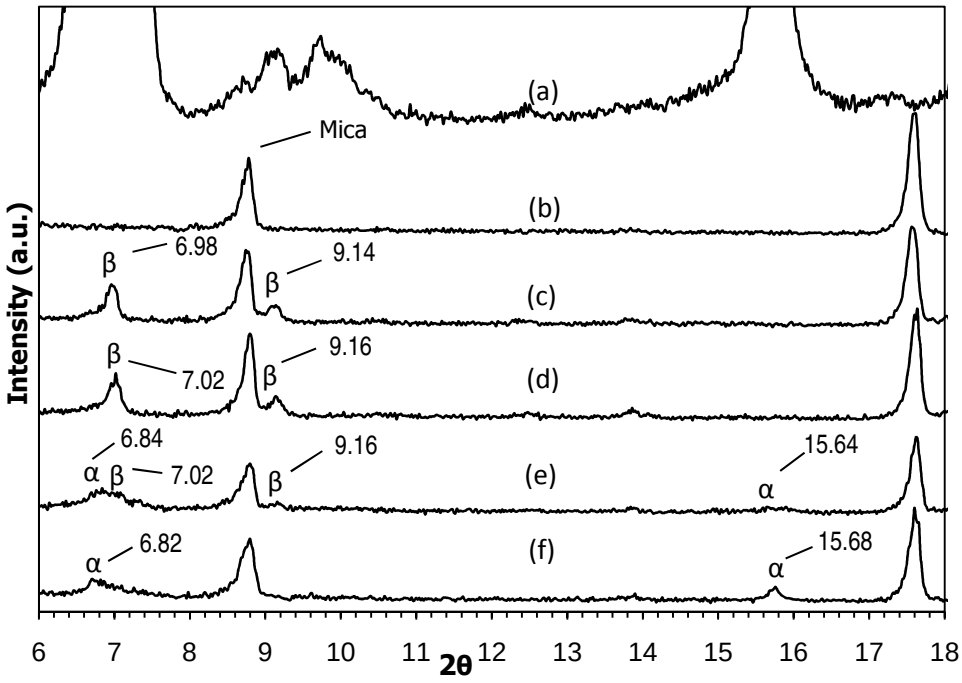

Figure 4.16 XRD patterns of (a) CP, (b) mica titania, CPM040 pigment at (c) 120°C, (d) 90°C, (e) 60°C (f) 25°C between 2θ=6-18.

4.5.2 FT-IR and XRD Analyse Results of TCPM0520 Pigment

Figure 4.17 shows the FT-IR of TCPM0520 pigment synthesized at different temperatures, mica titania pigment and CP pigment. Most of the peaks belong to TCPM0520 could not be seen in FT-IR because very small amount of TCP was deposited on the substrates; therefore they can not be distinguished not only in SEM analysis but also in FT-IR graphs.

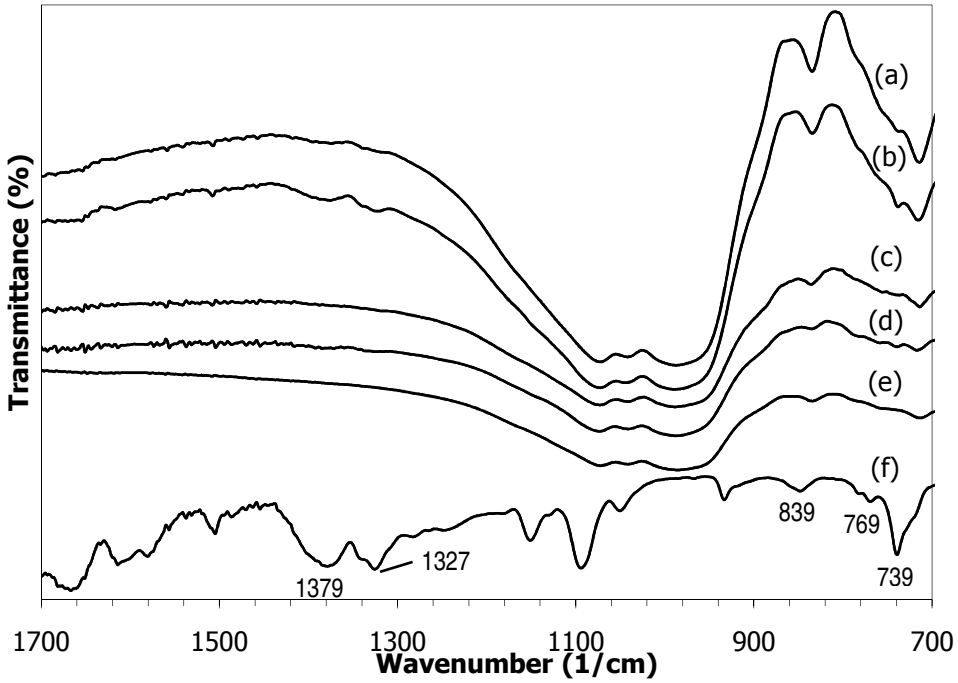

Figure 4.17 FT-IR spectra of TCPM0520 pigment at (a) 120°C, (b) 90°C, (c) 60°C (d) 25°C, (e) mica titania, (f) CP.

However, the most intense peaks at 739 cm^{-1} and 769 cm^{-1} that correspond to C-H out of plane deformations, peak at 839 cm^{-1} that corresponds to in plane vibration, and the peaks at 1329 cm^{-1} and 1379 cm^{-1} that correspond to C-C stretching in isoindole were significant. When the broad peak at 739 cm^{-1} was deconvoluted by using Peak Fit software, it was separated into three peaks of 739 cm^{-1}, 723 cm^{-1} and 715 cm^{-1}. The amide peaks at 1656 cm^{-1} and 1583 cm^{-1}, and also at 3163 cm^{-1} and 3317 cm^{-1} disappeared in Figure 4.18.

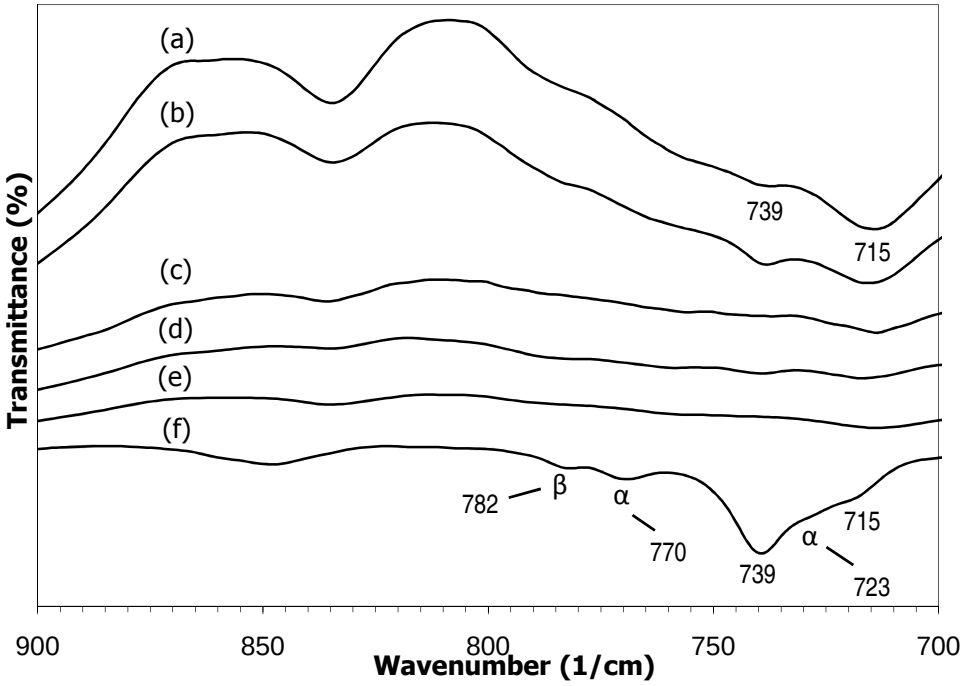

Figure 4.18 FT-IR spectra of TCPM052 pigment between 700- 900 cm^{-1} at (a) 120°C, (b) 90°C, (c) 60°C (d) 25°C, (e) mica titania, (f) CP.

The polymorphic form of the synthesized TCP powder was found to be alpha which was confirmed by peaks at 1190 cm^{-1}, 769 cm^{-1} and 723 cm^{-1}. Also some peaks belonging to beta form could be seen at 783 cm^{-1} and 985 cm^{-1} with very low intensities. As it could be seen in Figure 4.18, alpha and the beta peaks at 723 cm^{-1}, 770 cm^{-1} and 782 cm^{-1} disappeared in the spectra of TCPM052 pigments at all temperatures. It can be interpreted as TCP formed an amorphous structure on the mica titania substrate. The peaks at 739 cm^{-1} and 715 cm^{-1} belonging to out of plane deformation of macrocycle were significant.

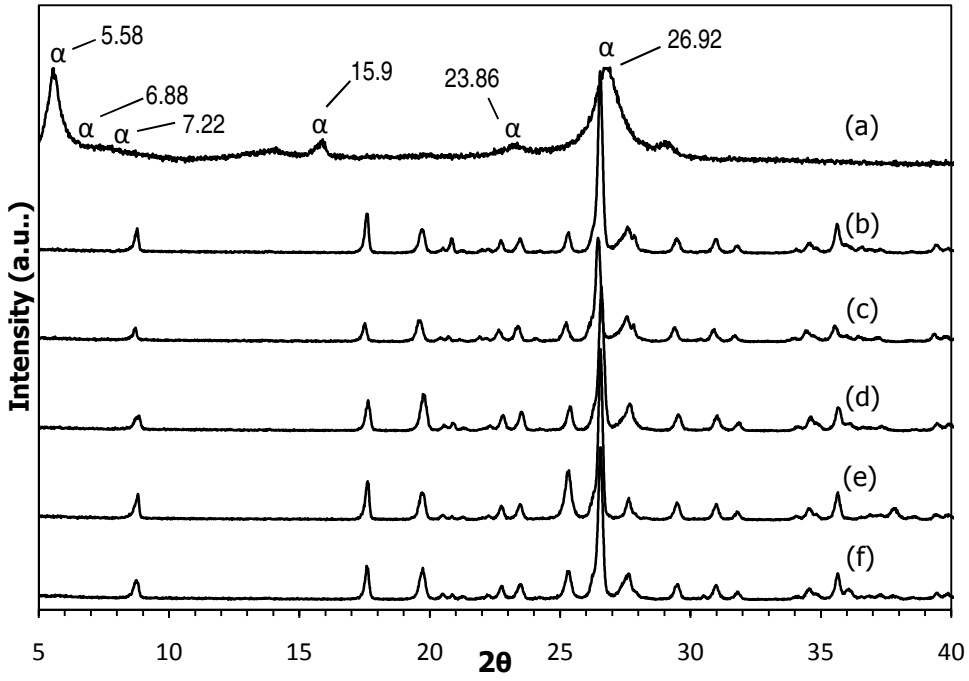

Figure 4.19 XRD patterns of (a) TCP, (b) mica titania, TCPM052 pigment at (c) 120°C, (d) 90°C, (e) 60°C (f) 25°C.

FT-IR results can also be confirmed by XRD analysis results which can be allowed in Figure 4.19. The TCP pigment shows a structure similar to alpha polymorphic form. The expected characteristic peaks of this polymorph appear at 2θ=6.88°, 7.22°, 15.9°, 23.36° and 26.92°. While the former three were identifiable, the peaks at 2θ= 6.88° and 7.22° could not be located. Upon deconvolution of the 2θ=5°-10° range, it was decided that the range was composed of three peaks and peaks that corresponded to 2θ=6.88° and 7.22° were extremely broad. The most intense peak located at 2θ=5.58° corresponds to an interplanar spacing of d=15.83Å. This peak is the third peak that is obtained in the deconvolution of the 2θ=5°-10° range. It is thought to be the (200) plane of TCP. Such a peak normally appears at 2θ=6.88° which corresponds to a smaller interplanar spacing of d=12.88Å. An increase in the interplanar spacing between the (200) planes could be

due to an increase of distance between TCP molecules because of the interactions between amide side groups. The peaks at 2θ=15.9° and 26.92° were observed to be shifted due to the amide substitution when compared to the CP.

When XRD pattern of TCPM0520 pigments was investigated, no TCP peaks could be seen which means that TCP forms XRD amorphous structure on mica-titania substrate at all temperatures. This is, because, the amide side groups prevented arrangement of molecules as crystals on the substrate by increasing the distance between the molecules. On the contrary, the interaction between the TCP molecules and mica-titania substrate must have been greater than the interaction among TCP molecules. This would lead to higher adhesive force between the deposit and the substrate and so a higher nucleation rate and an XRD amorphous fine-grain structure in the growth stage.

4.5.3 SEM Results of CPM Pigments

The SEM micrographs of CPM040 pigment samples at different temperatures are given in Figure 4.20. Table 4.3 also shows the average lengths of the crystallites calculated by using Image J program. (Appendix D). It can be clearly seen that with increasing temperature, the length of phthalocyanine crystalline rods increased significantly.

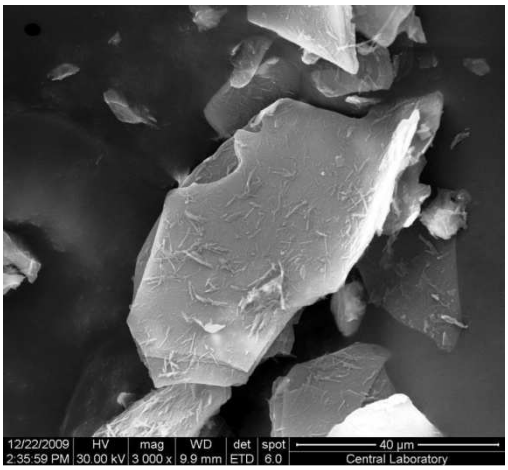
12/22/2009 | HV | mag | WD | det | spot | 40 µm
2:35:59 PM | 30.00 kV | 3 000 x | 9.9 mm | ETD | 6.0 | Central Laboratory

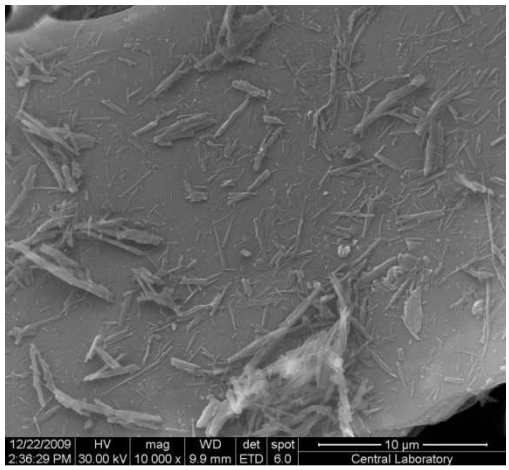
12/22/2009 | HV | mag | WD | det | spot | 10 µm
2:36:29 PM | 30.00 kV | 10 000 x | 9.9 mm | ETD | 6.0 | Central Laboratory

(a)

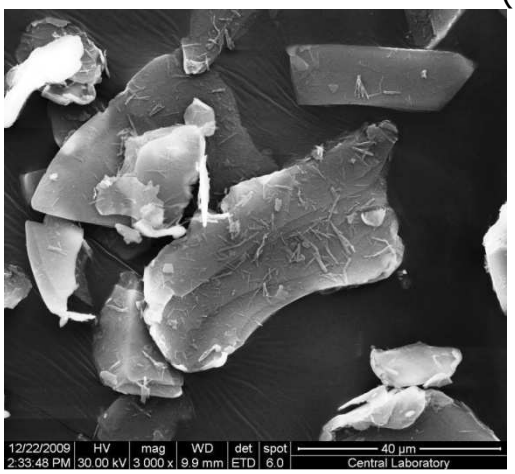
12/22/2009 | HV | mag | WD | det | spot | 40 µm
2:33:48 PM | 30.00 kV | 3 000 x | 9.9 mm | ETD | 6.0 | Central Laboratory

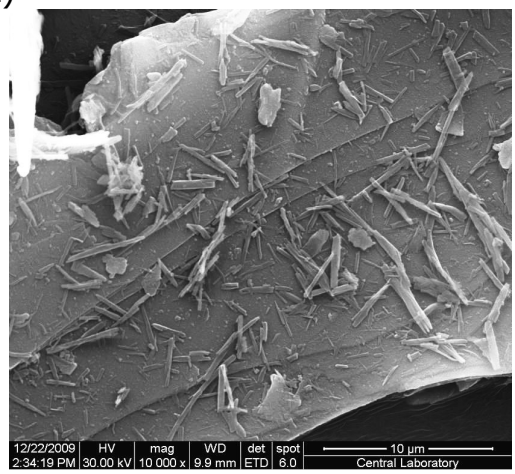
12/22/2009 | HV | mag | WD | det | spot | 10 µm
2:34:19 PM | 30.00 kV | 10 000 x | 9.9 mm | ETD | 6.0 | Central Laboratory

(b)

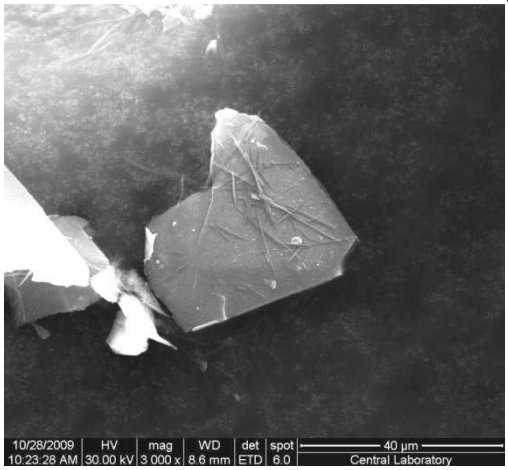
10/28/2009 | HV | mag | WD | det | spot | 40 µm
10:23:28 AM | 30.00 kV | 3 000 x | 8.6 mm | ETD | 6.0 | Central Laboratory

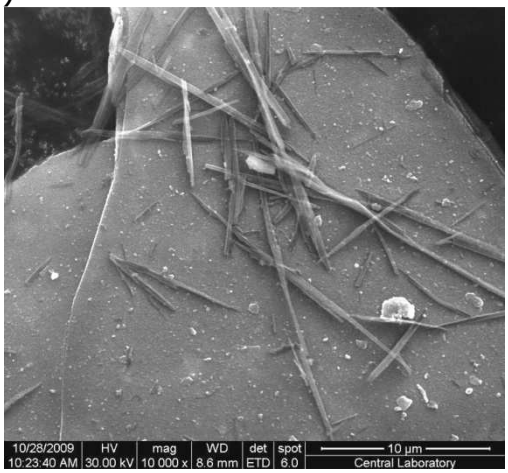
10/28/2009 | HV | mag | WD | det | spot | 10 µm
10:23:40 AM | 30.00 kV | 10 000 x | 8.6 mm | ETD | 6.0 | Central Laboratory

(c)

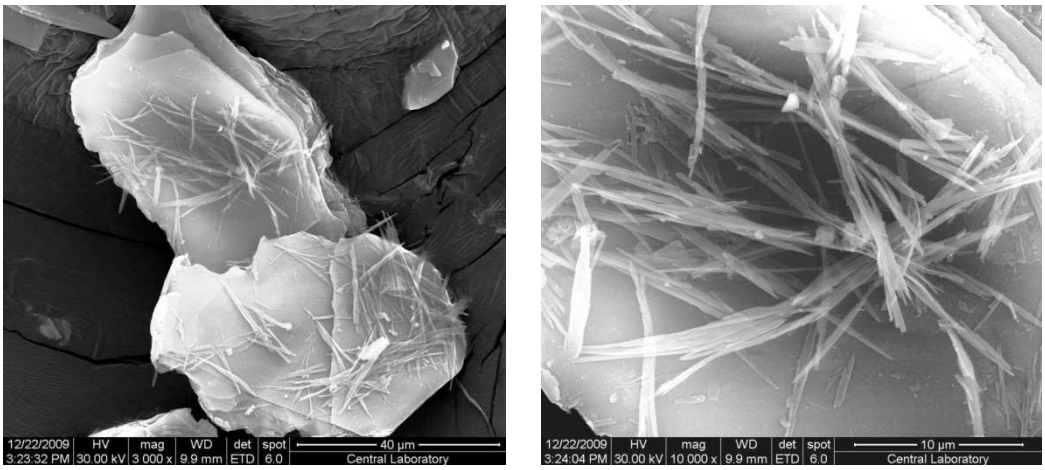

(d)

Figure 4.20 SEM micrographs of CPM040 at (a) 25°C, (b) 60°C, (c) 90°C (d) 120°C.

In the literature it is reported that α polymorphs are known to grow initially without transformation by thermal treatment or by exposure to some organic solvents and then they are transformed into stable beta form after they have grown to a certain size [45]. SEM results and the increase in the length of the phthalocyanine rods supported this information because significant increase in the length could be seen when alpha form is completely transformed to the beta form.

Table 4.3 Average length of CP rods at different temperatures.

Sample	Average Length of Rods (µm)
CPM040 (25°C)	2.50
CPM040 (60°C)	3.63
CPM040 (90°C)	6.09
CPM040 (120°C)	10.94

Varying the quantity of CP, did not introduce any significant change in the length of the phthalocyanine crystalline rods as seen in Figure 4.21.

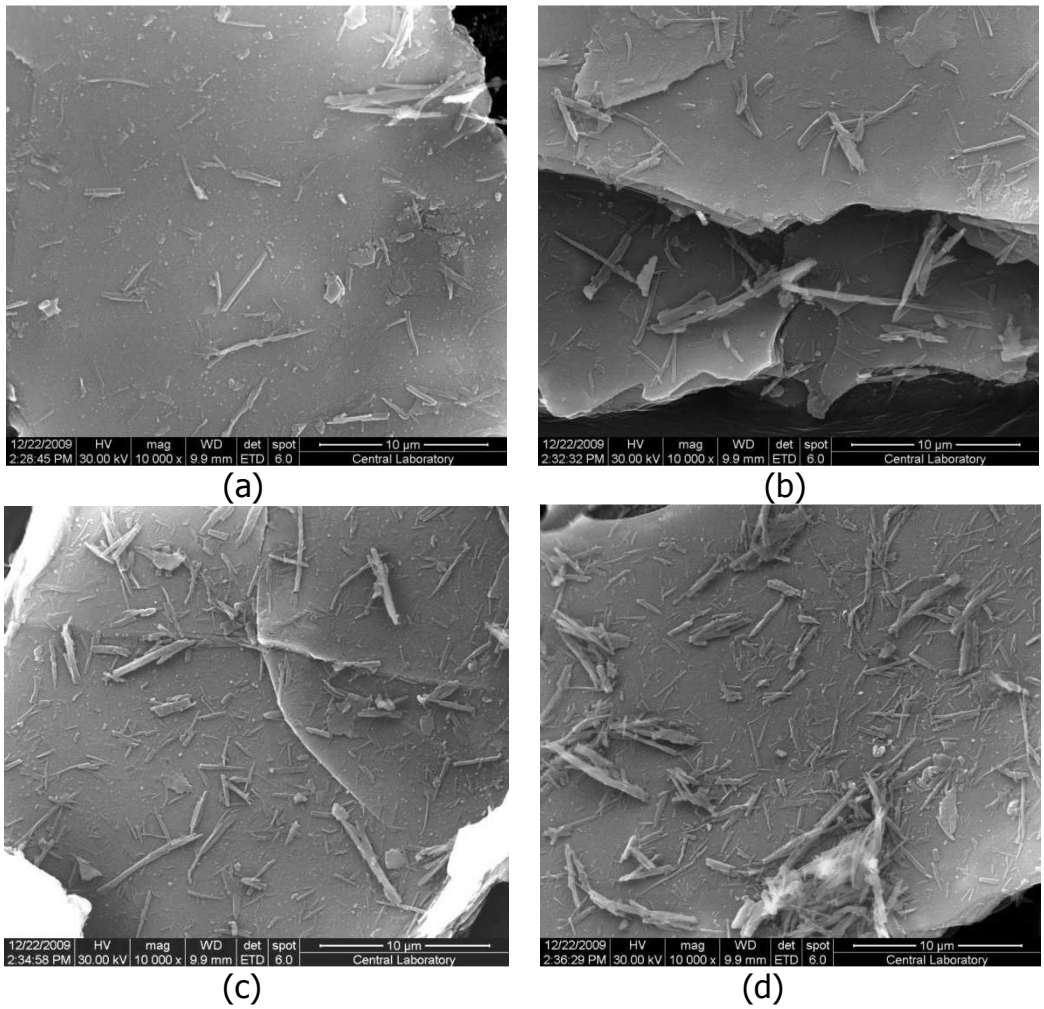

Figure 4.21 SEM micrographs of CPM pigments with different CP amounts at 25°C; (a) CPM005, (b) CPM010, (c) CPM020, (d) CPM040.

4.5.4 SEM Results of TCPM Pigments

In Figure 4.22, SEM micrographs of TCPM0520 synthesized at 120°C are given. SEM micrographs show that TCPM0520 pigment did not form any

crystalline structure on the substrate and only TiO_2 crystals could be noticed from the surface. So it could not be seen even at high magnifications which might be due to adhering of molecules all over the surface. Also, the same result was obtained with the other TCPM samples at all temperatures.

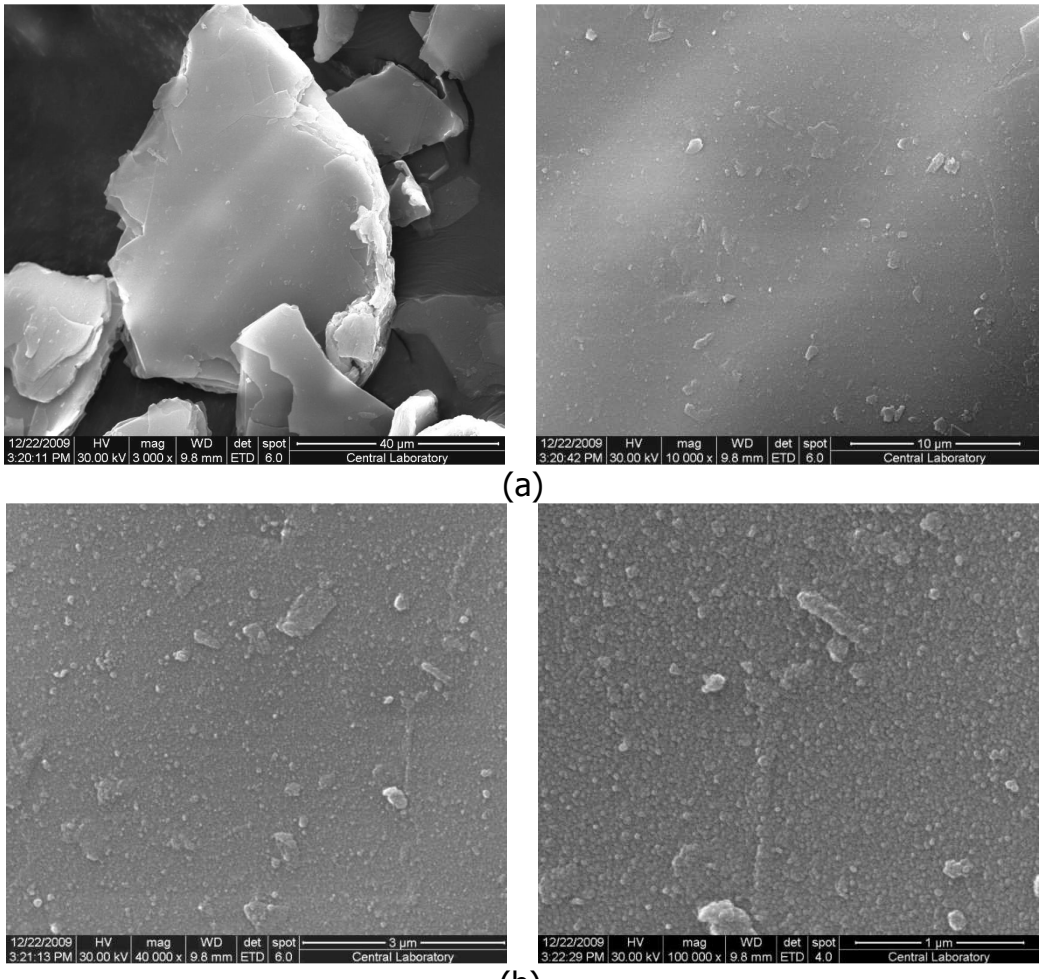

Figure 4.22 SEM micrographs of TCPM0520 synthesized at 120°C; (a) low magnifications, (b) high magnifications.

The reason of this result was due to amide substitution preventing TCP molecules to be arranged as stacks to form crystallites and rendering the

molecules to interact with the substrate instead of themselves by well disseminating on the substrate surface. This result agreed with the results of XRD and FT-IR analysis results which confirm amorphous structure of TCP on the mica-titania pigment.

4.5.5 Elemental Analysis Results of Combination Pigments

Elemental analysis (nitrogen) was performed on the combination pigments in order to see the effect of temperature on the deposition of phthalocyanine onto the mica-titania substrates. Table 4.4 shows mass percentages of the CP and TCP pigments on the substrate at different temperatures. Calculation details are given in Appendix C. It can be easily seen that with increasing temperature, the amounts of CP on the substrate increased until the reaction temperature of 90°C. However, at 120°C, the amount of CP was found to decrease slightly. It was obvious that the increment of CP was significant at 90°C that the α-β transformation was completed.

Table 4.4 Mass percents of CP and TCP pigments on mica titania.

Sample	Phthalocyanine (Mass%)
CPM040 (25°C)	4.26
CPM040 (60°C)	7.30
CPM040 (90°C)	8.12
CPM040 (120°C)	7.76
TCMP040 (25°C)	3.08
TCMP040 (60°C)	0.71
TCMP040 (90°C)	1.83
TCMP040 (120°C)	1.92

In the case of TCPM pigments, the amount of TCP as a function of deposition temperature changed inconsistently, i.e., there was no direct temperature dependency according to our observations as given in Table 4.4.

4.5.6 Paint Properties of Combination Pigments

CPM and TCPM pigments which were synthesized at 90°C were incorporated into paint formulation. For comparison, mica-titania with highest anatase and rutile form was also used to prepare paint samples.

Gloss of the paints were measured by gloss meter at different angles given in Table 4.5. Mica titania pigment with rutile form showed improved gloss with respect to mica titania pigment with anatase form.

Table 4.5 Gloss values of paints including CPM and TCPM pigments.

Sample	25^0	60^0	85^0
Mica_titania (Anatase)	40.0	65.6	67.2
Mica_titania (Rutile)	48.5	75.7	75.8
CPM005	58.7	79.6	80.8
CPM010	56.7	78.9	78.8
CPM020	50.7	78.5	77.6
CPM040	49.8	78.0	77.2
TCPM0065	59.8	84.9	87.6
TCPM0130	48.0	75.2	58.0
TCPM0260	47.3	74.8	50.1
TCPM0520	45.9	74.0	45.3

On the other hand, the higher gloss values of all CPM samples when compared to mica titania was the evidence of the enhancing luster property of copper phthalocyanines on the mica-titania substrates. The reason of the decrease in gloss value with an increasing amount of CP on the substrate could be due to the light scattering of the stacking of the CP molecules. In the case of TCPM only TCPM0065 had better gloss than mica-titania. The amorphous structure of the TCP on the mica-titania surfaces was confirmed by XRD and FT-IR analysis should cause this result. The gloss of TCPM0065 was not affected due to the presence of small amount of TCP on the substrates.

Hardness of the paints was measured with Pendulum Hardness Measuring Device, and the results are given in Table 4.6.

Table 4.6 Hardness of CPM and TCPM pigments synthesized at 90°C.

Sample	Hardness
Mica_titania (Anatase)	41.7
Mica_titania (Rutile)	41.5
CPM005	50.5
CPM010	54.0
CPM020	55.0
CPM040	65.5
TCPM0065	52.8
TCPM0130	45.3
TCPM0260	56.5
TCPM0520	55.1

Anatase and rutile phases of mica titania pigments showed similar hardness values while all CPM and TCPM samples showed improved hardness. This should be due to the better compatibility of CP and TCP with the alkyd resin due to copper phthalocyanine pigments on the surface. Thus, the increase in the amounts of CP on the mica titania promoted the increase in hardness of the CPM pigments. However, in case of TCM pigment the hardness values seemed to be random with the increase in amounts of TCP. This should be due to the amide substitution that distorts the adhesion in paint.

The L*a*b* is an important parameter for the characterization of optical properties of the pigments. Among them, L* is the lightness, a* is red or green, and b* is yellow or blue. From the different L*a*b* values, it can be indicated that the specimen different color at varying amounts of copper phthalocyanine pigment. dL*, da* and db* indicate how much a standard and sample differ from one another in L*, a* and b*. dE* represents the total color difference. In Table 4.7, dL*, da*, db* and dE* values are given for each pigment. These values were measured from paint samples.

Table 4.7 The L*a*b* values of paints of combination pigments.

	dL*	**da***	**db***	**dE***
TCPM0065 (standard)	0.00	0.00	0.00	0.00
TCPM0130	0.00	0.10	-1.73	1.74
TCPM0260	-2.13	1.65	-1.70	3.18
TCPM0520	-5.12	1.69	-3.97	6.00
CPM005	-3.80	5.26	-5.87	8.75
CPM010	-8.92	7.23	-10.07	15.28
CPM020	-11.48	7.61	-10.38	17.25
CPM040	-16.09	10.66	-10.06	21.77

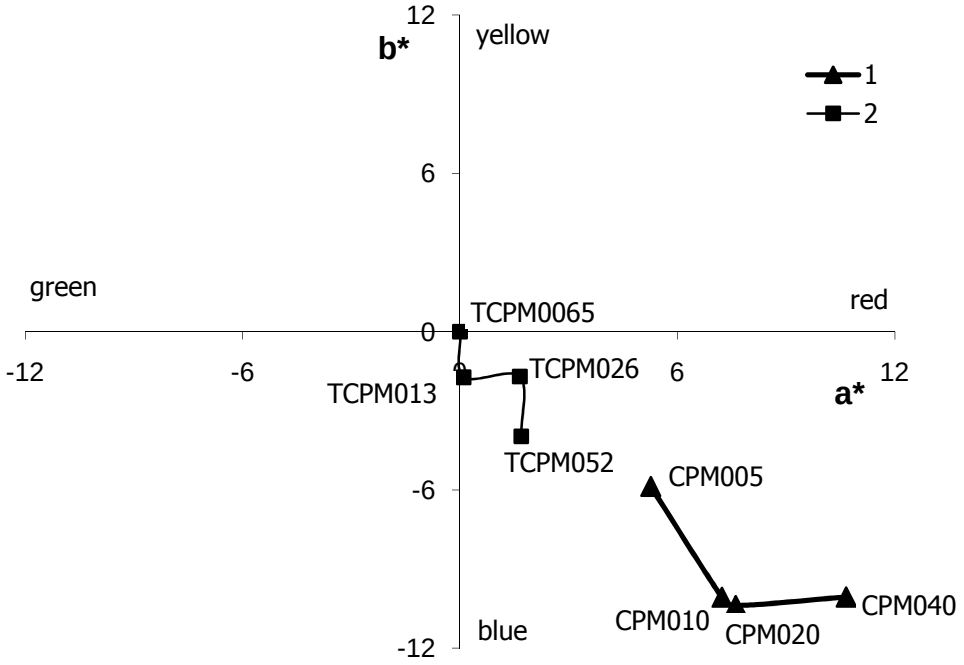

Figure 4.23 The comparative color properties of combination pigments based on different phthalocyanine deposition. Graph 1 and 2 represents CPM and TCPM pigments, respectively.

This effect could also be observed by evaluating the magnitude of individual color shifts as shown in Figure 4.23. Graph 1 which represents CPM pigments showed high red and blue shift while Graph 2 which represents TCPM pigments did not show significant blue or red shift with increasing amount of TCP. It can be interpreted as for CPM pigments, more CP pigments was deposited onto the mica titania substrate with increasing CP amount.

CHAPTER 5

CONCLUSIONS

1. Pearlescent pigment was synthesized by coating muscovite mica with TiO_2. Pre-treatments increased pearlescence effect.

2. Improved luster properties were obtained by achieving anatase to rutile crystalline phase transformation of TiO_2.

3. Unsubstituted copper phthalocyanine (CP) and tetracarboxamide copper phthalocyanine TCP) were synthesized by microwave irradiation.

4. Varying amounts of copper phthalocyanines (CP and TCP) were deposited onto mica-titania pigment at different temperatures. The phase transformations of copper phthalocyanines on mica pigments were investigated.

5. At 90^oC and 120^oC, beta phase of CP was obtained on the substrates which was the desired phase in paint applications.

6. TCP pigments were found to be amorphous on the mica titania substrate.

7. Paint formulations of combination pigments showed improved gloss and hardness properties with respect to mica titania based paints.

CHAPTER 6

RECOMMENDATIONS

1. Interference pigments can be obtained by increasing the amount of TiO_2 coating with yellow reflecting, red reflecting or blue reflecting appearance. Copper phthalocyanines can be deposited onto these interference pigments and paint properties (color, hardness, gloss) as well as crystalline forms can be investigated.

2. Copper phthalocyanines can be ground and/or dispersed in the solution before deposition in order to achieve nano-size coating instead of micro-size coating.

3. Copper phthalocyanines with different substituents can be used to synthesize combination pigments. Crystalline phases and surface morphologies of them on the mica titania substrates can be investigated.

4. Parameters that effect the alpha-beta phase transformation of CP on the mica titania substrate can be investigated.

REFERENCES

1. H. Du, C. Liu, J. Sun, Q. Chen, "An investigation of angle-dependent optical properties of multi-layer structure pigments formed by metal-oxide-coated mica," *Powder Technology* **185**, 291-296 (2008).

2. F. J. Maile, G. Pfaff, P. Reynders, "Effect pigments--past, present and future," *Progress in Organic Coatings* **54**, 150-163 (2005).

3. P. M. Tenório Cavalcante, M. Dondi, G. Guarini, F. M. Barros, A. Benvindo da Luz, "Ceramic application of mica titania pearlescent pigments," *Dyes and Pigments* **74**, 1-8 (2007).

4. C. Jing, S. X. Hanbing, "The preparation and characteristics of cobalt blue colored mica titania pearlescent pigment by microemulsions," *Dyes and Pigments* **75**, 766-769 (2007).

5. H. Giesche, "Preparation and Applications of Coated Powders in Ceramics and Related Fields," *Journal of Dispersion Science and Technology* **19**, 249 - 265 (1998).

6. G. Pfaff, P. Gabel, M. Kieser, F. J. Maile, W. Joachim, "Special Effect Pigments," (2008).

7. K. D. Franz, K. Ambrosius, "Iron oxide coated perlescent pigments," (1988).

8. N. Bayat, S. Baghshahi, P. Alizadeh, "Synthesis of white pearlescent pigments using the surface response method of statistical analysis," *Ceramics International* **34**, 2029-2035 (2008).

9. L. Armanini, F. Bagala, "Iron oxide coated mica nacreous pigments," (1979).

10. R. Vogt, H. D. Bruckner, "Interference pigments having a blue mass tone," (2001).

11. G. B. Song, J. K. Liang, F. S. Liu, T. J. Peng, G. H. Rao, "Preparation and phase transformation of anatase-rutile crystals in metal doped TiO2/muscovite nanocomposites," *Thin Solid Films* **491**, 110-116 (2005).

12. V. Carmine, Jr. Deluca, "Rutile titanium dioxide coated micaceous pigments formed without tin," (1995).

13. Y. C. Ryu, T. G. Kim, G. S. Seo, J. H. Park, C. S. Suh, S. S. Park, S. S. Hong, G. D. Lee, "Effect of substrate on the phase transformation of TiO2 in pearlescent pigment," *Journal of Industrial and Engineering Chemistry* **14**, 213-218 (2008).

14. C. J. Rieger, L. Armanini, "Exterior grade titanium dioxide coated mica," (1979).

15. M. Çamur, A. R. Özkaya, M. Bulut, "Novel phthalocyanines bearing four 4-phenyloxyacetic acid functionalities," *Polyhedron* **26**, 2638-2646 (2007).

16. A. Kalkan, Z. A. Bayir, "Phthalocyanines with rigid carboxylic acid containing pendant arms," *Polyhedron* **25**, 39-42 (2006).

17. D. Kulaç, M. Bulut, A. Altindal, A. R. Özkaya, B. Salih, Ö. Bekaroglu, "Synthesis and characterization of novel 4-nitro-2-(octyloxy)phenoxy substituted symmetrical and unsymmetrical Zn(II), Co(II) and Lu(III) phthalocyanines," *Polyhedron* **26**, 5432-5440 (2007).

18. S. Y. Al Raqa, "The synthesis and photophysical properties of novel, symmetrical, hexadecasubstituted Zn phthalocyanines and related unsymmetrical derivatives," *Dyes and Pigments* **77**, 259-265 (2008).

19. C. Alkan, L. Aras, G. Gündüz, "Synthesis, characterization, and electrical properties of diazophenylene bridged Co, Ni, Cu, Ce, and Er phthalocyanine polymers," *Journal of Applied Polymer Science* **106**, 378-385 (2007).

20. N. Akdemir, G. Erdem, "Synthesis and Characterization of Novel Phthalocyanines Containing (nOctyl) Mercapto Acetamid Substituents," *Synthesis and Reactivity in Inorganic, Metal-Organic, and Nano-Metal Chemistry* **35**, 819-824 (2005).

21. B. S. Sesalan, A. Koca, A. Gül, "Water soluble novel phthalocyanines containing dodeca-amino groups," *Dyes and Pigments* **79**, 259-264 (2008).

22. V. Verdree, S. Pakhomov, G. Su, M. Allen, A. Countryman, R. Hammer, S. Soper, "Water Soluble Metallo-Phthalocyanines: The Role of the Functional Groups on the Spectral and Photophysical Properties," *Journal of Fluorescence* **17**, 547-563 (2007).

23. N. B. McKeown, "Phthalocyanine-containing polymers," *Journal of Materials Chemistry* **10**, 1979-1995 (2000).

24. B. O. Agboola, "Catalytic activities of Metallophthalocyanines towards Detection and Transformation of Pollutants," (2007).

25. O. Seven, B. Dindar, B. Gultekin, "Microwave-Assisted Synthesis of Some Metal-Free Phthalocyanine Derivatives and a Comparison with Conventional Methods of their Synthesis," *Turkish Journal of Chemistry* **33**, 123-134 (2009).

26. K. S. Lokesh, N. Uma, B. N. Achar, "The Microwave-assisted syntheses and a conductivity study of a platinum phthalocyanine and its derivatives," *Polyhedron* **28**, 1022-1028 (2009).

27. A. Shaabani, R. Maleki Moghaddam, A. Maleki, A. H. Rezayan, "Microwave assisted synthesis of metal-free phthalocyanine and metallophthalocyanines," *Dyes and Pigments* **74**, 279-282 (2007).

28. T. Noguchi, T. Watanabe, "Flaky colored pigments, methods for their production, and their use in cosmetic compositions," (1988).

29. H. M. Smith, "High Performance Pigments," (2002).

30. L. Armanini, "Colored micaceous pigments," (1992).

31. C. Çağlar, "Kimyasal Yöntemlerle Çok Tabakalı Pigment Sentezi," (2004).

32. V. Stengl, J. Subrt, S. Bakardjieva, A. Kalendova, P. Kalenda, "The preparation and characteristics of pigments based on mica coated with metal oxides," *Dyes and Pigments* **58**, 239-244 (2003).

33. M. Ren, H. Yin, A. Wang, T. Jiang, Y. Wada, "Mica coated by direct deposition of rutile TiO2 nanoparticles and the optical properties," *Materials Chemistry and Physics* **103**, 230-234 (2007).

34. V. Carmine, Jr. Deluca, H. A. Miller, G. R. Waitkins, "Rutile-coated mica nacreous pigments and process for the preparation thereof," (1977).

35. V. D. Hildenbrand, S. Doyle, H. Fuess, G. Pfaff, P. Reynders, "Crystallisation of thin anatase coatings on muscovite," *Thin Solid Films* **304**, 204-211 (1997).

36. M. Özil, E. Agar, S. Sasmaz, B. Kahveci, N. Akdemir, I. E. Gümrükçüoglu, "Microwave-assisted synthesis and characterization of the monomeric phthalocyanines containing naphthalene-amide group moieties and the polymeric phthalocyanines containing oxa-aza bridge," *Dyes and Pigments* **75**, 732-740 (2007).

37. M. N. Yarasir, M. Kandaz, B. Filz Senkal, A. Koca, B. Salih, , "Selective heavy metal receptor functional phthalocyanines bearing thiophenes: Synthesis, characterization, spectroscopy and electrochemistry," *Dyes and Pigments* **77**, 7-15 (2008).

38. M. N. Yarasir, M. Kandaz, A. Koca, B. Salih, "Polytopic cation receptor functional phthalocyanines: Synthesis, characterization, electrochemistry and metal ion binding," *Polyhedron* **26**, 1139-1147 (2007).

39. C. S. Marvel, J. H. Rassweiler, "Polymeric Phthalocyanines," *Journal of the American Chemical Society* **80**, 1197-1199 (2002).

40. D. Villemin, M. Hammadi, M. Hachemi, N. Bar, "Applications of Microwave in Organic Synthesis: An Improved One-step Synthesis of Metallophthalocyanines and a New Modified Microwave Oven for Dry Reactions," *Molecules* **6**, 831-844 (2001).

41. A. T. Hu, T. Tseng, H. Hwu, "Novel Synthesis of Phthalocyanines by Microwave Irradiation," (2003).

42. K. S. Jung, J. H. Kwon, S. M. Son, J. S. Shin, G. D. Lee, S. S. Park, "Characteristics of the copper phthalocyanines synthesized at various conditions under the classical and microwave processes," *Synthetic Metals* **141**, 259-264 (2004).

43. B. J. Exsted, M. W. Urban, "Novel phthalocyanine/polyol high-solids coatings: Structure - property relationships," *Journal of Applied Polymer Science* **47**, 2019-2035 (1993).

44. R. Prabakaran, R. Kesavamoorthy, G. L. N. Reddy, F. P. Xavier, "Structural Investigation of Copper Phthalocyanine Thin Films Using X-Ray Diffraction, Raman Scattering and Optical Absorption Measurements," *physica status solidi (b)* **229**, 1175-1186 (2002).

45. F. Iwatsu, "Size effects on the alpha-beta transformation of phthalocyanine crystals," *The Journal of Physical Chemistry* **92**, 1678-1681 (1988).

46. S. Karan, B. Mallik, "Templating Effects and Optical Characterization of Copper (II) Phthalocyanine Nanocrystallites Thin Film: Nanoparticles, Nanoflowers, Nanocabbages, and Nanoribbons," *The Journal of Physical Chemistry C* **111**, 7352-7365 (2007).

47. K. R. Patil, S. D. Sathaye, R. Hawaldar, B. R. Sathe, A. B. Mandale, A. Mitra, "Copper phthalocyanine films deposited by liquid-liquid interface recrystallization technique (LLIRCT)," *Journal of Colloid and Interface Science* **315**, 747-752 (2007).

48. H. J. Emeleus, A. G. Sharpe, "Advances In Inorganic Chemistry And Radiochemistry," **7**, (1965).

49. F. Iwatsu, T. Kobayashi, N. Uyeda, "Solvent effects on crystal growth and transformation of zinc phthalocyanine," *The Journal of Physical Chemistry* **84**, 3223-3230 (1980).

50. G. D. Penrose, "Process of producing tinctorially stable phthalocyanine coloring matters," (1951).

51. H. E. Tillson, "Production of phthalocyanine colors in pigmentary state," (1957).

52. Y. L. Lee, W. C. Tsai, C. H. Chang, Y. M. Yang, "Effects of heat annealing on the film characteristics and gas sensing properties of substituted and un-substituted copper phthalocyanine films," *Applied Surface Science* **172**, 191-199 (2001).

53. J. J. Bardet, "Methods for treating mica and composition," (1951).

54. G. B. Song, H. Joly, F. S. Liu, T. J. Peng, P. Wan, J. K. Liang, "Surface and interface characteristics of TiO2-muscovite nanocomposites," *Applied Surface Science* **220**, 159-168 (2003).

APPENDIX A

FT-IR SPECTROSCOPY RESULTS FOR COMBINATION PIGMENTS

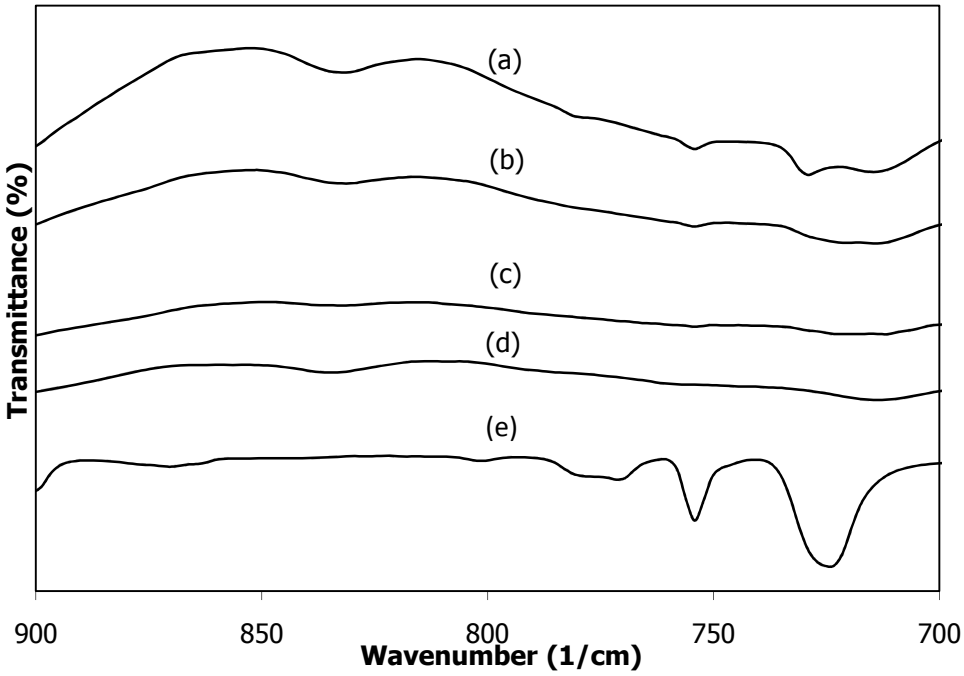

Figure A.1 FT-IR spectra of CPM005 pigment (a) 90°C, (b) 60°C, (c) 25°C, (d) mica-titania pigment and (e) CP.

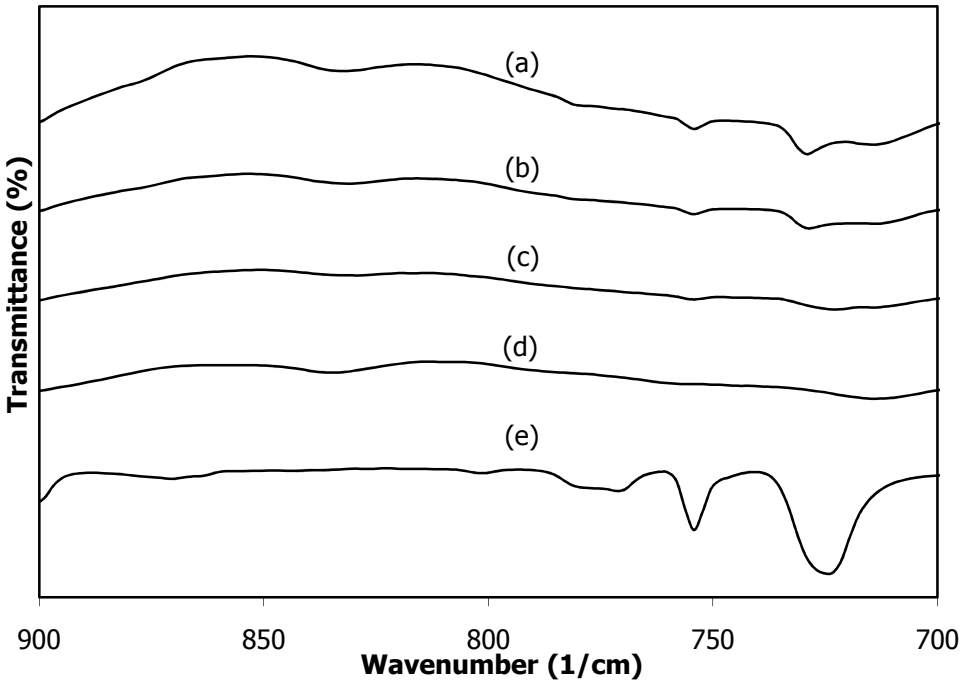

Figure A.2 FT-IR spectra of CPM010 pigment (a) 90°C, (b) 60°C, (c) 25°C, (d) mica-titania pigment and (e) CP.

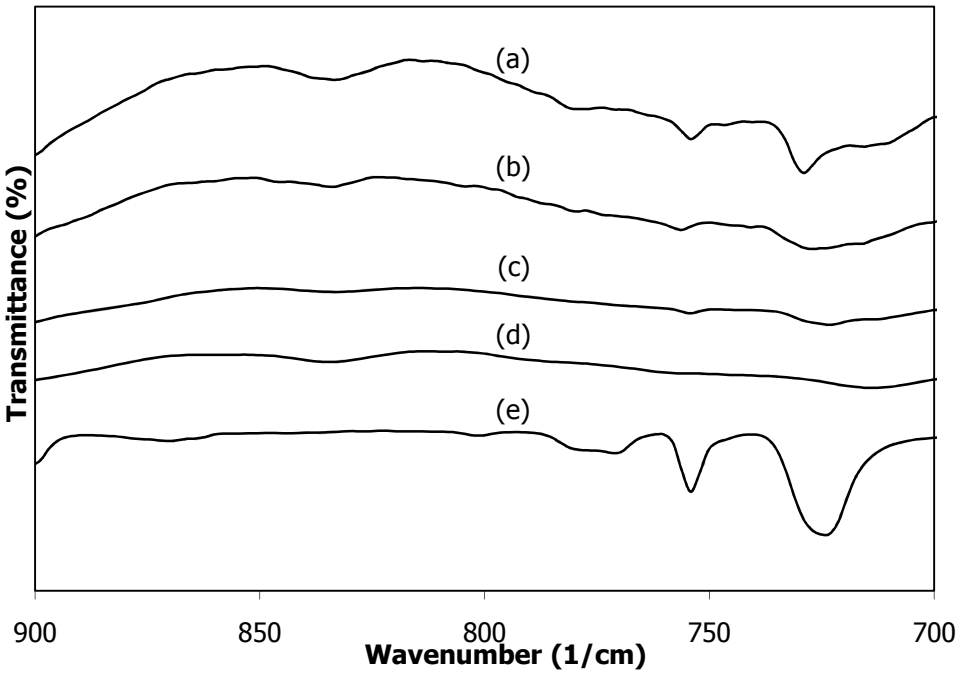

Figure A.3 FT-IR spectra of CPM020 pigment (a) 90°C, (b) 60°C, (c) 25°C, (d) mica-titania pigment and (e) CP.

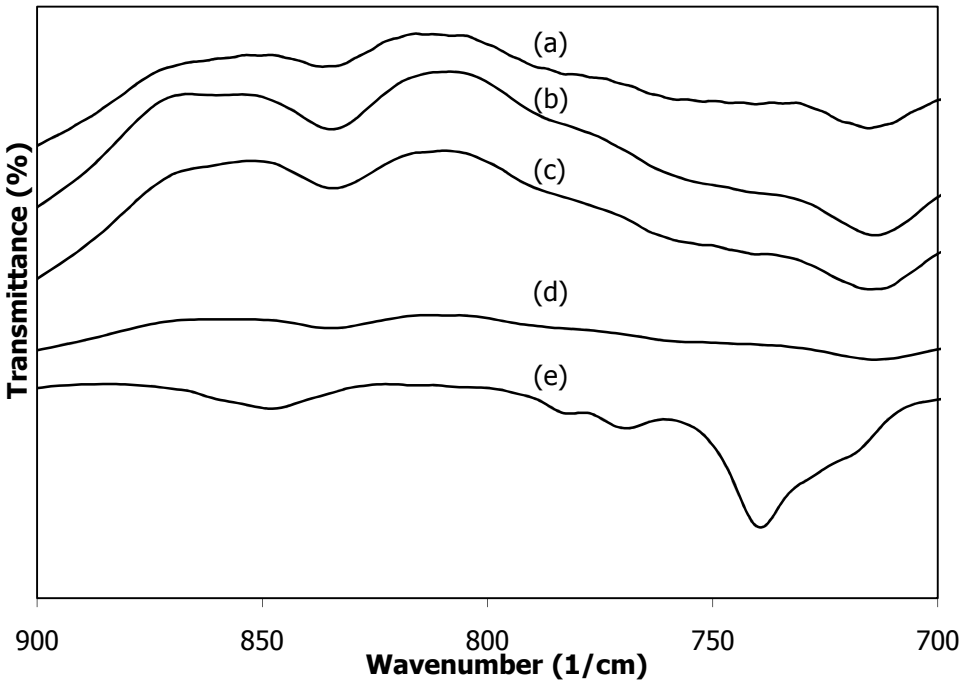

Figure A.4 FT-IR spectra of (a) TCPM0065 pigment (90°C), (b) TCPM pigment (60°C) , (c) TCMP pigment (25°C), (d) mica-titania pigment and (e) TCP.

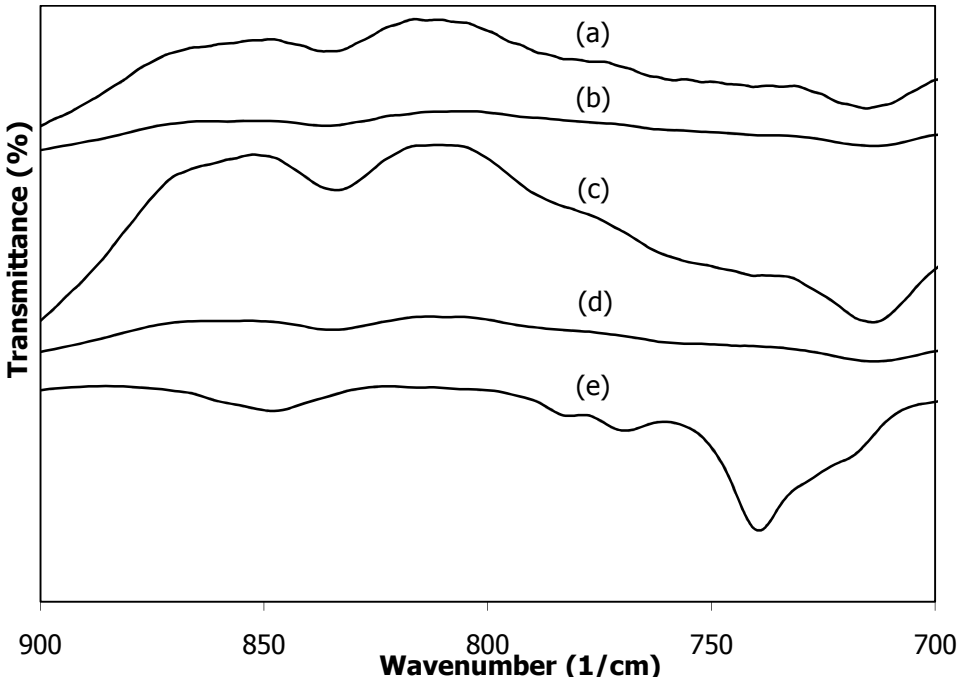

Figure A.5 FT-IR spectra of (a) TCPM0130 pigment (90°C), (b) TCPM pigment (60°C) , (c) TCMP pigment (25°C), (d) mica-titania pigment and (e) TCP.

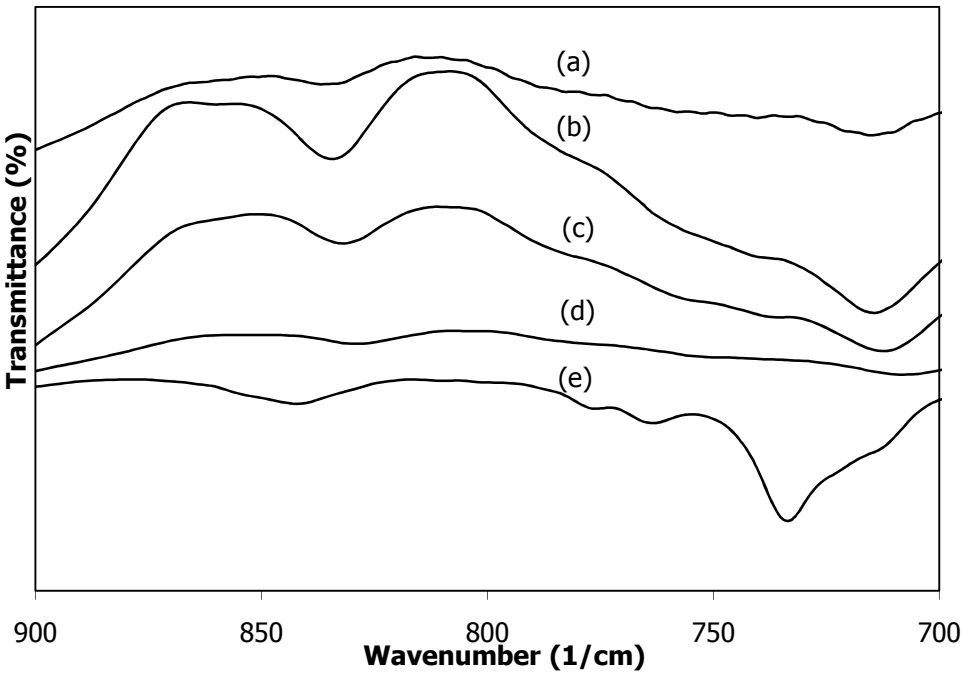

Figure A.6 FT-IR spectra of (a) TCPM0260 pigment (90°C), (b) TCPM pigment (60°C) , (c) TCMP pigment (25°C), (d) mica-titania pigment and (e) TCP.

APPENDIX B

MOLE PERCENT CALCULATIONS OF TiO_2 PHASES

Table B.1 shows the analytical areas of the most intense peaks of anatase and rutile which were deconvoled by using Peak Fit software.

Table B.1 Analytical areas of Rutile and Anatase Phases.

Sample	**Rutile Peak Area**	**Anatase Peak Area**
Mica Titania	4.72	200.11
Mica titania (0.22 % SnO_2)	22.52	76.78
Mica titania (0.44 % SnO_2)	107.94	48.25
Mica titania (0.66 % SnO_2)	199.19	10.07
Mica titania (0.88 % SnO_2)	141.18	14.29

Firstly the calculation of volume percents of phases were performed.

% (In Volume) Anatase = [200.11 / (4.72 + 200.11)] * 100 = 97.69 %.
% (In Volume) Rutile = [4.72 / (4.72 + 200.11)] * 100 = 2.30 %.

Theoretical densities of anatase (d=3.84 g/cm^3) and rutile phases (d=4.26 g/cm^3) and molecular weight of TiO_2 (M_w=79.88 g/mol) were utilized in order to determine the mole percent of phases.

Mol of Anatase = (97.69 * 3.84) / 79.88 = 4.69.

Mol of Rutile = (2.30 * 4.26) / 79.88 = 0.12.

% (In mole) Anatase = [4.69 / (4.69 + 0.12)] * 100 = 97.45 %.

% (In mole) Rutile = [0.12 / (4.69 + 0.12)] * 100 = 2.55 %.

The deconvoluted peaks of mica-titania pigment that were utilized to find the areas under them are shown in Figures below.

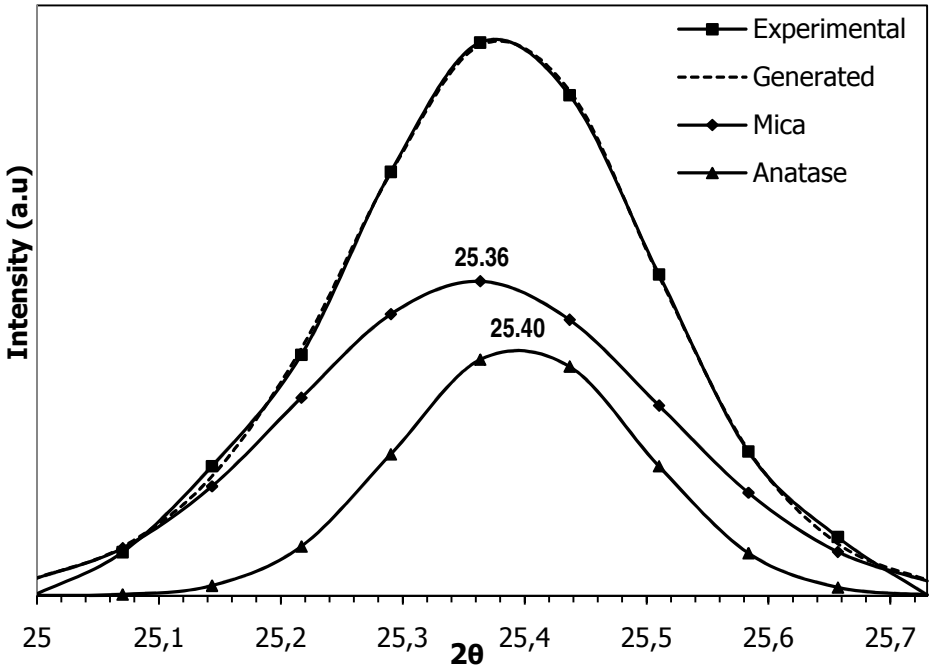

Figure B.1 Deconvoluted peaks of mica titania (anatase).

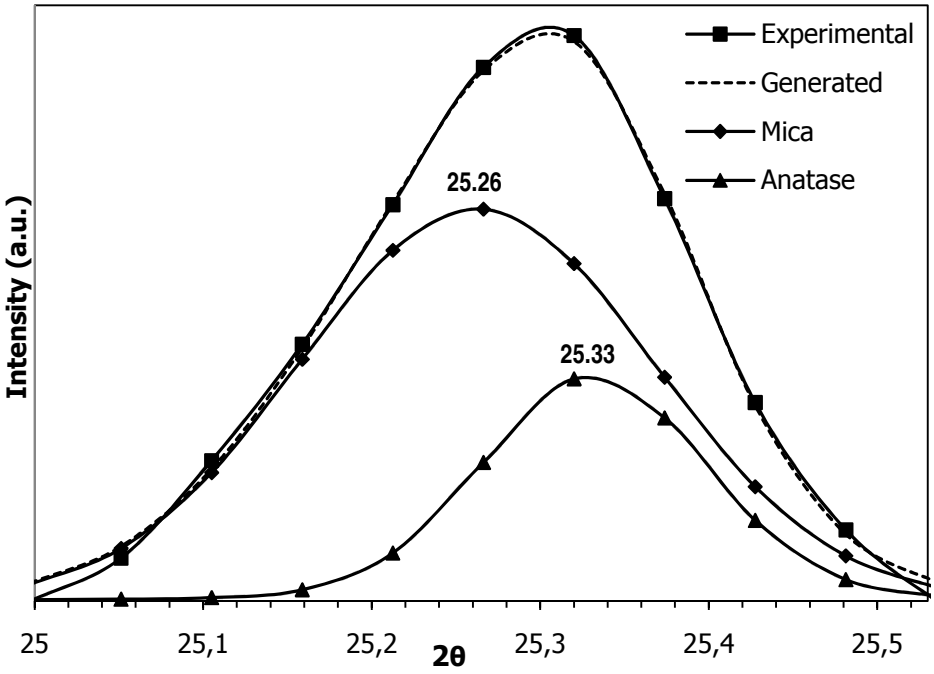

Figure B.2 Deconvoluted peaks of mica titania (anatase) with 0.22 % SnO_2.

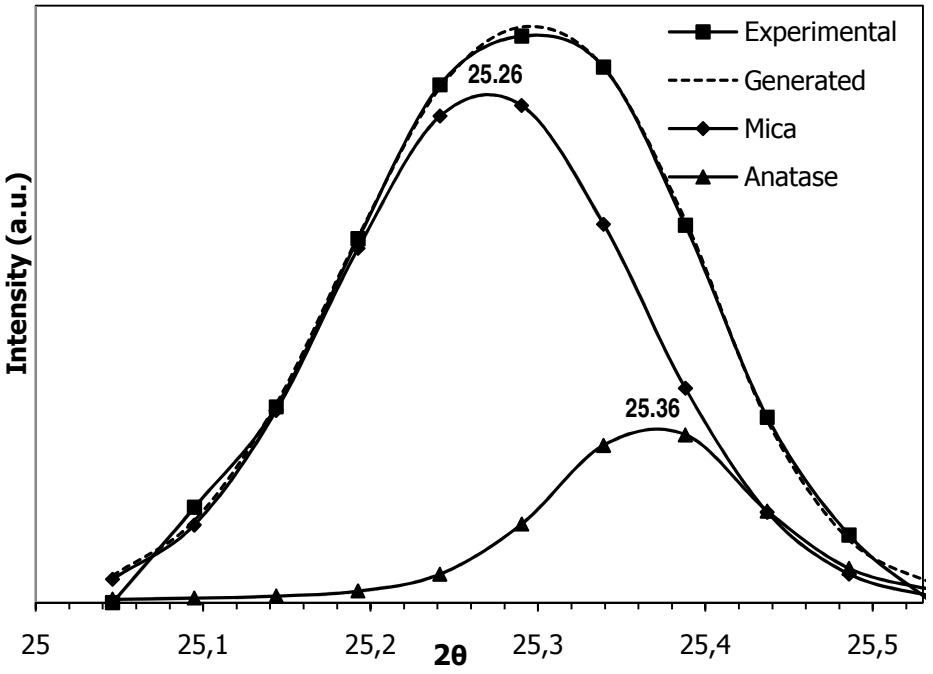

Figure B.3 Deconvoluted peaks of mica titania (anatase) with 0.44 % SnO_2.

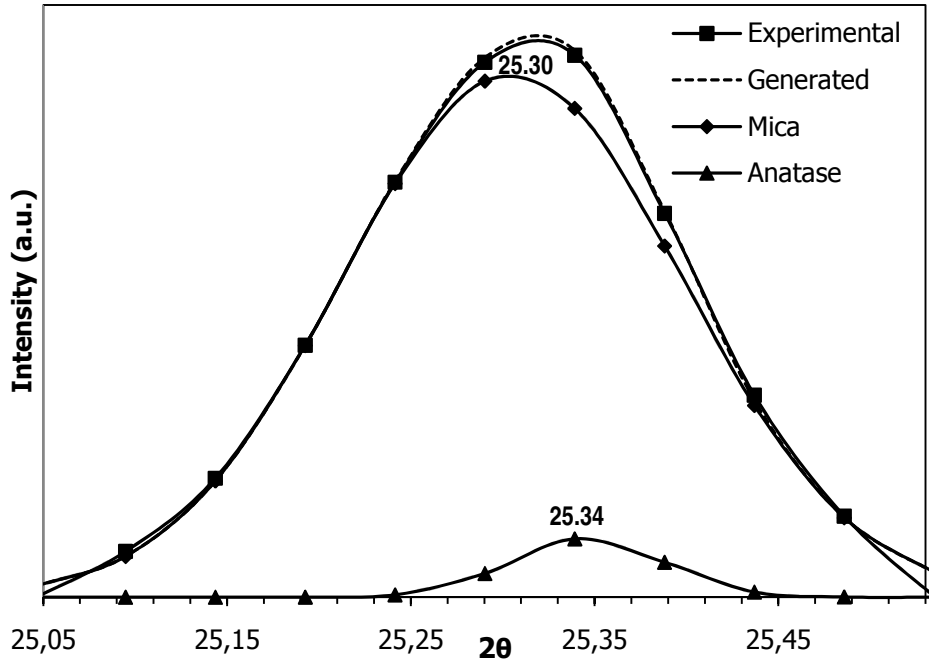

Figure B.4 Deconvoluted peaks of mica titania (anatase) with 0.66 % SnO_2.

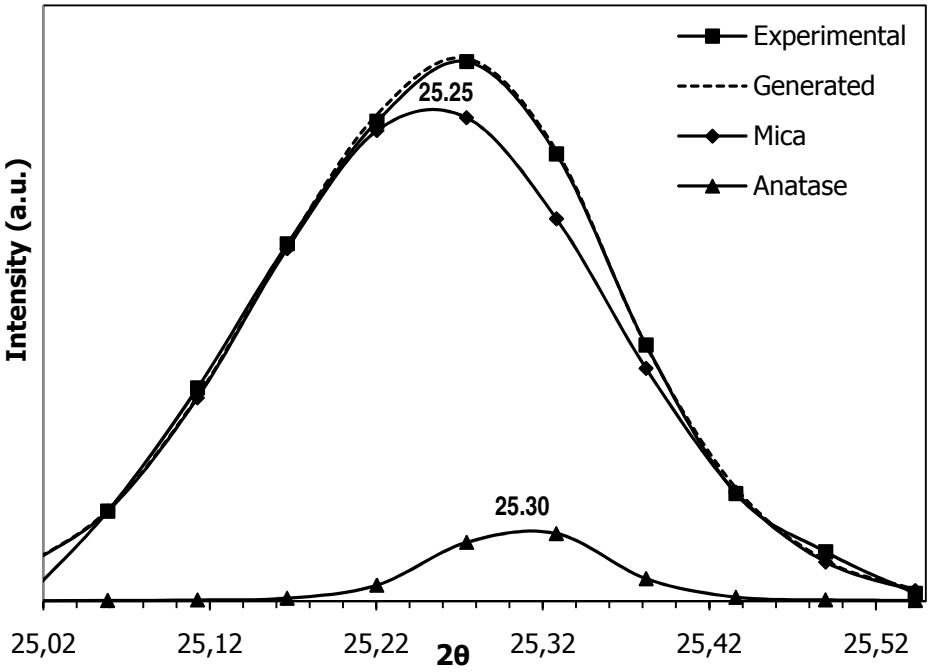

Figure B.5 Deconvoluted peaks of mica titania (anatase) with 0.88 % SnO_2.

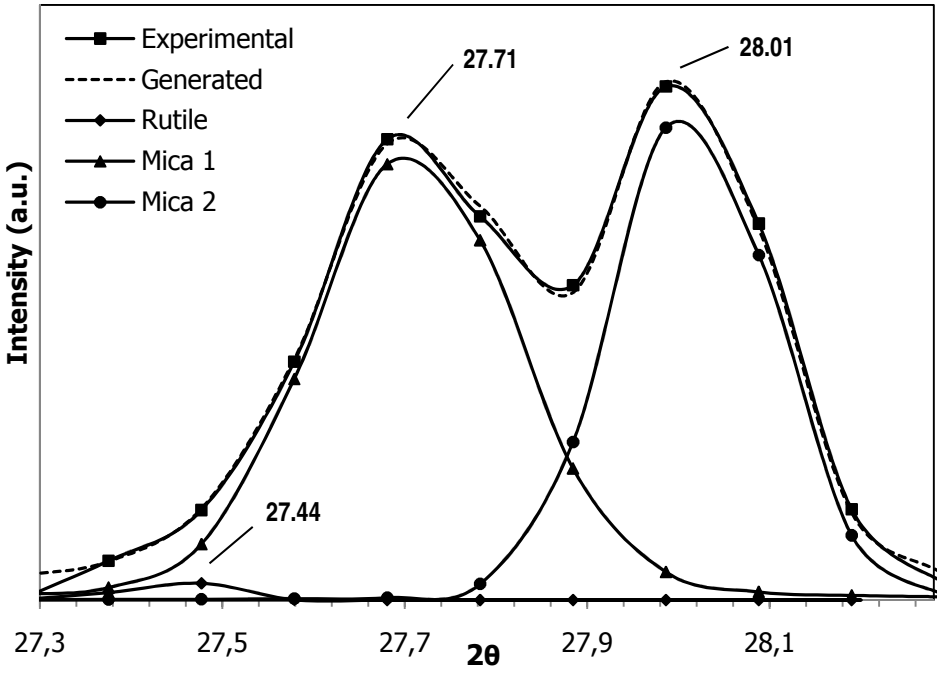

Figure B.6 Deconvoluted peaks of mica titania (rutile).

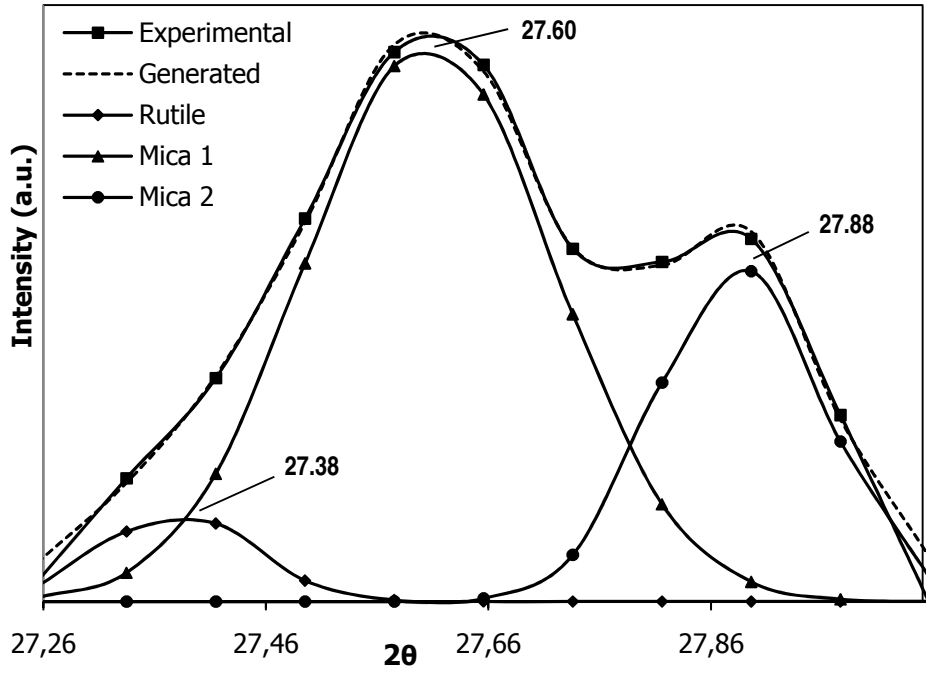

Figure B.7 Deconvoluted peaks of mica titania (rutile) with 0.22 % SnO_2.

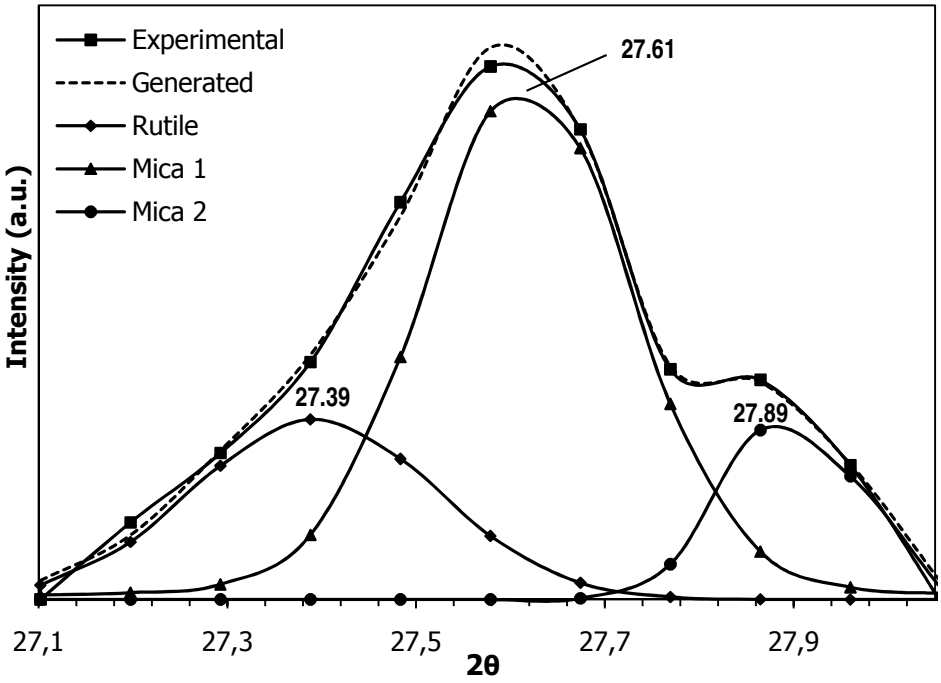

Figure B.8 Deconvoluted peaks of mica titania (rutile) with 0.44 % SnO_2.

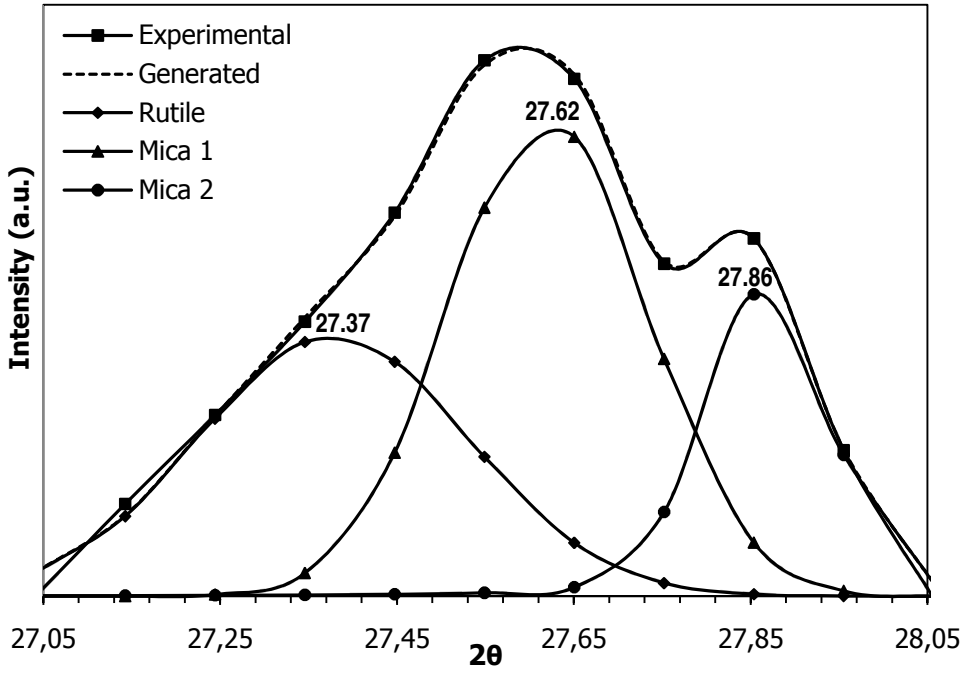

Figure B.9 Deconvoluted peaks of mica titania (rutile) with 0.66 % SnO_2.

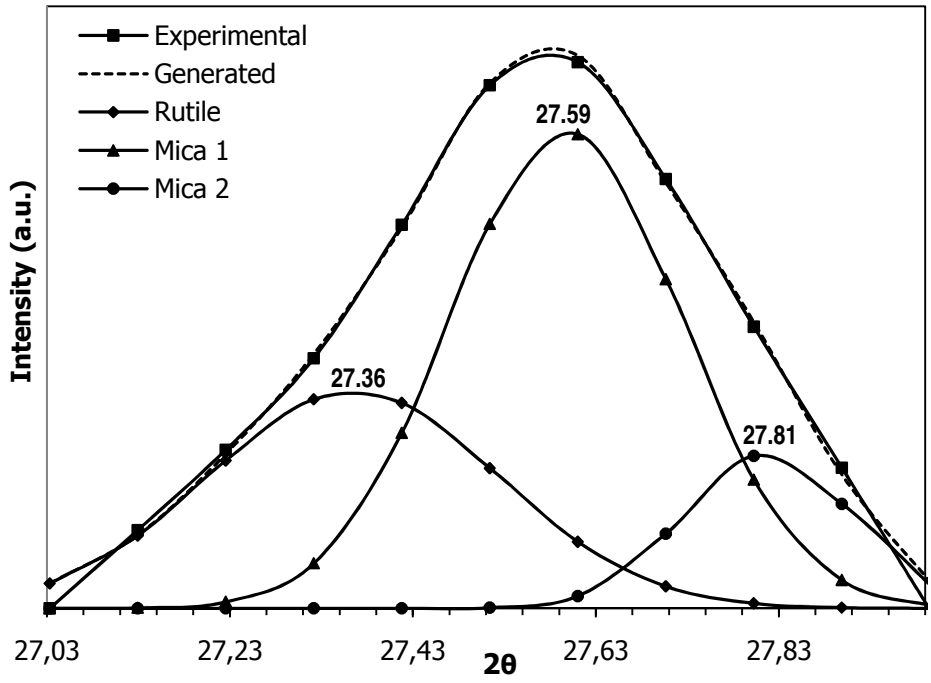

Figure B.10 Deconvoluted peaks of mica titania (rutile) with 0.88 % SnO_2.

APPENDIX C

ELEMENTAL ANALYSIS RESULTS OF COMBINATION PIGMENTS

Nitrogen Elemental Analysis results which was performed to determine CP and TCP amounts on the mica-titania substrate, were given in Table C.1.

Table C.1 Nitrogen % in combination pigments at different temperatures.

Sample	N (mass %)
CPM040 (25°C)	0.83
CPM040 (60°C)	1.42
CPM040 (90°C)	1.58
CPM040 (120°C)	1.51
TCMP040 (25°C)	0.69
TCMP040 (60°C)	0.16
TCMP040 (90°C)	0.41
TCMP040 (120°C)	0.43

Molecular weight of CP and TCP are 576.08g/mol and 752.08g/mol, respectively. 1 mol CP consists of 112 g nitrogen while 1 mol TCP consists of 168 g nitrogen. One of the mass percents of CP and TCP pigments on the substrate were calculated as an example below.

% CP = 0.83 * 576.08 / 112 = 4.26 %.

% TCP = 0.69 * 752.08 / 168 = 3.08 %.

APPENDIX D

THE LENGTHS OF PHTHALOCYANINE RODS ON MICA TITANIA

The lengths of CP rods were measured by Image J program which are given in Table D.1 below.

Table D.1 Lengths of CP rods on the mica titania substrate.

Number of CP rods measured	Length (μm) 25°C	Length (μm) 60°C	Length (μm) 90°C	Length (μm) 120°C
1	1.98	4.75	13.08	15.85
2	2.88	6.20	9.93	13.09
3	2.73	4.28	9.71	7.11
4	3.49	5.78	16.93	9.60
5	2.79	4.69	13.45	14.13
6	2.50	3.68	5.50	16.03
7	2.58	2.95	5.34	14.83
8	2.78	3.47	5.31	9.31
9	2.83	4.66	5.03	7.72
10	2.87	2.43	3.51	17.35
11	2.58	3.94	9.37	18.88
12	4.46	3.66	7.06	20.48
13	2.26	6.60	2.36	8.54
14	2.52	5.80	2.24	12.31
15	2.73	2.34	5.17	9.93
16	3.11	3.97	12.25	3.29
17	2.75	3.32	4.96	5.15
18	2.39	1.94	4.45	3.74
19	2.31	1.38	5.05	6.75
20	3.56	2.34	2.97	7.20
21	2.66	2.94	3.99	3.33
22	1.71	2.50	1.71	5.16
23	2.47	4.56	8.06	13.70
24	1.52	2.34	5.04	10.78
25	1.73	2.05	2.15	16.00